Thermal Conversion of Algal Biomass and its Derivative to Fuels and Petrochemicals

Submitted in fulfilment of the requirements for the degree of Doctor of Engineering: Chemical Engineering in the Faculty of Engineering and Built Environment at the Durban University of Technology

Sherif Ishola Mustapha

April 2021

Supervisor: Professor Yusuf Makarfi Isa

Co-supervisor: Professor Faizal Bux

DECLARATION

I confirm that this thesis is composed of my original work and contains no material previously submitted to the Durban University of Technology or any other institution for academic qualifications. The content of the thesis consists of work I have carried out since the commencement of my PhD studies. All information utilized and their sources have been duly acknowledged.

21/04/2021

Signature: ……. Date …….

Sherif Ishola Mustapha **(Candidate)**

As the candidate's supervisor, I approve this Thesis for submission:

Signature ……. Date …….

Prof. Yusuf Makarfi Isa **(Supervisor)**

As the candidate's co-supervisor, I approve this Thesis for submission:

Signature ……. Date …….

Prof. Faizal Bux **(Co-supervisor)**

SUMMARY

Thermal conversion processes have gained increased attention since they can be applied to whole microalgae (not lipids alone) resulting in higher biofuel yield with potential for production of other high-value products. The major challenges of microalgal thermal conversion are the high level of nitrogen and oxygen content present in the product stream, as well as high acidity which makes the bio-oil unstable and unfit for use as transportation fuels directly. Transportation fuels are expected to be low in oxygen and acid content for stability and also have low nitrogen content to meet environmental emission standards for combustion. Nutrient stress as a tool for enhancement of yields and quality of bio-oils produced from thermal conversion of microalgae has not received sufficient attention. This study investigated the conversion of *Scenedesmus obliquus* microalgae via three different thermal conversion processes which include pyrolysis, hydrothermal liquefaction and hydrothermal gasification. *Scenedesmus obliquus* microalgae were grown under nutrient stressed and unstressed conditions.

To better understand the effect of nutrient stressing on the process, pyrolysis experiments were conducted on unstressed *S. obliquus* microalgae biomass (N3), nutrient-stressed *S. obliquus* microalgae biomass (N1) and its residual algae biomass after lipid extraction (R-N1) at different temperatures (400 °C to 700 °C) and the results compared. Detailed biomass characterization which includes proximate analysis, ultimate analysis, biochemical analysis, Fourier-transform infrared spectroscopy (FTIR) analysis, and thermogravimetric analysis (TGA/DSC) were carried out on the microalgae biomass (N1, R-N1 and N3) to provide useful information about the combustion behaviour of the biomass during pyrolysis. The biomass characterization results indicated that nutrient-stressed condition altered the microalgae biomass composition and empirical formula for N1, R-N1, and N3 microalgae biomass were $CH_{2.00}N_{0.07}O_{0.71}$, $CH_{2.36}N_{0.08}O_{0.75}$, and

$CH_{2.35}N_{0.14}O_{0.71,}$ respectively. The maximum bio-oil yield for N1 (46.37 wt%) and R-N1 (34.85 wt%) were obtained at 500 °C, while the highest yield of bio-oil for N3 (41.94 wt%) was obtained at 600 °C. Also, the proportion of nitrogen compounds in N3 bio-oil (47.4 %) was significantly higher than that obtained in the nutrient stressed microalgae biomass (N1) bio-oil (5.92%) at pyrolysis temperature of 500 °C. Thus, nutrient stressed approach is considered more promising to produce a higher yield and good-quality pyrolytic bio-oil from microalgae biomass. A predictive model was developed based on artificial neural network (ANN) and can serve as a framework for the prediction of bio-oil yield from the pyrolysis of microalgae biomass.

Finding better heterogeneous catalysts that can enhance the quality of microalgal bio-oils to meet transportation fuels standards is seen as a major advance toward developing efficient and sustainable thermal conversion processes. In this study, pyrolysis of nutrient-stressed *Scenedesmus obliquus* microalgae over various supported metal M/Fe_3O_4-HZSM-5 catalysts (M = Zr, W, Co and Mo) was investigated. The synthesized catalysts were characterized by X-ray diffraction spectroscopy (XRD), thermogravimetric analysis (TGA), high-resolution scanning electron microscopy and energy dispersive spectroscopy (HRSEM/EDS). The catalyst: biomass ratio and temperature influence on pyrolysis product yield was also investigated. Between these, Co/Fe_3O_4-HZSM-5 catalyst showed better activity in enhancing the bio-oil quality and yield; it had the lowest nitrogen content (4.77 wt%) and highest bio-oil yield (17.73 wt %) as well as highest HHV (40.78 MJ/kg) which is almost similar to that of crude petroleum. The results showed that all the supported metal catalysts during pyrolysis promote aromatization and acid ketonization of bio-oils. The total amounts of acids present in pyrolytic bio-oil significantly decreased from 26.68% (non-catalytic) to between 0.58 – 9.68% (catalytic). Also, production of 2-pentanone was observed to increase from ~10% (non-catalytic) to 27.36 – 53.90% (catalytic). In terms of

energy recovery, Co/Fe_3O_4-HZSM-5 had about 40% energy recovery, which was the highest while the least performing catalyst was W/Fe_3O_4-HZSM-5 with 24.18% energy recovery in bio-oil. Overall, Co/Fe_3O_4-HZSM-5 was the most effective catalyst in enhancing the quality of pyrolytic bio-oil produced from nutrient stressed *Scenedesmus obliquus* microalgae with properties close to that of petroleum crude.

Hydrothermal liquefaction (HTL) of nutrient-stressed microalgae (*Scenedesmus obliquus*) (N1) with and without the use of Zr/HZSM-5 catalyst was investigated under temperature conditions ranging from 250 – 350 °C. The Zr/HZSM-5 catalyst was synthesized using wet impregnation technique and characterization was conducted on the synthesized catalyst for its crystalline nature, morphology and thermal stability using X-ray diffractometer (XRD), High-resolution scanning electron microscopy (HRSEM) and thermogravimetric analysis/differential scanning calorimetry (TGA/DSC). The HTL experiments were also conducted on the unstressed microalgae (N3) for comparison. Under the stressed condition, the protein content of the microalgae was reduced from 42.35% to 22.08% while the carbohydrate and lipid contents were increased from 25.36% to 42.55% and 17.16% to 21.62% respectively. The maximum HTL bio-oil yield of 52.80 wt% and 24.27 wt% were found for N1 and N3 respectively at 350 °C with addition of Zr/HZSM-5 catalyst. Higher denitrogenation and deoxygenation was achieved with N1 compared to N3. At high temperature of 350 °C, the most abundant fatty acid in N1 was found to be cis-vaccenic acid (omega-7- fatty acid), and this could be explored for possibility of extracting products of great value from the bio-oil for applications other than biofuels. Mainly, the use of Zr/HZSM-5 catalyst on nutrient-stressed *S. obliquus* microalgae resulted in enhanced bio-oil yield and characteristics which compared well with petroleum crude.

The potential of using whole algae, lipid and residual algae of *S. obliquus* microalgae as feedstocks for production of high-quality hydrogen and methane-rich gas via

hydrothermal gasification technique was also examined. The effect of operating parameters such as temperature, pressure and biomass concentration on the yield and composition of gaseous products using whole algae, lipid, and lipid extracted algae (LEA) as feedstocks was examined. The results showed that reaction pressure had minimal impact while temperature, biomass concentration and feedstock composition had significant effects on the composition of gaseous products. It was also found that low temperature (400 ^{o}C) and biomass concentration of 40 wt% favoured the production of methane-rich gas. In contrast, high temperature (700 ^{o}C) and low biomass concentration (10 wt%) favoured hydrogen-rich gas production in all the three feedstock considered. The highest mole fraction achieved for CH_4 was 53.45 mole%, 61.70 mole% and 52.20 mole% which corresponded to CH_4 yield of 31.14 mmol/g, 56.90 mmol/g and 30.15 mmol/g for whole algae, lipid and LEA respectively. For H_2 rich gas production, the highest mole fraction achieved were 55.77 mole%, 52.29 mole% and 55.34 mole% which corresponded to H_2 yield of 75.44 mmol/g, 105.51 mmol/g and 73.49 mmol/g for whole algae, lipid and LEA respectively. The ranking order for the yield and lower heating value (LHV) of the product gas from the HTG process was lipid > whole algae > LEA. This study has shown that hydrogen-rich and methane-rich gas can be produced from the hydrothermal gasification of microalgae as a function of the reaction conditions and feedstock composition. Also, the suitability of nutrient stressed approach and use of catalysts to enhance the quality of bio-oil produced from thermal conversion of microalgae biomass was established.

AKNOWLEDGEMENTS

My sincere gratitude and appreciation to my supervisor Prof. Yusuf Makarfi Isa for giving me the opportunity to do my doctorate degree under his supervision. I am grateful for your mentorship, sincere supervision, continuous encouragement, valuable, and constructive criticism. I will forever be grateful to you for this great accomplishment in my career. I also wish to sincerely appreciate my co-supervisor, Prof. Faizal Bux, for your support throughout my programme. I thank you for your supervision, technical inputs, and insightful contribution and for allowing me direct access to the facilities of the IWWT.

I also want to extend my appreciation to my colleagues in Fuels and Petrochemical Research Group, Chemical Engineering Department, DUT for their supports and encouragement during this study. Appreciation is also expressed to all my colleagues and staff members of the Department of Chemical Engineering and Institute of Water and Wastewater Technology (IWWT), Durban University of Technology for their cooperation and support.

Special thanks to my friend and brother in person of Dr Tijani Jimoh Oladejo for helping in proof reading my thesis. Also to Engr. Boldwin Mutsvene, I really appreciate your support and words of encouragement. Engr. Usman Aliyu and Engr. Alhafiz Mohammed thanks for always being there for me. I wish to sincerely appreciate Mr Jafar Bux, and his family for making my stay in South Africa a memorable one. To my Nigerian Muslim Community brothers and sisters resident in Durban, I appreciate you all. My brothers, Dr Taofeek Abayomi, Dr Amoo Oseni, Brother Bakr Olayemi and others too numerous to mention, I cannot thank you enough for your advices and support.

I thankfully acknowledge the financial support of the Durban University of Technology and my appreciation also goes to University of Ilorin for granting me study leave for this study.

I would like to express my sincere appreciation to my parents, my mother in-law and father in-law for their love, prayers and support. To my family and friends, thanks for your supports. I appreciate you all.

Lastly, I would like to express my deepest appreciation and love to my wife, DR Rukayat Murtala and my lovely children (Ibrahim, Naeemah and Khadijah). I cannot thank you enough for your constant support, understanding, perseverance, and endurance to make this milestone a reality. May God continue to strengthen our love and bless our children for us, Amin.

CONTENTS

DECLARATION ii

SUMMARY iii

AKNOWLEDGEMENTS vii

CONTENTS ix

LIST OF PAPERS xiv

CONFERENCE PRESENTATION xv

AWARDS AND HONOURS xvi

LIST OF FIGURES xvii

LIST OF TABLES xix

LIST OF ABBREVIATIONS xxi

CHAPTER 1 INTRODUCTION 1

1.1 Aim and Objectives 3

1.2 Thesis Outline / Framework 4

CHAPTER 2 LITERATURE REVIEW 7

2.1 Effect of Growth Conditions and Species Type on Microalgae Composition 7

2.2 Biofuel Production from Microalgae Biomass 8

2.3 Thermal Conversion Processes Using Microalgal Biomass as Feedstock 10

2.3.1 Hydrothermal Liquefaction (HTL) of Microalgae Biomass 10

2.3.2 Pyrolysis of Microalgae Biomass 15

2.3.3 Gasification of Microalgae Biomass 18

2.4 Microalgae Biomass Characterization Methods 21

2.4.1 Proximate Analysis 22

2.4.2 Ultimate Analysis 23

2.4.3 Calorific Value (Heating Value) 23

2.4.4 Biochemical Composition of Microalgae Biomass 26

2.4.5 Thermogravimetric Analysis (TGA) of Microalgae Biomass 29

2.4.6 Fourier-Transform Infrared Spectroscopy (FTIR) Analysis of Microalgae Biomass 29

2.4.7 Scanning Electron Microscopy (SEM) of Microalgae Biomass 29

CHAPTER 3 PYROLYSIS OF NUTRIENT-STRESSED MICROALGAE FOR HIGH-QUALITY BIO-OIL PRODUCTION 30

3.1 Introduction 30

3.2 Materials and Method 32

3.2.1 Raw Materials and Chemical Reagents 32

3.2.2 Characterization of Microalgae Samples 32

3.2.3 Pyrolysis Experiments 34

3.2.4 Bio-oil Analysis 36

3.2.5 Development of Predictive Model for Pyrolytic Bio-oil Yield using Artificial Neural Network (ANN) 36

3.3 Results and Discussion 37

3.3.1 Characterization of Microalgae Samples 37
3.3.2 Pyrolysis Product Distribution 44
3.3.3 Pyrolysis Bio-oil Analysis 46
3.3.4 Predictive Modelling of Bio-oil Yield 52
3.4 Conclusion 54
CHAPTER 4 CATALYTIC PYROLYSIS OF NUTRIENT-STRESSED MICROALGAE FOR HIGH-QUALITY BIO-OIL PRODUCTION 55
4.1 Introduction 55
4.2 Materials and Method 58
4.2.1 Feedstocks 58
4.2.2 Preparation of Catalyst and Characterization 58
4.2.3 Catalytic Pyrolysis Experiments 60
4.2.4 Bio-oil Analysis 61
4.3 Results and Discussion 61
4.3.1 Catalysts Characterization 61
4.3.2 Pyrolysis of *Scenedesmus obliquus* 65
4.3.3 Effect of Temperature 72
4.3.4 Effect of Catalyst to Biomass (C:B) Ratio 73
4.4 Conclusion 74
CHAPTER 5 CATALYTIC HYDROTHERMAL LIQUEFACTION OF NUTRIENT-STRESSED MICROALGAE FOR PRODUCTION OF HIGH-QUALITY BIO-OIL 76

5.1 Introduction 76

5.2 Materials and Methods 79

5.2.1 Materials 79

5.2.2 Microalgae Biomass Characterization 79

5.2.3 Catalyst Preparation and Characterisation 80

5.2.4 Hydrothermal Liquefaction Experiments 81

5.2.5 HTL Bio-oil Analysis 82

5.3 Results and Discussion 83

5.3.1 Characterisation of *Scenedesmus obliquus* Microalgae Biomass 83

5.3.2 Catalyst Characterisation 86

5.3.3 Liquefaction Product Yields 87

5.3.4 HTL Bio-oil Characterization 91

5.4 Conclusion 100

CHAPTER 6 HYDROTHERMAL GASIFICATION OF MICROALGAE AND ITS DERIVATIVES 102

6.1 Introduction 102

6.2 Experimental 102

6.2.1 Feedstock Characterisation 104

6.2.2 Hydrothermal Gasification Process Modelling with Aspen Plus 105

6.2.3 Process Model Assumptions 109

6.2.4 Effect of Pressure, Temperature, Biomass Concentration and Feedstock Composition 110

6.2.5 Model Validation 110

6.3 Results and Discussion 113

6.3.1 Effect of Pressure, Temperature and Biomass Concentration 113

6.3.2 Effect of Varying Feedstock Composition on the Hydrothermal Gasification Process 120

6.4 Conclusion 123

CHAPTER 7 CONCLUSION AND FUTURE WORK 125

7.1 Conclusion 125

7.2 Future Work 128

REFERENCES 129

APPENDIX A (CHAPTER 3) 152

APPENDIX B (CHAPTER 4) 155

APPENDIX C (CHAPTER 5) 162

APPENDIX D EXPERIMENTAL SET-UP, MATERIALS AND EQUIPMENTS 170

LIST OF PAPERS

I. **Sherif Ishola Mustapha**, Ismail Rawat, Faizal Bux, Yusuf Makarfi Isa (2020). Enhancing the efficiency of thermal conversion of microalgae: A review. (Manuscript under review at Journal of Cleaner Production)

II. **Sherif Ishola Mustapha,** Usman Aliyu Mohammed, Faizal Bux, Yusuf Makarfi Isa (2020). Catalytic hydrothermal liquefaction of nutrient-stressed microalgae for production of high-quality bio-oil over Zr/HZSM-5 catalyst. (Manuscript ready for submission)

III. **Sherif Ishola Mustapha,** Faizal Bux, Yusuf Makarfi Isa (2020). Pyrolysis of nutrient-stressed *Scenedesmus obliquus* microalgae for high-quality bio-oil production. (Manuscript ready for submission)

IV. **Sherif Ishola Mustapha,** Ismail Rawat, Faizal Bux, Yusuf Makarfi Isa (2020). Catalytic pyrolysis of nutrient-stressed *Scenedesmus obliquus* microalgae for high-quality bio-oil production. (Manuscript ready for submission)

V. **Sherif Ishola Mustapha,** Usman Aliyu Mohammed, Faizal Bux, Yusuf Makarfi Isa (2021). Hydrothermal gasification of *Scenedesmus obliquus* microalgae and its derivatives: A thermodynamic study using Aspen Plus. (Manuscript accepted at Biofuels, Bioproducts and Biorefining Journal)

VI. **Sherif Ishola Mustapha,** Faizal Bux, Yusuf Makarfi Isa (2021). Techno-economic analysis of biodiesel production over lipid extracted algae derived catalyst. *Biofuels*, 1-12.

Other Publications

VII. **Mustapha, S. I.,** and Isa, Y. M. (2020). Utilization of quaternary solvent mixtures for extraction of lipids from *Scenedesmus obliquus* microalgae. *Cogent Engineering*, *7*(1), 1788877

VIII. Aderibigbe, F. A., **Mustapha, S. I.**, Adewoye, T. L., Ishaq, A. M., Gbadegesin, A. B., Faith, E. N., ... and Saka, H. B. (2020). Qualitative role of heterogeneous catalysts in biodiesel production from *Jatropha curcas* oil. *Biofuel Research Journal*, *7*(2), 1159.

CONFERENCE PRESENTATION

Sherif Ishola Mustapha, Yusuf Makarfi Isa, Faizal Bux (2019). Synthesis and characterization of lipid extracted algae derived nano - catalyst for biodiesel production. Oral presentation at 5th International Conference Catalysis for Renewable Sources: Fuel, Energy, Chemicals (CRS-5). Crete, Greece, September 2 – 6, 2019.

Sherif Ishola Mustapha, Faizal Bux**,** Yusuf Makarfi Isa (2019). Zirconium – phosphide doped magnetic zeolite as a catalyst for enhancing microalgae volarization to biofuels. Oral presentation at 7th International Conference on Bio-refinery (ICB 2019), Johannesburg, South Africa, 18 – 21 August, 2019

Mustapha SI, Aliyu UM, Bux F**,** and Isa YM (2019). Synthesis and Characterization of Supported Nickel-Based Heterogeneous Catalyst for Biofuel Application. Oral presentation at 4th Interdisciplinary Research and Innovation Conference, Hilton, Durban, South Africa, 17 -20 September 2019

Aliyu Mohammed U, **Mustapha SI**, Rathilal S**,** and Isa YM (2019). Synthesis and Characterization of Zeolite A from South African Clay and its Application in Water Desalination. Oral presentation at 4th Interdisciplinary Research and Innovation Conference, Hilton, Durban, South Africa, 17 -20 September 2019

Sherif Ishola Mustapha, Usman Aliyu Mohammed, Faizal Bux, and Yusuf Makarfi Isa (2020). Simulation of Supercritical Water Gasification of Microalgae for Hydrogen and Methane-rich Gas Production. 18th JOHANNESBURG International Conference on Science, Engineering, Technology and Waste Management (SETWM-20), Johannesburg, South Africa, 16 – 17 November 2020.

U M Aliyu, S Rathilal**, S I Mustapha**, and Y M Isa (2020). Hydrothermal Synthesis and Characterization of Zeolite A from Grahamstown South Africa Kaolin. 18th JOHANNESBURG International Conference on Science, Engineering, Technology and Waste Management (SETWM-20), Johannesburg, South Africa, 16 – 17 November 2020.

S.I. Mustapha, F. Bux, Y.M. Isa (2021). Catalytic and non-catalytic pyrolysis of *Scenedesmus* sp. grown on nitrogen stressed condition for high-quality biofuel production. 10th International Conference on Algal Biomass, Biofuels & Bioproducts. Pittsburgh, PA, USA

AWARDS AND HONOURS

Best oral presentation at 18th JOHANNESBURG International Conference on Science, Engineering, Technology and Waste Management (SETWM-20), Johannesburg, South Africa, 16 – 17 November 2020.

LIST OF FIGURES

Figure 2.1 Technologies used for the production of biofuels from microalgae biomass ……..9

Figure 2.2 Outline of experimental methods used for characterization of microalgae .22

Figure 3.1 Schematic diagram of the experimental pyrolysis set-up ……..35

Figure 3.2 FTIR of *Scenedesmus obliquus* microalgae grown under different conditions ……42

Figure 3.3 (a) TGA (b) DSC plot of *Scenedesmus obliquus* microalgae grown under different conditions ……44

Figure 3.4 Product yields of the pyrolysis of microalgae samples at different reaction temperature ……46

Figure 3.5 Distribution of main compounds in pyrolytic bio-oils produced from *Scenedesmus obliquus* microalgae samples at 500 °C ……..50

Figure 3.6 ANN architecture used for the prediction of the bio-oil yield ……..52

Figure 3.7 Regression plots of predicted versus experimental bio-oil yield for the ANN model ……53

Figure 4.1 XRD patterns of the synthesized catalysts ……62

Figure 4.2 Thermogravimetric analysis (TGA) of the synthesized catalysts ……..63

Figure 4.3 SEM image of (a) HZSM-5 (b) Fe_3O_4-HZSM-5 (c) W/Fe_3O_4-HZSM-5 (d) Zr/Fe_3O_4-HZSM-5 (e) Co/Fe_3O_4-HZSM-5 (f) Mo/Fe_3O_4-HZSM-5 ……..64

Figure 4.4 Product yields during the catalytic and non-catalytic pyrolysis of *S. obliquus* microalgae (temperature: 500 °C, catalyst to biomass ratio of 1:1) ……..66

Figure 4.5 Distribution of main compounds in catalytic and non-catalytic pyrolytic bio-oils from *S. obliquus* microalgae (temperature: 500 °C, catalyst : biomass ratio 1:1) …..69

Figure 4.6 Effect of temperature on product yields obtained from pyrolysis of *S. obliquus* over Co/Fe_3O_4-HZSM-5 catalyst (catalyst to biomass ratio of 1:1) ……73

Figure 4.7 Effect of catalyst to biomass ratio on product yields obtained from pyrolysis of *S. obliquus* over Co/Fe_3O_4-HZSM-5 catalyst at 500 ^oC ……74

Figure 5.1 (a) XRD pattern (b) TGA/DSC (c) SEM image of HZSM-5 (d) SEM image of Zr/HZSM-5 ……87

Figure 5.2 Product distribution from HTL of nutrient stressed and unstressed *Scenedesmus obliquus* microalgae with and without Zr/HZSM-5 catalyst ……90

Figure 5.3 FTIR spectra of bio-oil produced from HTL of nutrient stressed and unstressed *Scenedesmus obliquus* microalgae with and without Zr/HZSM-5 catalyst at 300 °C and 350 °C ……..96

Figure 5.4 Distribution of main compounds in HTL bio-oils produced from nutrient stressed and unstressed *Scenedesmus obliquus* microalgae with and without Zr/HZSM-5 catalyst at 300 °C and 350 °C ……98

Figure 6.1 Aspen Plus flow diagram of the hydrothermal gasification model ……..107

Figure 6.2 Composition of product gases from the HTG of different algae samples at 500 °C, 36 MPa, and 5wt% biomass feed concentration ……..112

Figure 6.3 Effect of temperature at three different pressures on gas composition obtained from HTG of raw microalgae with 10 wt% biomass concentration ……..115

Figure 6.4 Effect of biomass concentration at different temperatures on (a) composition of H_2 and CH_4 (b) yield of H_2 and CH_4 obtained from HTG of whole algae (P = 30 MPa) ……..117

Figure 6.5 Effect of biomass concentration at different temperatures on lower heating value (LHV) obtained from HTG of *Scenedesmus obliquus* microalgae (P = 30 MPa) ...119

Figure A3.1 Bovine Serum Albumin (BSA) calibration curve…….……155

Figure A3.2 D-glucose calibration curve…….……155

Figure B4.1 EDS Analysis of the synthesized catalysts ……...161

LIST OF TABLES

Table 2.1 Basic gasification reactions ……19

Table 2.2 Some of the important correlation reported for determining HHV of microalgae ……25

Table 3.1 Properties of the *Scenedesmus obliquus* microalgae samples ……39

Table 3.2 Elemental analysis, atomic ratios and HHV of pyrolytic bio-oil at 500 °C and 600 °C ……..49

Table 4.1 Elemental analysis, atomic ratios and HHV of pyrolytic bio-oil at 500 °C .68

Table 5.1 Properties of the *Scenedesmus obliquus* microalgae samples ……84

Table 5.2 Elemental analysis, atomic ratios and HHV of HTL bio-oil from *Scenedesmus Obliquus* microalgae at 350 °C ……93

Table 6.1 Feedstock composition for the hydrothermal gasification process ……...105

Table 6.2 Description of Aspen plus unit operation blocks used in the simulation model ……...109

Table 6.3 Difference in experimental and Aspen simulation model results (Experimental data – Aspen model data) ……112

Table 6.4 Influence of operating conditions on LHV, yield, and composition of gaseous product using varying feed composition ……121

Table A3.1 Relative abundance (area %) of the main compounds of the pyrolytic bio-oil from N1 at 500 °C ……...152

Table A3.2 Relative abundance (area %) of the main compounds of the pyrolytic bio-oil from R-N1 at 500 °C ……..153

Table A3.3 Relative abundance (area %) of the main compounds of the pyrolytic bio-oil from N3 at 500 °C ……..154

Table B4.1 Relative abundance (area %) of the main compounds of the non-catalytic pyrolytic bio-oil at 500 °C ……..156

Table B4.2 Relative abundance (area %) of the main compounds of the catalytic pyrolytic bio-oil using W/Fe_3O_4-HZSM-5 at 500 °C ……..157

Table B4.3 Relative abundance (area %) of the main compounds of the catalytic pyrolytic bio-oil using Zr/Fe_3O_4-HZSM-5 at 500 °C ……158

Table B4.4 Relative abundance (area %) of the main compounds of the catalytic pyrolytic bio-oil using Co/Fe_3O_4-HZSM-5 at 500 °C ……..159

Table B4.5 Relative abundance (area %) of the main compounds of the catalytic pyrolytic bio-oil using Mo/Fe_3O_4-HZSM-5 at 500 °C ……..160

Table C5.1 GC-MS results of the HTL bio-oil from NSM at 300 ˚C …….162

Table C5.2 GC-MS results of the HTL bio-oil from NSM with a catalyst at 300 ˚C .163

Table C5.3 GC-MS results of the HTL bio-oil from CM at 300 ˚C …….164

Table C5.4 GC-MS results of the HTL bio-oil from CM with a catalyst at 300 ˚C …165

Table C5.5 GC-MS results of the HTL bio-oil from NSM at 350 ˚C ……..166

Table C5.6 GC-MS results of the HTL bio-oil from NSM with a catalyst at 350 ˚C ..167

Table C5.7 GC-MS results of the HTL bio-oil from CM at 350 ˚C …….168

Table C5.8 GC-MS results of the HTL bio-oil from CM with a catalyst at 350 ˚C …169

LIST OF ABBREVIATIONS

NSM	Nutrient Stressed Microalgae
CM	Control Microalgae
LEA	Lipid Extracted Algae
LHV	Lower Heating Value
HHV	Higher Heating Value
XRD	X-ray Diffractometer
HRSEM	High-resolution Scanning Electron Microscopy
EDS	Energy Dispersive Spectroscopy
TGA	Thermogravimetric Analysis
DSC	Differential scanning calorimetry
HTL	Hydrothermal Liquefaction
ANN	Artificial Neural Network
FTIR	Fourier-Transform Infrared Spectroscopy
BBM	Bold's Basal Medium
N	Nitrogen
HTG	Hydrothermal Gasification
SCWG	Supercritical Water Gasification
MC	Moisture Content
VM	Volatile Matter
FC	Fixed Carbon
ASE	Accelerated Solvent Extraction
BSA	Bovine Serum Albumin
TN	Total Nitrogen
N-P	Nitrogen-to-Protein
GC/MS	Gas Chromatography / Mass Spectrometer

NIST	National Institute of Standards and Technology
MLP	Multi-Layered Perceptron
MSE	Mean Square Error
PAH	Polycyclic Aromatic Hydrocarbons
PR-BM	Peng Robinson-Boston Mathias
IWWT	Institute of Water and Wastewater Technology
DUT	Durban university of Technology

CHAPTER 1

INTRODUCTION

Biofuels are considered as a sustainable and strategically important alternative fuel source to fossil fuels (Wu *et al.* 2012; Chen *et al.* 2015; Milano *et al.* 2016). They are important for a number of reasons; reduction of emission of greenhouse gases, improvement of air quality and finally as an alternative source of energy (Nigam and Singh 2011). Algae biomass is a highly regarded renewable energy resource and could potentially fulfil the global need for fuels in the future (Lam and Lee 2012; Vassilev and Vassileva 2016).

Over the last decade, extensive works have been carried out on biodiesel production from microalgal lipids using the transesterification process route (Cheng *et al.* 2014; Guldhe *et al.* 2014; Singh *et al.* 2014; Taleb *et al.* 2016). Most of the attention has been given to cultivation, improving lipid productivity, lipids extraction, and lipids conversion into biodiesel through transesterification. However, due to the prohibitive costs associated with its production process, the benefits of the microalgae to biodiesel technology with regards to the economic, social and environmental aspects have not been adequate to justify commercial-scale production of microalgal biofuel (Ziolkowska and Simon 2014; Bharathiraja *et al.* 2015; Ullah *et al.* 2015). It has been suggested that microalgae for biodiesel production may become more acceptable and competitive if considered along with the production of other important by-products from the residual algae. These by-products could be used as feed for animals, aquaculture, biofertilizers, biomethane and other bioproducts (Singh *et al.* 2014; Singh *et al.* 2015; Vassilev and Vassileva 2016). Thermal conversion is another microalgae conversion approach that is gaining increasing attention in recent years since the processing can be applied to whole microalgae and not just lipid extracts, and as a result, higher product yields have been demonstrated (Guo *et al.* 2019; Raheem *et al.* 2019; Lu *et al.* 2020; Xu *et al.* 2020; Brindhadevi *et al.* 2021; Liu,

Wang and Feng 2021; Lu *et al.* 2021). Although the thermal conversion option seems very promising, available data shows that the high content of nitrogen and oxygen-containing compounds in the microalgae bio-oil could limit its utilisation as a transportation fuel (Vassilev and Vassileva 2016). The presence of oxygenates and nitrogenates in the bio-oil can result in emission of NOx and also lower the calorific values. Hence, upgrading processes on the bio-oil such as denitrogenation and deoxygenation becomes necessary.

The use of different catalysts to enhance the processes of thermal conversion is one commonly used method to improve bio-oil yield and quality. However, the use of catalysts may result in an additional cost to the process without necessarily being able to address the problems caused by high nitrogen content. Another approach yet to be explored with the thermal conversion process may involve the use of nitrogen stressed condition to alter the biomass feedstock composition for improved bio-oil product yield and quality. Nutrient alterations during cultivation have been widely used for the improvement of lipid accumulation in microalgae. They are no doubt a preferred option due to its easy applicability at both laboratory and commercial-scale cultivation (Řezanka *et al.* 2011; Markou, Chatzipavlidis and Georgakakis 2012; Ikaran *et al.* 2015; Li *et al.* 2016). Among other nutrients, nitrogen and phosphorous alterations have been considered to be the most effective for the enhancement of lipid and consequently, could change the microalgae composition. Although both nitrogen and phosphorus stressing may result in a relative increase in carbohydrate and/or lipid content of microalgae, more attention is given to nitrogen alteration, especially for biofuel application via thermochemical conversion processes. Bio-oil with high content of nitrogen remains one of the biggest challenges affecting the fuel quality produced from thermal conversion processes and research efforts should be focused on developing strategies for improving the fuel quality. Some previous studies have shown that the most notable changes under nitrogen stressed condition involve

the enhancement of carbohydrates and/or lipids and reduction of protein (Griffiths, van Hille and Harrison 2012; Huang *et al.* 2013b; Depraetere *et al.* 2015; Liu *et al.* 2016). Most of the nitrogen in the bio-oil products are attributed to the protein content of the microalgae feedstock, and it is believed that the starting composition of nitrogen will have a great influence on product quality. Thus, nitrogen alteration is seen as an approach that could provide the needed solution towards developing efficient and sustainable thermal conversion process for quality biofuel production from various species of microalgae. This study explored the use of nutrient-stressed approach towards improving quality of microalgal bio-oils produced via thermal conversion processes. The search for catalyst with better characteristics for microalgae conversion is still ongoing. In this study, different multifunctional heterogeneous catalysts were synthesised and their performance during the thermal conversion of microalgae were investigated to identify catalysts that showed better activity in enhancing the quality and yield of bio-oil produced. The potential of using whole algae, lipid and residual algae of *S. obliquus* microalgae as feedstocks for production of high-quality hydrogen and methane-rich gas via hydrothermal gasification technique was also examined.

1.1 Aim and Objectives

The aim of this study focused on the thermal conversion of microalgae and its derivatives into biofuels and other co-products. This aim was set to be achieved through the following outlined objectives:

1. Characterization of lipids, lipid extracted biomass and whole cell algae grown under varying conditions to compare their composition.
2. Synthesis and characterization of zeolite-supported metal catalysts for application in the hydrothermal liquefaction process.

3. Synthesis and characterization of metal - based catalyst loaded on different supports for application in the pyrolysis process.
4. Establishing the optimum process conditions for the thermal conversion processes (pyrolysis, hydrothermal liquefaction and gasification) via optimization studies.
5. Using Artificial Neural Networks to predict production of biofuels and other co-products from microalgae based on feedstock composition and type of thermal conversion process.

1.2 Thesis Outline / Framework

This thesis comprises of seven (7) chapters which are outlines below:

Chapter 1: Introduction

Chapter 1 outlines the introduction and gives a brief overview of the topic, aim and objectives of the study, and the thesis framework.

Chapter 2: Literature Review

Chapter 2 gives an overview of technologies for converting microalgae and its derivatives to biofuels, providing more insights on the prospects of altering microalgae growth conditions and their effect on biomass composition, comprehensive microalgae biomass characterization techniques, recent progress on thermal conversion processes, and the role of catalyst in improving the thermal conversion processes.

Chapter 3: Pyrolysis of Nutrient Stressed Microalgae for High-Quality Bio-oil Production.

Chapter 3 focuses on the pyrolysis of nutrient stressed *S. obliquus* microalgae (N1) and its residual algae after lipid extraction (R-N1) at different temperatures (400 °C - 700 °C). Pyrolysis experiment on unstresed *S. obliquus* microalgae (N3) was also carried out

for comparison. Detailed characterization which includes proximate analysis, ultimate analysis, biochemical analysis, Fourier-transform infrared spectroscopy (FTIR) analysis, and thermogravimetric analysis (TGA/DSC) were carried out on the microalgae biomass (N1, R-N1 and N3) to provide useful information about the combustion behaviour of biomass during pyrolysis. A model based on artificial neural network (ANN) was developed to predict the yield of bio-oil produced from pyrolysis of microalgae.

Chapter 4: Catalytic Pyrolysis of Nutrient Stressed Microalgae for High-Quality Bio-oil Production

Findings from chapter 3 showed that the bio-oil from the nutrient stressed biomass (N1) was better in terms of quality and yield than R-N1 and N3 in all the experimental conditions. Hence, this chapter focuses on the use of catalyst to further enhance the quality of bio-oil obtained from nutrient-stressed *Scenedesmus obliquus* microalgae. In chapter 4, various metals (Zr, W, Co and Mo) supported on Fe_3O_4-HZSM-5 catalysts were applied in the pyrolysis of nutrient-stressed *Scenedesmus obliquus* microalgae. This study investigated the effect of various supported metal catalysts (Mo/Fe_3O_4-HZSM-5, Zr/Fe_3O_4-HZSM-5, W/Fe_3O_4-HZSM-5, and Co/Fe_3O_4-HZSM-5) on pyrolytic bio-oil quality and yield at temperature 500 °C using catalyst-to-biomass ratio 1:1. The synthesized catalysts were characterized by X-ray diffraction spectroscopy (XRD), thermogravimetric analysis (TGA), high-resolution scanning electron microscopy and energy dispersive spectroscopy (HRSEM/EDS). The catalyst: biomass ratio and temperature influence on pyrolysis product yield was also investigated. The target of this study is to aid in finding catalysts capable of enhancing the quality of pyrolytic bio-oils produced from microalgae.

Chapter 5: Catalytic Hydrothermal Liquefaction of Nutrient Stressed Microalgae for High-Quality Bio-oil Production

Chapter 5 presents the effect of Zr/HZSM-5 catalyst on product yield and quality during the HTL of *Scenedesmus obliquus* microalgae grown under nutrient-stressed condition. The Zr/HZSM-5 catalyst was synthesized using wet impregnation technique and characterization was conducted on the synthesized catalyst for its crystalline nature, morphology and thermal stability using X-ray diffractometer (XRD), High-resolution scanning electron microscopy (HRSEM) and thermogravimetric analysis/differential scanning calorimetry (TGA/DSC) respectively. The HTL experiments were conducted at reaction temperatures of 250 °C, 300 °C and 350 °C, with and without Zr/HZSM-5 catalyst. The HTL of unstressed microalgae with and without catalyst was also evaluated as control for comparison.

Chapter 6: Hydrothermal Gasification of Microalgae and its Derivatives

Chapter 6 aimed to evaluate the potential of using whole algae, lipid and lipid extracted algae of *Scenedesmus obliquus* microalgae as feedstocks for the production of high-quality hydrogen-rich and methane-rich gas via hydrothermal gasification technique. The effects of temperature (400-700 ºC), pressure (24-36 MPa) and biomass concentration (10-40%) on the yield and composition of the gaseous products were evaluated. The simulation model developed in this work will serve as a framework for predicting the yield and composition of gaseous products from HTG at any given microalgae feedstock composition and operating conditions.

Chapter 7: Conclusion and Recommendations

In chapter 7, the overall findings of the study and recommendations for further studies based on the outcome of the research are provided.

CHAPTER 2

LITERATURE REVIEW

2.1 Effect of Growth Conditions and Species Type on Microalgae Composition

As a novel resource, with the ability to generate large amounts of proteins, carbohydrates and lipids in a short period, microalgae has gained great attention. The production of biofuels as well as other useful co-products is the main reason for the attention to microalgae (Brennan and Owende 2010; Sambusiti *et al.* 2015; Chew *et al.* 2017). Several studies have shown that the composition of constituents of microalgae varies according to organisms, conditions of growth, source, and geographical location. For example, the composition of *Chlorella vulgaris* species was found to differ depending on the growth condition and the source of the strain of microalgae (Biller, Riley and Ross 2011; Xu *et al.* 2011; Wang *et al.* 2013; Gong *et al.* 2014).

Xu *et al.* (2011) cultivated *Chlorella vulgaris* in an open pond system equipped with an additional CO_2 supplier under standard nitrogen nutrient (0.150 kg/m^3) and low nitrogen (0.049 kg/m^3) nutrient condition. Comparatively, nitrogen stress conditions in microalgae resulted in reduced protein composition from 29 wt % to 6 wt %, while a significant increase was reported in the carbohydrate content (19.70 wt % to 51 wt %) resulting from low nitrogen nutrient in the growth media. Wang *et al.* (2013) further supports how growth conditions could affect the composition of the *Chlorella vulgaris* microalgae. They obtained a low lipid and high protein biomass by growing *Chlorella vulgaris* in Bold's Basal Medium (BBM) coupled with continuous illumination (338 µmol m^{-2} s^{-1}) at room temperature and constant CO_2 and air purging. The use of high nitrogen nutrient used during cultivation of microalgae could contribute to the high protein content, since protein accounts for the major intracellular nitrogen pools in microalgae (Sajjadi *et al.* 2018).

2.2 Biofuel Production from Microalgae Biomass

Previous studies focusing on sustainable biofuel production reveal that algae can be transformed into a broad spectrum of products depending on their composition and the conversion techniques employed (Debiagi *et al.* 2017; Sajjadi *et al.* 2018; Nagappan *et al.* 2019; Ramesh Kumar *et al.* 2019; Yang *et al.* 2019; Xu *et al.* 2020; Liu, Wang and Feng 2021). To achieve sustainability of the microalgae biofuel technology, two important areas have been identified, including the search for high biomass-productive microalgae strains and the development of sustainable conversion technologies. Numerous studies have focused on achieving high microalgae growth rate or improving lipid productivity by selecting strains and altering the cultivation conditions, which may result in different microalgae biomass composition (Yee 2015; Hu *et al.* 2016; Sibi, Shetty and Mokashi 2016; Singh *et al.* 2016; Taleb *et al.* 2016; Vlaskin *et al.* 2017). While research efforts towards improving biomass productivity are yielding positive results, choosing efficient downstream conversion technologies are crucial for any significant advancement. Presented in Figure 2.1 is an overview of technologies for the conversion of biomass from microalgae to biofuels.

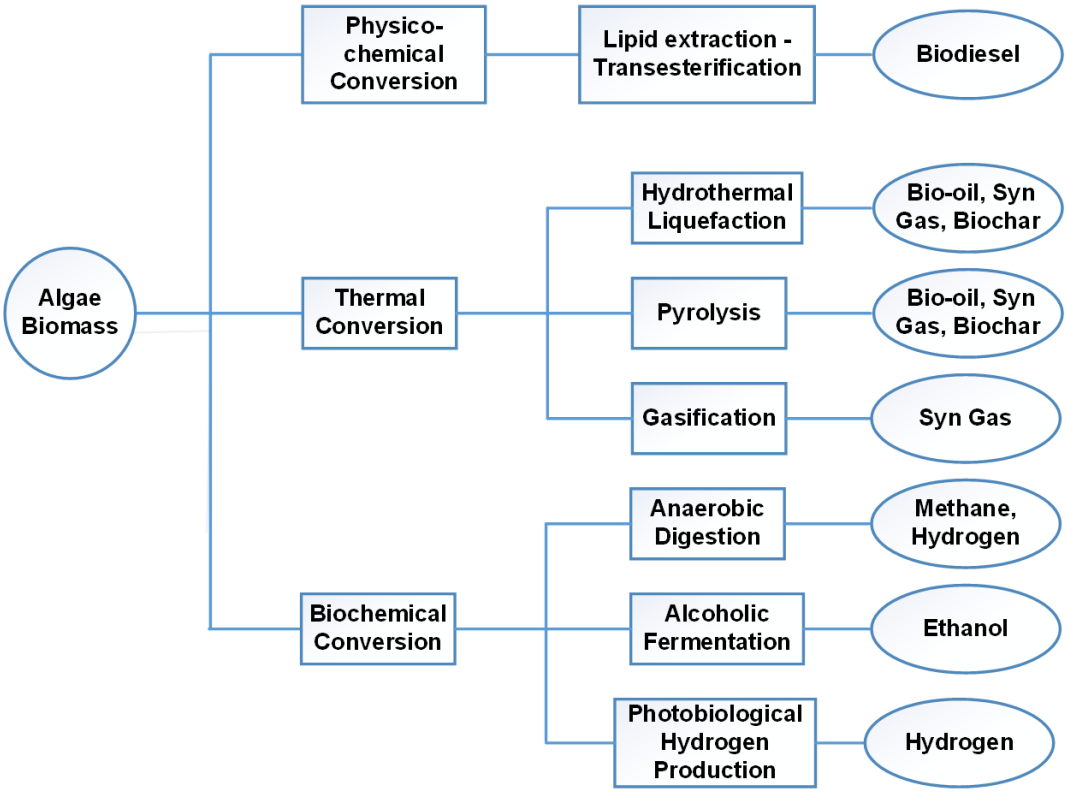

Figure 2.1. Technologies used for the production of biofuels from microalgae biomass (Adapted from Brennan and Owende (2010).

The commonly used downstream conversion technologies for microalgae to biofuel include chemical conversion (lipid extraction – transesterification), biochemical conversion and the thermal conversion processes as shown in Figure 2.1. Among the different conversion methods, the thermal conversion method is regarded as a more promising way of generating biofuels. Thermal conversion processing can be applied to whole microalgae, resulting in higher yields of biofuel products, and can generate other high-value products. Also, biomass feedstock varieties can be converted through the thermal processing route within a brief period. Whereas only lipids are converted to biodiesel in the chemical conversion process leaving behind large residual defatted algae unused (Brennan and Owende 2010). Also, the high costs associated with its production process could render the microalgal biodiesel technology less competitive to fossil fuel (Rashid, Rehman and Han 2013).

Albeit, it is believed that finding a use for the residual algae for other value-added applications can lower the cost of microalgal biodiesel production and result in economically beneficial algal technology (Ansari *et al.* 2015; Ansari *et al.* 2020).

Production of biofuels via biochemical conversion technique like fermentation requires several days and achieving sustainability towards commercialization is still very challenging (Nahak *et al.* 2011). Thus, thermal conversion technology is considered to be promising for the valorisation of microalgae to produce biofuel and other valuable co-product. However, the high nitrogen content in bio-oils produced via the thermal conversion processes is still far from the desired quality and is focused on seeking ways to increase the quality and yield of bio-oils. The next section presents the different thermal conversion and approaches to enhance the biofuel yield and quality were discussed.

2.3 Thermal Conversion Processes Using Microalgal Biomass as Feedstock

Thermal conversion requires the organic matter in microalgal biomass to be decomposed thermally, which can be accomplished through various methods, such as hydrothermal liquefaction, pyrolysis or gasification (Raheem *et al.* 2019; Xu *et al.* 2020; Brindhadevi *et al.* 2021; Lu *et al.* 2021). Bio-oils, biochars and gases are the primary products of pyrolysis and hydrothermal liquefaction of microalgae. While gasification process is mainly carried out to produce a mixture of syngas and some light hydrocarbons.

2.3.1 Hydrothermal Liquefaction (HTL) of Microalgae Biomass

Hydrothermal liquefaction (HTL) is an intriguing technique that produces bio-oil, biochar, water-soluble compounds and some gases using the whole biomass of microalgae in a wet state (Guo *et al.* 2015). HTL can be performed with or without a catalyst at a temperature range of (200-370 ºC) and a pressure range of (2-20 MPa) (Chiaramonti *et al.* 2017; Liu, Wang and Feng 2021). HTL is seen as the most appropriate thermal conversion

technique for aquatic biomass such as microalgae because it performed with the wet biomass, thereby eluding the drying step related energy costs (Barreiro *et al.* 2013b). When compared to the other thermal conversion methods such as pyrolysis, HTL is considered more efficient in the utilization of resources. For instance, HTL can lead to a reduction of energy needed by at least 50% and enables the separation and reusability of recovered nutrients for microalgae growth (Venteris *et al.* 2014). Furthermore, higher bio-oil yield and quality at lower energy consumption can be achieved with HTL compared to pyrolysis (Peterson *et al.* 2008). Despite the benefits, bio-oils created by hydrothermal microalgae liquefaction contain large quantities of nitrogen and oxygen compounds that need further processing before they can be used as a transport fuel (Gollakota, Kishore and Gu 2017). Just like other thermal conversion processes, various process parameters such as microalgae strains selection and composition, biomass concentration, reaction temperature, and catalysts can influence the HTL of microalgae (Guo *et al.* 2015).

Other studies have reportedly used different species of microalgae such as *Chlorella* sp., *Nannochloropsis* (Shakya *et al.* 2017b), *Spirulina* (Jena, Das and Kastner 2011), *Porphridium perpureum*, *Tetraselmis suecica*, *Scenedesmus* sp. (Barreiro *et al.* 2013b), *Botryococcus braunii* (Ren *et al.* 2018), *Aurantiochytrium* sp. (Vo *et al.* 2016) among others for HTL. The variation in the composition of the different microalgae strains may result in different HTL product distributions, bio-oil yield and quality.

Previous studies have shown that microalgal biomass concentration has an impact on the yield and quality of bio-oil, compared to the quality of the microalgal biomass. For instance, Jena, Das and Kastner (2011) found the optimum biomass concentration for *S. platensis* liquefaction to be 20 wt% and increasing the biomass concentration above the optimum no major impact on the yield of bio-oil was seen. Another researcher found that rising *Chlorella* sp. biomass concentration from 5-35 wt% increases bio-oil yield from 36-

46 wt% (Valdez *et al.* 2012). On the contrary, Zou et al. (2010) observed a decrease in bio-oil yield with an increase in biomass concentration Zou *et al.* (2010); hence the need for optimization studies to establish the optimum biomass concentration for each microalgae biomass becomes necessary. Considering from an engineering point of view and economic reasons, the preferred biomass concentration was suggested to be 15 - 20 wt% (Peterson *et al.* 2008).

In the HTL process of bio-oil production from microalgae, reaction temperature is an important factor. The optimum bio-oil yield for the HTL process reported from previous studies was found between 250 -375 ºC temperature range for microalgae biomass (Brown, Duan and Savage 2010; Jena, Das and Kastner 2011; Yu *et al.* 2011; Valdez *et al.* 2012; Yoo *et al.* 2015; Wądrzyk *et al.* 2018; Hu *et al.* 2019). Different temperature ranges are dominated by competing reactions, which influences the choice of temperature for optimal yield of bio-oil. For instance, hydrolysis usually dominates at low temperatures below 220 ºC but as the temperature increases, other reactions such as isomerization, reforming, depolymerization and repolymerization reactions occur which could result in higher bio-oil yield (Guo *et al.* 2015). The bio-oil quality is also found to be highly dependent on the temperature of the reaction. Yu *et al.* (2011) noted that with an increase in temperature, the hydrogen and carbon content increase in the bio-oil while the oxygen content was reduced. Although the authors did not provide information on the nitrogen distribution, however, with the knowledge that some of the nitrogen content is transferred to the aqueous phase during HTL process, the nitrogen content in the initial microalgae feedstock is projected to be greater than that contained in the bio-oil product due to the conversion of some of the nitrogen to the aqueous and gaseous product (Brown, Duan and Savage 2010). Although a slight reduction in nitrogen content in the bio-oil may be observed when compared to raw biomass due to transfer of N to the aqueous and gaseous phase, the value is however still

very high, suggesting that bio-oil produced from microalgae through the HTL will require further upgrading such as denitrogenation to make it suitable as transportation fuels. One of the most widely investigated approaches employed as a control strategy for addressing the problem of yield and quality of HTL bio-oils is the use of various catalysts.

2.3.1.1 Catalytic Hydrothermal Liquefaction

It has been shown that catalysts play an integral role in improving the yield and quality of bio-oil generated using microalgae by HTL. The use of catalyst has been shown in previous studies to have beneficial effects on the improvement of bio-oil yield and features such as oxygen content reduction and H/C ratio increase (Vlaskin *et al.* 2017). The commonly employed catalysts for the hydrothermal liquefaction of microalgae can be grouped into the homogeneous and the heterogeneous catalysts (Galadima and Muraza 2018).

Homogeneous catalysts which include hydroxides, carbonates and organic acids have been employed in the HTL of microalgae (Barreiro *et al.* 2013a; Yeh *et al.* 2013). The bio-oil yield is a function of the form of micro-algae species, the hydrothermal conditions and the catalyst used. Ross *et al.* (2010) used alkalis (Na_2CO_3, KOH) and organic acids (HCOOH, CH_3COOH) catalysts for hydrothermal liquefaction of *Spirulina* and *Chlorella* microalgae at 350 ^oC. The author's findings showed that the bio-oil yield observed in the presence of the studied catalysts is in the order Na_2CO_3 >CH_3COOH>KOH>HCOOH. In terms of denitrogenation efficiency, the alkalis catalysts performed better than the organic acids.

Due to their ease of separation, reusability and selectivity, heterogeneous catalysts are considered to be more promising for HTL of microalgae (Vlaskin *et al.* 2017; Galadima and Muraza 2018). Among the heterogeneous catalysts, the most widely considered for

microalgae hydrothermal liquefaction include zeolites, supported metals, SiO_2, Al_2O_3, and CoMo based catalyst (Biller, Riley and Ross 2011; Barreiro *et al.* 2013a; Xu *et al.* 2014). Due to their enhanced activity and selectivity properties, the application of zeolite catalyst systems has been the most common approach for bio-oil upgrading as well as for the liquefaction of microalgae biomass (Yeh *et al.* 2013; Xu *et al.* 2014; Dimitriadis and Bezergianni 2017). Xu *et al.* (2014) used Ce/HZSM-5 and HZSM-5 to catalyze the hydrothermal liquefaction of *Chlorella pyrenoidosa.* In the presence of H-ZSM-5 and Ce/H-ZSM-5, bio-oil yield of 32% has been reported without the use of catalyst and increased to 38% and 52%, respectively. Ma *et al.* (2019) studied the HTL of *Ulva prolifera* using Mordenite, ZSM-5 and Y-Zeolite, these are all zeolites based catalysts. In comparison with other zeolite catalysts, the ZSM-5 catalyst performed better in the yield of bio-oil achieved. Higher deoxygenation was obtained with the ZSM-5 catalyst with a maximum bio-oil yield of 29.3 wt%. In general, zeolites have shown to be promising catalysts for improving the properties and yield of bio-oil from the HTL of microalgae. However, deactivation of the zeolite catalysts could occur under hot compressed water due to the depletion of exposed active sites in the catalyst frameworks (Yeh *et al.* 2013). Both the degradation of zeolitic frameworks and pore blockage resulting from carbonaceous deposits have been identified as a possible challenge that could affect the catalyst efficiency. These challenges can be addressed in many ways that include phosphide or metals incorporation on the zeolite support and preparation of the zeolite catalyst in fluoride media (Galadima and Muraza 2018). More studies are required on catalytic HTL of biomass microalgae, especially to achieve denitrogenation and deoxygenation of the bio-oil product. Some other areas that demand further investigations include the search for better recyclable catalyst materials that are stable and can resist deactivation under the subcritical or supercritical water condition.

2.3.2 Pyrolysis of Microalgae Biomass

Pyrolysis is a conversion technique which thermally decomposes microalgae biomass in a reactor devoid of oxygen or air. Pyrolysis is operated between temperature range (400 – 700 ºC) and residence time (0 – 2 hr) with or without the addition of catalyst (Brennan and Owende 2010; Chiaramonti *et al.* 2015). The main pyrolysis products are; solids (which is the biochar), Liquid (bio-oil), and the non-condensable gases (fuel gas). The distribution of products depends largely on the microalgae species composition and conditions of reaction (Chen *et al.* 2015; Yang *et al.* 2019).

Different species of microalgae have reportedly been used as feedstock for pyrolysis. The microalgae species include *Chlorella* sp. (Babich *et al.* 2011; Du *et al.* 2011; Borges *et al.* 2014; Huang *et al.* 2017), *Spirulina* sp. (Chaiwong *et al.* 2013), *Chlorella vulgaris* (Thangalazhy-Gopakumar *et al.* 2012; Gong *et al.* 2014), *Spirulina platensis* (Jena and Das 2011), *Nannochloropsis* sp. (Pan *et al.* 2010), *Microcystis sp.* (Hu *et al.* 2013), *Saccharina japonica* (Ly *et al.* 2016), *Scenedesmus* sp. (Kim, Koo and Lee 2014), *Pavlova* (Aysu *et al.* 2017), *Tetraselmis chuii, Synechococcus, Chaetocerous muelleri, Dunaliella tertiolecta* (Grierson *et al.* 2009), and *Chlamydomonas reinhardtii* (Andrade *et al.* 2018). The product yields at different pyrolysis temperatures for different microalgae species are found to be in the ranges of 10.2 -64.9 wt% for bio-oil, 12.0 - 63.0 wt% for biochar and 2.70 - 60.0 wt% for the gas content. The varying composition from the different microalgae species and reaction temperatures are known to have a strong impact on the combustion behaviour during pyrolysis (Peng, Wu and Tu 2001; Peng *et al.* 2001; Vassilev *et al.* 2010). High combustion yield is more likely with microalgae biomass composition with high volatile matter content and low ash content (Vassilev *et al.* 2010). Proteins and carbohydrates have been found to decompose between 150 and 360 ºC, while lipid decomposition occurs between 330 and 560 ºC (Peng, Wu and Tu 2001; Peng *et al.* 2001).

The high content of nitrogen and oxygen in the fuel, which makes the bio-oil unfit and unstable to be directly used as transport fuels, is the major challenge associated with the pyrolysis process. Research efforts to address this obstacle are ongoing, and the use of catalysts and co-pyrolysis of microalgae with other feedstocks has been proposed as possible options (Fang *et al.* 2018; Xu *et al.* 2020). The use of catalysts on the pyrolysis of microalgae needs to be well understood for the development of optimal processing techniques.

2.3.2.1 Catalytic Pyrolysis of Microalgae Biomass

Solid heterogeneous catalysts have been investigated as catalytic materials for the improvement of the yield and quality of bio-oils produced from microalgae pyrolysis, such as zeolite-based materials, acidic metal oxides and basic oxides (Thilakaratne 2016). To date, biofuels generated from microalgae thermal degradation are still far from the fuel yield and quality required. In microalgal bio-oils, the oxygen and nitrogen content is still high, requiring a further upgrade process to boost bio-oil stability, prevent condensation and polymerization reactions (Liang 2013). Pyrolysis is a commonly used method in the presence of a catalyst to boost bio-oil production from microalgae and achieve higher bio-oil yields with less oxygenic compounds (Suali and Sarbatly 2012). Thangalazhy-Gopakumar *et al.* (2012) conducted catalytic pyrolysis of *Chlorella vulgaris* in a packed bed reactor using HZSM-5 as a catalyst. The researchers have found that with an increase in the catalyst to biomass ratio from zero to nine, there was an increase in the carbon yield of aromatic hydrocarbons from 0.9 to 25.8 wt%.

In another study, Borges *et al.* (2014) investigated the pyrolysis of *Nannochloropsis* and *Chlorella* sp. microalgae biomass in the presence of HZSM-5 catalyst. They found that pyrolysis of *Nannochloropsis* at a temperature of 500 ^{o}C and in the presence of catalyst gave an optimum liquid yield of 59 wt%. Wang and Brown (2013) investigated the fate of

nitrogen from *C. vulgaris* fast pyrolysis in the presence of HZSM-5 (catalyst: biomass ratio of 20:1) at 700 ºC. They found that in the bio-oil, the nitrogenated and oxygenated compounds completely vanished, but the yield of bio-oil also decreased significantly. Although the presence of HZSM-5 at very high temperature reduced the oxygen and nitrogen content, however, it was found to be at the expense of the bio-oil yield. Thus, it was suggested that pyrolysis be conducted below 600 ºC if the pyrolytic bio-oils are the preferred product.

Besides the use of HZSM-5 as a pyrolytic catalyst, activated carbon was reported by Fang *et al.* (2018) for the co-pyrolysis of *Chlorella* and waste tire. The authors concluded that the addition of waste tire could increase the hydrocarbon production but reduce the bio-oil yield. Huang *et al.* (2017) reported the use of magnetite (Fe_3O_4) and activated carbon (AC) as microwave receptor for pyrolysis of microalgae biomass. The mass ratio of microalgae and AC/Fe_3O_4 was maintained as 8:2, and the temperature was varied between 350 – 650 ºC. They found that the presence of composite AC/Fe_3O_4 during pyrolysis increased the bio-oil yield but have no effect on the bio-oil total nitrogen content. Other catalysts that have reportedly been used in the pyrolysis of microalgae include TiO_2, CeO_2, Co/TiO_2, Ce/TiO_2 and Ni supported catalyst (Aysu *et al.* 2017; Zainan *et al.* 2018). Nickel-based catalysts are reported to promote decarboxylation and decarbonylation reactions resulting in a higher amount of hydrocarbons. To date, no significant reduction in the nitrogen content of bio-oils has been reported with the presence of microalgae pyrolysis catalysts without significantly compromising the bio-oil yield. The nitrogen content of the pyrolysis bio-oil may be substantially reduced at a higher temperature. However, under this situation, at the cost of bio-oil yield, the gaseous product is favoured, which becomes another issue of concern if the chosen product is pyrolytic bio-oils.

2.3.3 Gasification of Microalgae Biomass

Microalgae can be processed either as wet or dry biomass. Based on the nature of microalgae, the gasification technique is in two categories: (1) traditional gasification (dry biomass) and (2) hydrothermal gasification (wet biomass).

In traditional gasification, in a partial oxidation environment, dry microalgae react with a gasifying agent, such as oxygen, steam, air, or water , and work at a known temperature (800-1000 ^{o}C) and pressure (1-10 bar) (Khoo *et al.* 2013). Many overlying sub-processes, such as dehydration or drying, devolatilization or pyrolysis, reduction and combustion/oxidation, constitute the gasification reaction. Therefore, during the traditional gasification, microalgae could undergo combinations of numerous reactions in the gasifier, as shown in Table 2.1. For instance, moisture content which is usually high for wet microalgae biomass is removed in the drying section of a gasifier. The volatiles content of the biomass is converted to light hydrocarbons, liquid long-chain hydrocarbons (tar), CO and CO_2 in the pyrolysis zone. The biomass is completely gasified in the reduction zone to produce syngas. This serves as the main process where biomass reacts with the gasifying agent (oxygen, air and/or steam) via a series of endothermic reactions as presented in Table 2.1 (Díaz-Rey *et al.* 2015; Sikarwar *et al.* 2017). Lastly, the residual char matrix is further burned in the combustion portion, providing more gaseous products and the requisite heat for the reduction zone reactions.

Table 2.1. Basic gasification reactions (Díaz-Rey *et al.* 2015; Sikarwar *et al.* 2017)

Name of reaction	Chemical Equation	$\Delta H^{o}_{r(298)}$[kJmol^{-1}]
Devolatilation	$Biomass + Q = Char + tar + gases(CO + CO_2 + H_2 + CH_4 + C_nH_m)$	Endothermic
Heterogeneous water gas	$C + H_2O = CO + H_2$	130.4
Water-gas shift	$CO + H_2O = CO_2 + H_2$	-41.2
Partial oxidation	$2C + O_2 = 2CO$	-246.4
Complete oxidation	$C + O_2 = CO_2$	-408.8
Hydrogasification	$C + 2H_2 = CH_4$	-75.0
Boudouard	$C + CO_2 = 2CO$	172.0
Steam reforming of methane	$CH_4 + H_2O = CO + 3H_2$	206.1
Dry reforming of methane	$CH_4 + CO_2 = 2CO + 2H_2$	247.3
Tar cracking	$Tar + Q = CH_4 + H_2 + H_2O + C_nH_m$	Endothermic
Tar steam reforming	$C_nH_m + nH_2O = nCO + \left(n + \frac{m}{2}\right)H_2$	Endothermic
Tar dry reforming	$C_nH_m + nCO_2 = 2nCO + \left(\frac{m}{2}\right)H_2$	Endothermic

The traditional gasification of coal and other low ash lignocellulose biomass is popular, and the technology has been commercialized (Chen *et al.* 2015; Bharath *et al.* 2018; Karatas and Akgun 2018; Lajili *et al.* 2018; Liu *et al.* 2018; Widjaya *et al.* 2018; Xiao *et al.* 2018). However, studies on the traditional gasification or co-gasification using microalgae as feedstock are still very limited. This area requires further study, particularly into the energy balance of biomass drying for gasification.

On the other hand, hydrothermal gasification sometimes referred to as supercritical water gasification (SCWG) is typically operated at temperature (400–700 ºC) and pressure (24–36 MPa) with or without the use of catalysts (Chen *et al.* 2015). SCWG works at lower temperatures than those used in conventional dry biomass feedstock gasification. This gasification technique (SCWG) is seen as a more promising pathway for wet biomasses such as microalgae. Higher thermal and gasification efficiency as well as low tar, have been reported via this route (Stucki *et al.* 2009; Miller *et al.* 2012; Onwudili *et al.* 2013; Duan *et al.* 2018). For instance, Onwudili *et al.* (2013) observed the highest hydrogen gas yield of 15.1 mol/kg from *Saccharina* a carbohydrate-rich macro-alga when three different algae (*Spirulina platensis*, *Chlorella vulgaris*, and *Saccharina latissima*) were tested under supercritical water gasification conditions at 500 ºC and 36 MPa. Also, the process waters derived from *Saccharina* conversion process can be reused as growth media for cultivation of microalgae. The variation in their biochemical composition could be attributed to the differences in product distributions from the three algae samples. *Saccharina*, a carbohydrate-rich macroalgae, was found to be more suitable for hydrothermal gasification than the microalgae of *Chlorella* and *Spirulina*, which could be better suited for the production of bio-oils. The possibility of achieving maximum gasification of *Spirulina platensis* microalgae into methane-rich gas in supercritical water with ruthenium as a

catalyst was demonstrated in another study by Stucki *et al.* (2009). They observed that the biomass recovered as methane had a heating value of about 60-70%.

The hydrothermal gasification of *Chlorella pyrenoidosa* microalgae via a two-component catalyst mixture of Ru/C and Rh/C has recently been studied by Duan *et al.* (2018). The influence of operating conditions such as reaction temperature (380-600 ^{o}C), water density (0-0.197 g/cm^3), and catalyst loading (0-20 wt%) on the composition and performance of the gaseous products was examined. The main gaseous products obtained include H_2, CH_4, CO, CO_2, and traces of C_2-C_3 hydrocarbons were also observed. From the study, temperature and water density have significant effects on the supercritical water gasification process. Specifically, carbon gasification efficiency was found to be more dependent on the water density, whereas hydrogen gasification efficiency was more dependent on the temperature. The gasification efficiency of hydrogen exceeded 100% during the supercritical water gasification process possibly due to hydrogen atoms transfer from biomass water content to the gaseous product. So far, studies on the gasification of microalgae under supercritical conditions are limited, and the commercial techniques are still underdeveloped. Therefore, this technology still needs substantial research and development in the direction of commercialization.

2.4 Microalgae Biomass Characterization Methods

The methods used in characterization of microalgae biomass include proximate, ultimate and compositional analyses (Naik et al. 2010; Bi and He 2013). Other tests include calorific value, Fourier-transform infrared spectroscopy (FTIR) analysis, thermogravimetric analysis (TGA/DSC) and scanning electron microscopy (SEM). An outline of characterization techniques for microalgae biomass is shown in Figure 2.2.

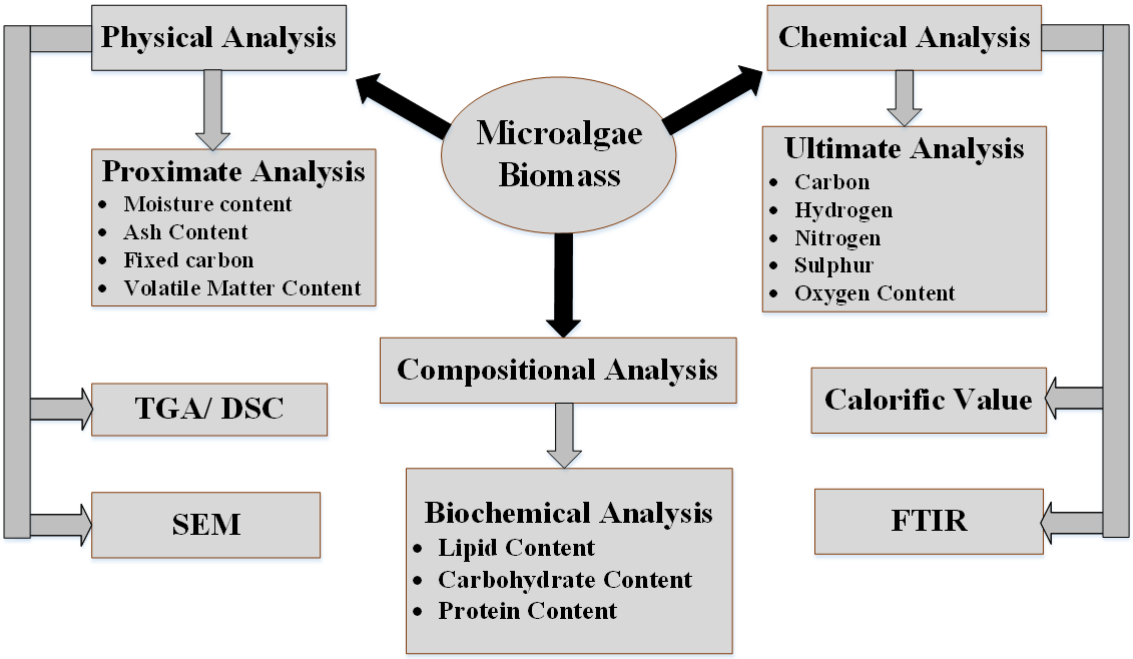

Figure 2.2. Outline of Experimental Methods used for Characterization of Microalgae

2.4.1 Proximate Analysis

Proximate analysis is one of the most important characterization methods when considering the thermal conversion of microalgae biomass. The results of the proximate analysis which include moisture content, ash content, volatile matter and fixed carbon content could help to understand the combustion behavior during the conversion process. Ash content can have a strong impact on the combustion rate in the biomass sample, transportation as well as handling and management costs of the process. Whereas, volatile matter/fixed carbon ratios are more related to the fuel's reactivity. Conventionally, proximate analysis can be determined using different international standards, such as ASTM E-830, D-1102, D-3174 or UNE-EN 14775 for ash content, ASTM E-871 for moisture content (MC) measure, ASTM E-872 and ASTM E-1755 for determination of volatile matter (VM) (Demirbas 2004; Sluiter *et al.* 2005; Khalil *et al.* 2008). The percentage of fixed carbon (FC) is usually determined by difference (FC = 100 – %MC – %VM – %Ash).

2.4.2 Ultimate Analysis

The ultimate analysis which is also known as the elemental analysis, is usually performed to determine the elemental composition of the sample (Bi and He 2013). The elemental analyzer is mostly used to determine the elemental composition (C, H, N, S, and O) of microalgae biomass as reported by many researchers (Ehimen *et al.* 2009; Jena *et al.* 2011; Biller *et al.* 2012). The fuel efficiency and quality largely depend more on the elemental ratio such as H:C, N:C and O:C.

2.4.3 Calorific Value (Heating Value)

The heating value of any fuel is the amount of heat produced by the complete combustion of the fuel per unit mass or unit volume of the fuel and can be expressed in terms of lower heating value (LHV) or higher heating value (HHV) (Singh, Mahanta and Bora 2017). The HHV refers to the condition where water is condensed out of the combustion products. While the LHV refers to the condition where water vapour remains in the combustion product. The calorific value of a material can be measured using bomb calorimeter (Phukan *et al.* 2011). Some researchers make use of the proximate and elemental analysis to estimate the calorific value based on established empirical correlations (see Table 2.2). Dulong correlation (Mott and Spooner 1940; Selvig 1945) have been reportedly used for estimating the HHV of the microalgae biomass and biofuel based on their respective elemental analysis (Huang *et al.* 2013a; Ly *et al.* 2016; Wang, Sheng and Yang 2017; Yan *et al.* 2017). Another correlation proposed by Friedl *et al.* (2005) was used by Maddi, Viamajala and Varanasi (2011) to determine the HHV of microalgae biomass. Recently, Odetoye *et al.* (2018) used the correlation proposed by Channiwala and Parikh (2002) for estimating the HHV of agricultural biomass and the same correlation was recently reported by Rahman, Fermoso and Sanna (2018) for determining the HHV of a microalgae biomass.

The correlation makes use of the results obtained from the elemental analysis and ash content, expressed in terms of their weight percentages.

Table 2.2. Some of the Important Correlation Reported for Determining HHV of Microalgae

Correlation	Expression	Reference
Dulong (1940)	$HHV = 0.338C + 1.428\left(H - \frac{O}{8}\right) + 0.095S$	(Ly *et al.* 2016; Wang, Sheng and Yang 2017; Yan *et al.* 2017)
Channiwala and Parikh (2002)	$HHV = 0.3491C + 1.1783H + 0.1005S - 0.1034O - 0.0151N - 0.0211Ash$	(Rahman, Fermoso and Sanna 2018)
Friedl et al. (2015)	$HHV\ (OLS) = 1.87C^2 - 144C - 2802H + 63.8C * H + 129N + 20147$ $HHV\ (PLS) = 5.22C^2 - 319C - 1647H + 38.6C * H + 133N + 21028$ $HHV = \frac{HHV(OLS) + HHV(PLS)}{2}$	(Maddi, Viamajala and Varanasi 2011)

2.4.4 Biochemical Composition of Microalgae Biomass

2.4.4.1 Determination of Lipid Content in Microalgae

The main methods used for lipid extraction can generally be classified into solvent extraction methods, mechanical methods, solvent-free methods and combination methods (Ranjith-Kumar, Hanumantha Rao and Arumugam 2015). At present, solvent extraction methods are most commonly used for lipid extraction as they provide high lipid recovery. The utilization of single organic solvent or combined solvent mixtures for efficient lipid extraction from microalgal biomass has been an important area of interest to many researchers due to its ease of operation and potential to scale-up for industrial application (Ranjith-Kumar, Hanumantha Rao and Arumugam 2015; Al-Ameri and Al-Zuhair 2019). The Bligh and dyer's (Bligh and Dyer 1959) and Folch (Folch, Lees and Stanley 1957) extraction methods are considered to be the most widely used solvent extraction technique for lipid extraction (Rawat *et al.* 2011; Samarasinghe and Fernando 2015). The Folch method employs the use of chloroform-methanol (2:1 v/v) for extraction of lipids from microalgae cells while the Bligh and Dyer method is done by extracting lipids from homogenized cell suspension using 1:2 (v/v) chloroform/methanol. Accelerated solvent extraction (ASE) process, using heat or pressure, has also been used to achieve better lipid recovery, shorten process time, and recover solvent for re-use (Cooney, Young and Nagle 2009). Many improved solvent extraction methods as well as combined solvent/physical extraction systems are being researched across the globe; however, the highly toxic nature of these solvents is still a concern, especially for industrial scale application (Ghasemi Naghdi *et al.* 2016; Kumar *et al.* 2017b).

The use of mechanical methods presents an effective approach because of less dependence on the type of microalgae species to be processed and they are also less likely to

cause contamination of the extracted lipid product. Some of the mechanical extraction processes that do not necessarily require solvent assistance include microwave-assisted extraction (Du *et al.* 2011; Zhou *et al.* 2019), ultrasound-assisted extractions (Jeevan Kumar and Banerjee 2019; Sallet *et al.* 2019), bead mills (Richmond 2004; Meullemiestre *et al.* 2016), and expeller press procedure (Ramesh 2013). The use of mechanical methods, though environment-friendly and cheap, is not a wise option because of poor recovery and the possible degradation of lipids due to the heat generated during mechanical disruptions. Furthermore, high energy and equipment costs and the need for the provision of a cooling system during the extraction of heat sensitive products will also heighten the process cost (Lee, Lewis and Ashman 2012).

2.4.4.2 Determination of Carbohydrate Content in Microalgae

The main component in the carbohydrates of microalgal cells is starch, and some microalgae species such as *Chlorella*, *Dunaliella*, *Chlamydomonas* and *Scenedesmus* have been reported to accumulate up to 50% carbohydrates based on their dry cell weight under appropriate cultivation conditions (Chen *et al.* 2013). For quantification of total carbohydrate content, some colorimetric procedures like phenol-based (Dubois *et al.* 1956) or anthrone-based (Morris 1948) methods are available, giving good and robust results in a very short time. Also, some researchers have reportedly determined total carbohydrate content from the results obtained from the proximate analysis, the lipid and protein content analysis using the equation 2.1 as reported by (Huang *et al.* 2013a) or When expressed in terms of percentage carbohydrate mass fraction (Wang *et al.* 2013; Gong *et al.* 2014) as shown in equation 2.2:

$$Total\ carbohydrate\ (wt\%) = volatile\ matter\ (wt\%) - (crude\ protein + crude\ lipid)\ (wt\%) \quad (2.1)$$

$$\%mf_{carbohydrate} = 100 - \%mf_{protein} - \%mf_{lipid} - \%mf_{moisture} - \%mf_{ash} \qquad (2.2)$$

2.4.4.3 Determination of Protein Content in Microalgae

The common methods identified to have been used in quantification of protein content in microalgae include Lowry's method (González López *et al.* 2010; Phukan *et al.* 2011; Slocombe *et al.* 2013; Kassim *et al.* 2014; Ansari *et al.* 2017), Bradford's method (Barbarino and Lourenço 2005; Geun Goo *et al.* 2013; Chia *et al.* 2015; Guldhe *et al.* 2016), and the use of nitrogen to protein conversion factor (Ho *et al.* 2013; Grossmann *et al.* 2018). The bovine serum albumin (BSA) remains the most commonly used protein standard for calibration curves in spectrophotometry (Phukan *et al.* 2011). In the case of the use of nitrogen to the protein conversion factor for estimation the protein content, the total nitrogen content (TN) is relatively simple to measure and the nitrogen-to-protein factors (N-P factors) can then be used to determine the crude protein content. The total nitrogen (TN) analysis can be carried out by Kjeldahl's method (Kelrich 1990), Hach techniques (Hach 1987) or directly using the CHN/S elemental analyser and subsequently the TN is converted to crude protein using the conversion factors. The use of conversion factors allows for protein estimation without a demanding extraction process and possible losses of protein are avoided. The conventional conversion factor used to calculate protein content is 6.25 and this is found to be suitable for microalgae and several other materials. Although the conversion factor of 6.25 is found suitable for estimating crude protein in microalgae (Sajjadi *et al.* 2018), care must be taken in the use of conversion factor for other plant materials and fungi.

2.4.5 Thermogravimetric Analysis (TGA) of Microalgae Biomass

Prior to the thermal conversion of microalgae biomass, thermogravimetric analysis (TGA) is usually conducted on the biomass feedstock to understand its thermochemical profile at different temperatures. Thermogravimetric analysis (TGA) can be used to understand the thermal behaviors of microalgae biomass (Mani *et al.* 2010; Qi *et al.* 2018; Sotoudehniakarani, Alayat and McDonald 2019). TGA study is useful for understanding pyrolysis degradation processes and the mechanisms involved.

2.4.6 Fourier-Transform Infrared Spectroscopy (FTIR) Analysis of Microalgae Biomass

The Fourier-transform infrared spectroscopy (FTIR) analysis are conducted to know about the functional groups present in microalgae biomass during the thermal conversion processes. The identified functional groups could give an indication of the components present in the sample and this characterization technique finds application to both solid and liquid samples (bio-oil).

2.4.7 Scanning Electron Microscopy (SEM) of Microalgae Biomass

Scanning electron microscopy (SEM) provides good visual images of possible microalgal cell structure and/or morphology changes after treatment, such as drying, lipid extracted algae, and it has been used to examine the biochar surface structure after thermal conversion processes (Suárez-Garcıa *et al.* 2002). For instance, Bi and He (2013) used SEM analysis to investigate the effect of different drying method and different lipid extraction method on mixed marine green microalgae. The SEM images showed that both the Soxhlet and Bligh-Dyer extractions method do not significantly impact the cell structure of the microalgae biomass. However, the microalgal cells after different drying processes show considerably different structures.

CHAPTER 3

PYROLYSIS OF NUTRIENT-STRESSED MICROALGAE FOR HIGH-QUALITY BIO-OIL PRODUCTION

3.1 Introduction

Pyrolysis of microalgae for biofuel production has gained attention among researchers owing to the application of the process to whole microalgae and production of higher yield of biofuel product (Ly *et al.* 2016; Aysu *et al.* 2017; Huang *et al.* 2017). However, high nitrogen content in the bio-oil product remains a major challenge limiting the direct use of pyrolytic bio-oil as transportation fuels (Vassilev and Vassileva 2016; Yang *et al.* 2019). High amounts of oxygen and nitrogen compounds in the bio-oil usually lower the calorific values and also result in NOx emissions (Du *et al.* 2011). Hence, upgrading processes towards reducing the nitrogen content of the bio-oil product becomes necessary.

Microalgae subjected to pyrolytic reaction using a suitable catalyst is a novel approach to enhance the quality of bio-oil, especially the reduction of oxygen content resulting in bio-oil product of higher calorific value (Suali and Sarbatly 2012; Wang and Brown 2013; Aysu *et al.* 2017). Some studies have also shown that specific product selectivity could be enhanced with the use of catalyst (Bennett *et al.* 2017; Dimitriadis and Bezergianni 2017). Aysu *et al.* (2017) studied pyrolysis of *Pavlova* sp. over Ce/Al_2O_3-based catalyst and concluded that use of catalysts increased the bio-oil yield with reduction of oxygen content in bio-oil relative to the non-catalytic process. They also observed nitrogen was removed from the catalytic bio-oils to the gas phase in the form of ammonia as well as hydrogen cyanide. In a related study, Wang and Brown (2013) reported the complete disappearance of nitrogen and oxygen containing compounds from the pyrolytic bio-oil produced at 700 ºC with HZSM-5 catalyst, but the bio-

oil yield significantly decreased. Some other catalysts such as TiO_2, CeO_2, Co/TiO_2, Ce/TiO_2 and Ni supported catalyst have been applied to pyrolysis of microalgae (Borges *et al.* 2014; Aysu *et al.* 2017; Zainan *et al.* 2018; Yang *et al.* 2019). Thus, pyrolysis of microalgae via catalytic route did not decrease the nitrogen content in the bio-oil without greatly affecting the yield of the bio-oil. At temperature beyond 700 °C, the nitrogen content could be greatly reduced but at the expense of bio-oil yield, which becomes another issue of concern if the pyrolytic bio-oils are the preferred product.

Another promising approach may involve the use of nitrogen alteration to manipulate the microalgae composition before the pyrolysis of the biomass. Previous studies have shown that the most notable changes under nitrogen stressed condition involve the enhancement of lipids and/or carbohydrates and reduction of protein (Griffiths, van Hille and Harrison 2012; Huang *et al.* 2013b; Depraetere *et al.* 2015; Liu *et al.* 2016). Under nitrogen stressed condition, an increase of high-energy store compounds in the form of carbohydrates, and/or neutral lipids can be achieved (Lamers *et al.* 2012). The increase in the stored high-energy compounds was linked to some changes in the processes of metabolism as a response to the decline of needed nutrient (Sajjadi *et al.* 2018). The amount of nitrogen nutrient used during cultivation could have a direct influence on the quality of pyrolytic bio-oil. This is because protein accounts for the major intracellular nitrogen pools in microalgae and most nitrogen product in bio-oils possibly emanate from protein content of the microalgae (Sajjadi *et al.* 2018). Thus, nitrogen alteration with a possible reduction in protein content as well as the increase in lipid and/or carbohydrate is seen as an approach that can improve the quality of pyrolytic bio-oil obtained from microalgae species.

3.2 Materials and Method

3.2.1 Raw Materials and Chemical Reagents

Scenedesmus obliquus microalgae grown under nitrogen stressed condition (N1) was collected from the Institute of Water and Wastewater Technology, Durban University of Technology, Durban, South Africa. The cultivation of algae was done in a 3000-litre capacity open raceway pond using a modified BG 11 media with reduced nitrogen (150 mg/L). Residual algae after lipid extraction from the N1 biomass was obtained and referred to as R-N1. Another sample of *Scenedesmus obliquus* microalgae was grown using the full BG 11 media as a control sample (N3) for comparison. The dried microalgal biomass flakes obtained from both N1 and N3 samples were crushed to power form using single 5 MT industrial blender and sieved to a particle size of <125µm, and later kept in air tight bag for further analysis.

Chloroform (ACS reagent, ≥ 99.8%) and methanol (ACS reagent, ≥ 99.8%) used for lipid extraction were supplied by Sigma-Aldrich®. The N_2 gas (99.995%, purity) used during the pyrolysis process was obtained from Afrox®. D-glucose (≥ 99.5% purity) and Bovine serum albumin (BSA) (≥ 98% purity) were purchased from Sigma-Aldrich®. All chemicals were of analytical grade and used without further purification.

3.2.2 Characterization of Microalgae Samples

3.2.2.1 Proximate, Ultimate and Biochemical Composition of the Microalgae Biomass

The proximate, ultimate and biochemical analysis, thermogravimetric analysis/differential scanning calorimetry (TGA/DSC) and Fourier-transform infrared spectroscopy (FTIR) analysis of the microalgae biomass samples, were carried out. Elemental analyzer (Vario EL-II Elementar Analysensysteme GmbH, Hanau, Germany) was used for the

ultimate analysis of the samples. Based on elemental composition of the microalgae, the Dulong correlation (Equation 3.1) was used to estimate the biomass higher heating value (HHV) (Saber *et al.* 2016).

$$HHV\left(\frac{MJ}{kg}\right) = 0.338C + 1.428\left(H - \frac{O}{8}\right) + 0.095S \quad (3.1)$$

C, H, O, and S depict weight percentage of carbon, hydrogen, oxygen, and sulphur in the microalgae biomass, respectively.

The proximate analysis, which comprises moisture content, volatile matter and ash content of the microalgae samples were determined according to ASTM standards (E-871), (D1102), and (E872) respectively.

For the biochemical composition of the biomass, lipids content was determined according to the procedure described by Ansari *et al.* (2017) with little modification. The dried biomass samples were mixed with an equal volume (1:1 v/v) of chloroform and methanol and the lipid fraction subsequently separated from the biomass residue using GF/C filter. After that, the rotary evaporator was employed to get rid of the solvent from the lipid fraction and the recovered lipids were determined by gravimetry method. Lowry's method was employed for the extraction of total protein as described by González López *et al.* (2010). The mixture absorbance was measured at 750 nm using spectrophotometer (SpectroquantPharo 300, Merck). Protein quantification was estimated from the calibration curve prepared with bovine serum albumin (BSA) standard (Figure A3.1). The phenol-sulfuric acid method was adopted for estimating the total carbohydrates in the biomass (Ansari *et al.* 2017). The absorbance of the solution set at 490 nm was measured using spectrophotometer (SpectroquantPharo 300,

Merck). Quantification of the total carbohydrates content was carried out using calibration curve prepared with D-glucose standard (Figure A3.2).

The functional groups of samples (N1, R-N1, N3) were obtained using FTIR (model Bruker Vertex 70 spectrometer, Bruker Optics, Billerica, MA, USA) equipped with a Platinum ATR sampling module. FTIR spectra range of 400–4000 cm^{-1} was selected at a resolution of 4 cm^{-1}. Thermogravimetric analysis/differential scanning calorimetry (TGA/DSC) was carried out on the biomass samples (N1, R-N1, N3) using TA instrument (SDT Q600) to analyze their decomposition behaviour. The samples were heated under N_2 atmosphere at rate of 10 ^oC/min from 25 ^oC to 800 ^oC.

3.2.3 Pyrolysis Experiments

The nitrogen-stressed *Scenedesmus obliquus* microalgae (N1) and its residual algae after lipid extraction (R-N1) were used as feedstock for the pyrolysis experiment. The pyrolysis of the unstressed algae (N3) was also carried for comparison. A stainless steel reactor with the following specifications (length = 450 mm, inner diameter = 10.6 mm and outer diameter = 12.7 mm) heated in an electric furnace with the temperature measured by K type thermocouple placed in the reactor was used to carry out the pyrolysis experiment. Figure 3.1 is the schematic diagram of the pyrolysis experiment and procedure by Chaiwong *et al.* (2013) was adopted for the pyrolysis experiments. The reactor was in vertical configuration and quartz wool was used to immobilize the microalgae feedstock as well the biochar left after pyrolysis. Prior to pyrolysis, the biomass was dried at 105 ^oC until constant weight was achieved. 1g each of the dried microalgae biomass sample was used, and the whole reactor system was first purged with N_2 for 30 min at 30 mL/min flow rate to get rid of residual air in the system and ensure inert atmosphere. The pyrolysis tests were performed as follows: Firstly the reactor was heated at

10 ^{o}C/min until the temperature reaches the set temperature between 400 and 700 $^{\circ}$C and held for 60 min. Thereafter, the sweeping gas was allowed to continue to flow until the vapour in the reactor condensed and kept at 0 ^{o}C. The biochar was left in the reactor while condensed liquid product (bio-oil) was collected into the storage flask. After allowing reactor to cool to room temperature, the solid residue was recovered from the reactor. The bio-oil was recovered by washing the collection flask with acetone after complete reaction time. Also, the residual bio-oil or biochar that might be stuck on the side of the reactor was recovered by washing the reactor with acetone. Then, evaporation of acetone from the bio-oil was done at 60 ^{o}C for 12 h, and the bio-oil obtained was measured gravimetrically. The yield of bio-oil and biochar recovered from a known weight of the dry biomass was determined. The non-condensable gases with any other losses were calculated by difference (gas yield = 100 – (bio-oil yield + biochar yield)). All the pyrolysis experiments were repeated twice and the mean values reported.

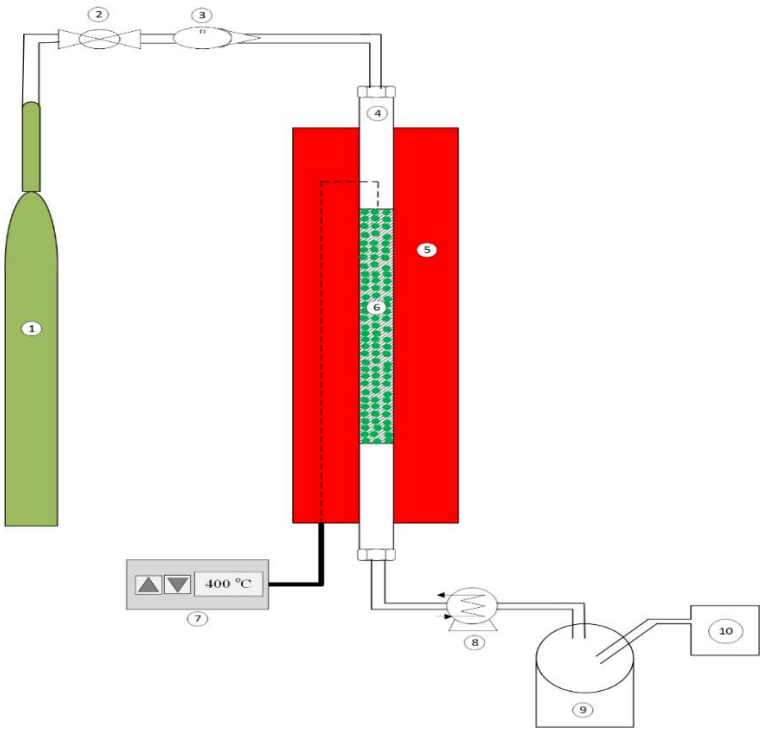

Figure 3.1. Schematic diagram of the experimental pyrolysis set-up: (1) Nitrogen cylinder, (2) Nitrogen controller valve (3) Rotameter (4) Reactor (5) Furnace (6) Algae biomass (7) Furnace temperature controller (8) Condenser (9) Bio-oil storage (10) Gasbag

3.2.4 Bio-oil Analysis

The gas chromatography / mass spectrometer (Agilent 7890-5975C) was used to determine the chemical constituents of the produced pyrolytic bio-oils under the following measurement conditions: DB-1701 column; Helium as carrier gas at flow rate of 1.76 mL/min; 1 µL injection size; and 1: 60 split ratio. Starting GC oven temperature was kept at 42 °C for 1 min; then the temperature was increased to 300 °C at a rate of 5.5 °C/min and held for 10 min; Scan mode (35.00 to 550.00 m/z); injector and detector temperature of 220 °C and 250 °C respectively. The compounds were identified using the National Institute of Standards and Technology (NIST) mass spectral data library. Furthermore, the elemental composition of the bio-oils produced was determined using an elemental analyzer (Vario EL-II Elementar Analysensysteme GmbH, Hanau, Germany) and bio-oils higher heating value (HHV) were estimated using the earlier mentioned Dulong correlation (Equation 3.1).

3.2.5 Development of Predictive Model for Pyrolytic Bio-oil Yield using Artificial Neural Network (ANN)

The predictive model for the pyrolysis bio-oil yield based on the composition of the feedstock (H/C, N/C and O/C) and temperature (T) was developed using artificial neural network (ANN) toolbox of MATLAB R2015a (Mathworks, Inc., Natick, MA, USA). To obtain desired model, the data set was classified into three categories: 70% (for training), 15% (for validation), and lastly 15% (reliability test of the model). A multi-layered perceptron (MLP)

feed forward neural network was employed using back-propagation based on Levenberg-Marquardt algorithm. The ANN framework with input layer of four neurons (H/C, N/C, O/C, T), an output layer of one neuron (Bio-oil yield), and a hidden layer was employed. The number of neurons in the hidden layer of the MLP was evaluated through identification of the number of neuron with a minimum mean square error (MSE) value from a range of neuron numbers tested (Adetiba and Olugbara 2015). The hyperbolic tangent sigmoid (tansig) was utilized as the transfer function for input layer to hidden layer mapping and hidden layer to output layer mapping. The following equations (3.2) – (3.4) were employed in developing the ANN model (Soji-Adekunle *et al.* 2018).

$$x = w^h v + b^h \tag{3.2}$$

$$g(t) = tansig(t) = \frac{1-e^{-t}}{1+e^{-t}} \tag{3.3}$$

$$y = w^{out} f(x) + b^{out} \tag{3.4}$$

where x stands for hidden layer output, w^h represent the hidden layer weight, v is the vector of network input, b^h stands for hidden layer bias, g(t) is the activation transfer function, y is the network output, w^{out} is the output layer weight, and b^{out} is the output layer bias.

3.3 Results and Discussion

3.3.1 Characterization of Microalgae Samples

3.3.1.1 Proximate, Ultimate and Biochemical Composition of the Microalgae Biomass

The results of the proximate, ultimate and biochemical composition of the nutrient stressed *Scenedesmus obliquus* microalgae (N1), the residual algae from N1 (R-N1) and the full BG 11 media grown *Scenedesmus obliquus* microalgae (N3) are presented in Table 3.1. When

compared with the N1 biomass, the N3 biomass have a lower lipid content and higher protein content. The relatively low lipid content (17.16 wt%) of the N3 biomass made this microalga not too suitable for biodiesel production. Likewise, its high protein content (42.35 wt%) will also have impact on pyrolytic bio-oil quality owing to high nitrogen composition in the bio-oil product. Koley et al. [26] also reported high protein content (56.1 wt%) for *Scenedesmus obliquus* microalgae. Under nitrogen stressed condition (N1), the lipid content (21.62 wt%) was slightly increased, and the protein content (22.08 wt%) decreased compared to N3. This is an indication that the N1 biomass could be the ideal for producing high-quality pyrolysis bio-oil, especially with the reduced protein content. It is believed that the starting nitrogen composition in the feedstock will have a great influence on pyrolysis product quality since most of nitrogen compounds found in the pyrolysed bio-oils are attributed to the protein content of the microalgae feedstock (Yang *et al.* 2019). The lipid composition of residual algae (R-N1) was 5.71 wt% while the protein content (24.31 wt%) was found to be significantly lower when compared to the N3 biomass and suggest R-N1 algae could be potentially suitable for pyrolysis. The use of residual algae (R-N1) as feedstock for pyrolysis can provide a reasonable alternative for converting waste algae to high-value products.

Table 3.1. Properties of the *Scenedesmus obliquus* microalgae samples

	Nitrogen stressed microalgae (N1)	Residual Algae after lipid extraction (R-N1)	Control microalgae (N3)
Biochemical composition (wt%)			
Lipid	21.62	5.73	17.16
Protein	22.08	24.31	42.35
Carbohydrate	42.55	56.38	25.36
Proximate Analysis (wt%)			
Moisture	4.38	5.98	10.05
Ash	10.17	11.42	14.91
Volatile matter	81.77	80.98	73.26
Fixed carbon (by difference)[a]	3.68	1.62	1.78
Ultimate Analysis (wt%)			
C	45.03	43.51	43.25
H	7.50	8.55	8.46
N	3.59	3.89	6.83
S	0.98	0.46	0.63
O (by difference)[b]	42.90	43.59	40.83
H/C	2.00	2.36	2.35
N/C	0.07	0.08	0.14
O/C	0.71	0.75	0.71
Heating value (MJ/kg)			
HHV	18.37	19.18	19.47

[a] Fixed carbon content (%)= 100% - (%moisture content + %Ash + % volatile matter)

[b] O composition (%) = 100% - %C + %H + %N + %S

According to Table 3.1, it can be noticed that the volatile and ash content of the nutrient stressed algae (N1) were 81.77 wt% and 10.17 wt% respectively. The residual algae (R-N1)

showed very close volatile content (80.98 wt%) and ash content (11.42 wt%) compared to the N1 algae. However, lower volatile content (73.26 wt%) and higher ash content (14.91 wt%) was observed with the N3 algae when compared to N1 and R-N1. The higher volatile content and lower ash content observed with both N1 and R-N1 indicate the potential of higher conversion of bio-oil by pyrolysis. High volatile and low ash content in biomass strongly determined the thermal properties and provide information about the potential bio-oil yield (Phukan *et al.* 2011; Rahman, Fermoso and Sanna 2018). The elemental composition of the microalgae biomass (N1, R-N1 and N3) are also shown in Table 3.1. The empirical formula for N1, R-N1 and N3 microalgae biomass are $CH_{2.00}N_{0.07}O_{0.71}$, $CH_{2.36}N_{0.08}O_{0.75}$, and $CH_{2.35}N_{0.14}O_{0.71,}$ respectively. Due to its high protein content, higher nitrogen content was observed with N3 (6.83) when compared to N1 (3.59) and R-N1 (3.89). As shown in Table 3.1, higher O/C (0.75) was observed with the R-N1when compared with N1 and N3 possible due to high carbohydrate content present in the residual algae. Although N1 has the lowest N/C (0.07), however, the biomass showed lower H/C value when compared to R-N1 and N3. On the other hand, lower oxygen content and lower O/C with N3 is responsible for its higher HHV. Microalgae biomass with a higher value of H/C implies the biomass has more hydrogen with a tendency to produce more saturated hydrocarbons (Demirbas 2002). This is also in agreement with previous studies which have shown biomass with lower O/C, and high H/C has higher HHV (López-González *et al.* 2014; Zainan *et al.* 2018). In the present study, the results from the proximate, ultimate and biochemical show that nitrogen-stressed condition during cultivation altered the microalgae composition. Therefore, both N1 and R-N1 could be potential biomass feedstock for pyrolysis.

3.3.1.2 FTIR Analysis of the Microalgae Biomass

The Fourier-transform infrared spectroscopy (FTIR) spectra for N1, R-N1 and N3 are presented in Figure 3.2. The identified functional groups suggest the components present in the biomass samples. According to Figure 3.2, it can be observed that most of the identified functional group frequencies were common across the three biomass. However, the intensities of absorption bands differ due to the variation in composition. The absorption peak at 3100–2800 cm^{-1} was observed for all the three biomass with the intensity of N1 more prominent than others (N3 and R-N1). This suggests that more lipid content is present in the N1 biomass compared to N3 and R-N1.

Furthermore, the presence of protein was confirmed by absorption peak of 1800–1500 cm^{-1}, and the peak from N3 was more prominent, and this depicts the likely presence of higher protein content. The bands at 1200–1000 cm^{-1}, which relates to the stretching of C-O, C-C, and C-O-C suggests the presence of carbohydrates. The work of Dumas and Miller (2003) also confirmed the absorption bands for proteins and carbohydrates to be in the region of 1800–800 cm^{-1} while absorption bands for lipids is in region of 3100–2800 cm^{-1}. Phukan *et al.* (2011) also found prominent bonds in the microalgae biomass which is an evidence of progressive degradation in their intensity in the spectra of the de-oiled cake.

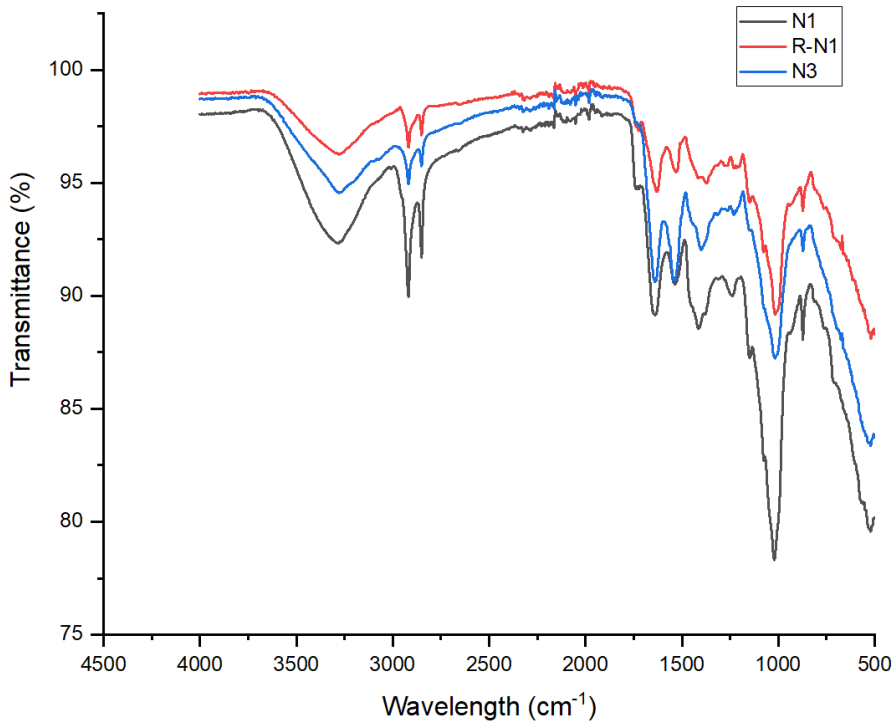

Figure 3.2. FTIR of *Scenedesmus obliquus* microalgae grown under different conditions

3.3.1.3 Thermogravimetric Analysis of the Microalgae Biomass

The TGA plot (Figure 3.3a) shows the relationship between the weight losses at different temperature while the differential scanning calorimetry (DSC) (Figure 3.3b) provides information about the heat flow changes against temperature. The TGA curves in Figure 3a for N1, R-N1 and N3 show multiple stages. The first stage for all the three biomass is dehydration, which occurs from 25 ºC to 150 ºC**.** The loss in weight of the samples at this temperature was due to evaporation of moisture from the biomass samples, and small change was also observed on the DSC curve in the form of endothermic peak caused by evaporation of moisture from the microalgae biomass. The other stages may depend on the composition of the major components (proteins, lipids, and carbohydrates) of microalgae. For instance, the second stage for N1 biomass is devolatilization of the major microalgal components which occurred between 150

and 600 ºC. This was assigned to the major weight loss during pyrolysis process and over this second phase, the TGA curve falls sharply. The higher lipid content in N1 may be possibly responsible for differences observed when compared to R-N1 and N3. This suggestion corroborated the previous studies on the decomposition of proteins and carbohydrates to which often occurred between 150 and 360 ºC while decomposition of lipid usually occurs within the range of 330 to 560 ºC (Peng, Wu and Tu 2001; Peng *et al.* 2001). This is also an indication of the large quantities of volatile organic matter in the biomass, an evidence of possible higher bio-oil yield (Phukan *et al.* 2011). The last stage was linked to the decomposition of carbonaceous material in the solid residue at a slower rate. For the N1 biomass, the third stage occurred at a temperature range of 600–800 ºC with a slight decrease in the TG curve. On the other hand, the second stage for R-N1 and N3 occurred between 150 and 500 ºC. The DSC plots obtained during the thermal decomposition of N1, R-N1 and N3 are shown in Figure 3.3b. The DSC curves shows an active reaction mechanism with a steady increase in heat flow from ambient to 500 ºC for all the three biomass considered. However, towards the completion stages at temperature > 600 ºC, the DSC curves showed a slight decrease in heat flow which indicated that the thermal decomposition activity was completed or the major component of the biomass was transformed before this temperature (Ahmad *et al.* 2019). The exothermic peak on the DSC curve of N1 when compared to R-N1 and N3 at temperature between 500 and 600 ºC is related to the energy released by the decomposition of the fixed carbon and residual lipids of N1.

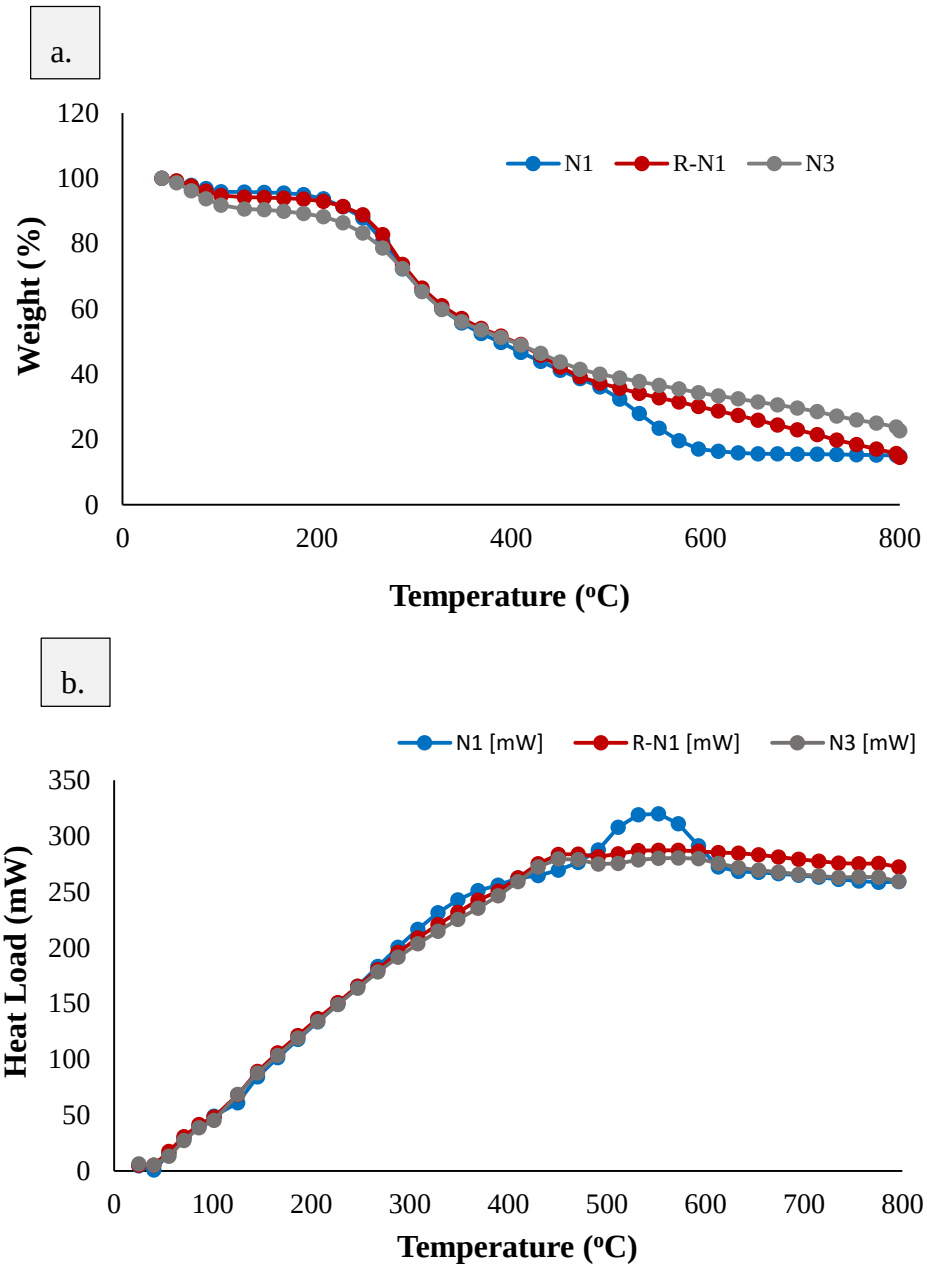

Figure 3.3. (a) TGA (b) DSC plot of *Scenedesmus obliquus* microalgae grown under different conditions

3.3.2 Pyrolysis Product Distribution

The pyrolysis product yield (bio-oil, biochar and gas) for the microalgae biomass (N1, R-N1 and N3) at different temperature is displayed in Figure 3.4. It was found that temperature

increase from 400 °C to 500 °C was responsible for the corresponding increase in yield of bio-oil produced from microalgae coded as N1 from 44.68 wt% to 46.37 wt%. While further increase in temperature to 600 °C and even 700 °C resulted in decrease in the bio-oil yield to 43.05 wt% and 40.38 wt% respectively. The decline in the bio-oil yield despite the corresponding increase in temperature above the optimum (500°C) was due to further cracking of the oil vapours via secondary reactions into non-condensable gas products. Similar trend was observed for bio-oil yield from the residual algae (R-N1) with the optimum bio-oil yield of 34.85 wt% at 500 °C, and temperature increase above the optimum increased the yield of gas product while the yield of bio-oil product decreased. Unlike the N1 and R-N1 with optimum yield at 500 °C, the maximum bio-oil yield (41.94 wt%) for N3 biomass was observed at a temperature of 600 °C. This is an indication that pyrolytic product distribution depends on both the feedstock composition and reaction temperature. The pyrolytic bio-oil yield from the nutrient-stressed microalgae (N1) was higher than R-N1 and N3 in all the experimental conditions. The higher bio-oil yield derived from the nutrient-stressed biomass (N1) was linked to the biomass high volatile matter content and low ash content (Vassilev *et al.* 2010). With increasing temperature from 400 °C to 700 °C, the biochar yields reduced while the gas yields correspondingly risen in all the three biomass considered. These results also corroborated the thermogravimetric analysis earlier discussed. Previous studies have also shown that varying feed composition and reaction conditions have a strong impact on combustion behavior during pyrolysis (Peng, Wu and Tu 2001; Peng *et al.* 2001; Vassilev *et al.* 2010).

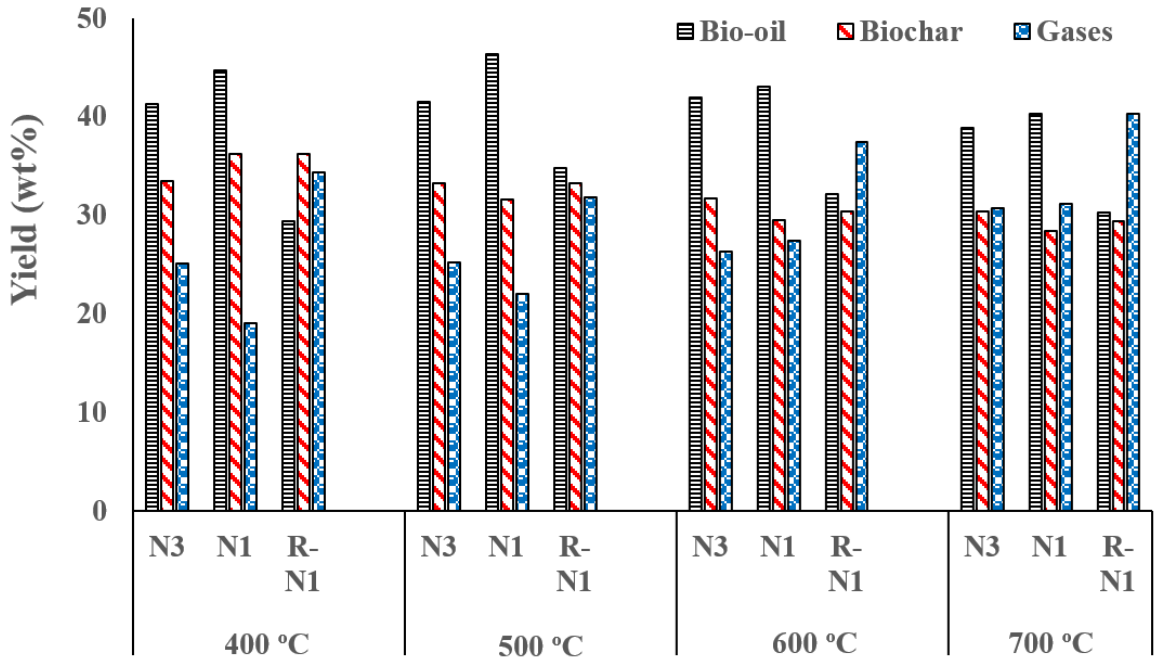

Figure 3.4. Product yields of the pyrolysis of microalgae samples at different temperature

3.3.3 Pyrolysis Bio-oil Analysis

3.3.3.1 Elemental Analysis

The elemental analysis, HHV and atomic ratios of the pyrolytic bio-oil produced from N1, R-N1and N3 at temperatures of 500 ˚C and 600 ˚C are presented in Table 3.2. At 500 ˚C, the carbon content (70.77 wt%) of the pyrolytic bio-oil obtained from N1 was higher than that of R-N1 (67.50 wt%) but almost the same with N3 (70.73 wt%). With increasing the temperature to 600 ˚C, the carbon content of N3 (67.61 wt%) slightly decreased while little or no change was observed on the carbon content of N1 and R-N1 (see Table 3.2). For all the biomass composition considered, there was no significant change in the hydrogen content of the bio-oils under the influence of temperature variation. However, the oxygen content of the bio-oil from N3 (7.78%) was lower when compared to N1 (11.84%) and R-N1 (12.06%) at

500 °C. The residual algae (R-N1) with higher carbohydrate content produced higher oxygen content at both 500 °C and 600 °C. In the same vein, the high oxygen composition of the bio-oil from R-N1 collaborated its lower HHV when compared to N1 and N3. There was no significant difference observed between the H/C ratio for all the pyrolytic bio-oils because of the closeness of their hydrogen values. Another reason is attributed to the fact that their hydrogen contents were significantly lower to the carbon contents. Interestingly, a significant difference was observed when the nitrogen content of bio-oil from N1 (5.46 wt%) was compared to N3 (8.84 wt%) at 500 °C. With the residual algae, the nitrogen content (8.59 wt%) was similar to that obtained with N3 but decreased to 6.44 wt% as the temperature was increased from 500 °C to at 600 °C. The N/C ratio further confirms the N1 bio-oil with the lower nitrogen when compared to N3 and R-N1. Notably, increasing the temperature to 600 °C has little or no effect on the nitrogen content of both N1 and N3 possibly due to complete decomposition of the protein content of the biomass at the temperature of 500 °C. This suggests that the nitrogen content of pyrolytic bio-oils was more dependent on feedstock composition than temperature. The sulphur content from both the raw biomass and that of bio-oils produced at all conditions considered were found to be < 1 wt% and fall within the range of 0.1 to 1.5 wt% reported for petroleum crude (Saber *et al.* 2016). The reason why the major challenge of pyrolytic bio-oils from microalgae remains a high amount of nitrogen and oxygen content but not sulfur. These findings have shown that nitrogen stressing during cultivation of microalgae could enhance the pyrolytic bio-oil yield as well as reduce the nitrogen content present in the bio-oil significantly. Thus, it could be seen as a promising approach to produce high-quality pyrolytic bio-oil from microalgae.

3.3.3.2 GC-MS Analysis

The chemical composition of the bio-oils derived from the pyrolysis of the microalgae biomass (N1, R-N1 and N3) at 500 °C were analyzed by gas chromatography (GC) / mass spectrometer (MS). The identified major compounds found in pyrolytic bio-oils were categorized into aliphatic hydrocarbons, aromatic hydrocarbons, nitrogen-containing aliphatic and aromatics, acids, and others (such as ketones, aldehyde, alcohol, esters and ethers). The distribution of the major compounds found in bio-oils from N1, R-N1 and N3 based on the above classification is shown in Figure 3.5. The relative abundance of the individual chemical compounds present in the pyrolytic bio-oils from N1, R-N1 and N3 are presented in Table A3.1 – 3.3, respectively. As shown in Figure 3.5, the distribution of the main compounds in the bio-oils is strongly dependent on the feedstock composition. The proportion of aliphatic hydrocarbons and acids in the bio-oil from N1 biomass was higher than that of R-N1 and N3. The higher amounts of aliphatic hydrocarbons and acids in N1 bio-oil may be as a result of the higher lipid content in N1 biomass being cracked into acids and hydrocarbons during pyrolysis (Yang *et al.* 2019). In addition to acetic acid, which accounts for the major proportions of the acids in the bio-oil from N1 biomass, other higher acids found in the bio-oil include hexanoic and fumaric acids. The compositions of aliphatic hydrocarbons in the pyrolytic bio-oils are 37.54%, 5.55% and 13.51% for N1, R-N1 and N3 biomass respectively, whilst the aromatic hydrocarbons compositions are 5.62%, 37.4% and 12.51% for N1, R-N1 and N3 biomass respectively.

Table 3.2. Elemental analysis, atomic ratios and HHV of Pyrolytic bio-oil at 500 ˚C and 600 ˚C

Condition	Elemental analysis					Atomic ratios			HHV (MJ/kg)
	C (%)	H (%)	N (%)	S (%)	O (%)	H/C	N/C	O/C	
Temperature = 500 °C									
N3	70.73	12.05	8.84	0.60	7.78	2.04	0.11	0.08	39.77
N1	70.77	11.50	5.46	0.43	11.84	1.95	0.07	0.13	38.27
R-N1	67.50	11.51	8.59	0.33	12.06	2.05	0.11	0.13	37.14
Temperature = 600 °C									
N3	67.61	11.40	8.55	0.59	11.85	2.02	0.11	0.13	37.07
N1	70.40	11.82	5.78	0.47	11.53	2.01	0.07	0.12	38.66
R-N1	67.35	11.39	6.44	0.49	14.34	2.03	0.08	0.16	36.51

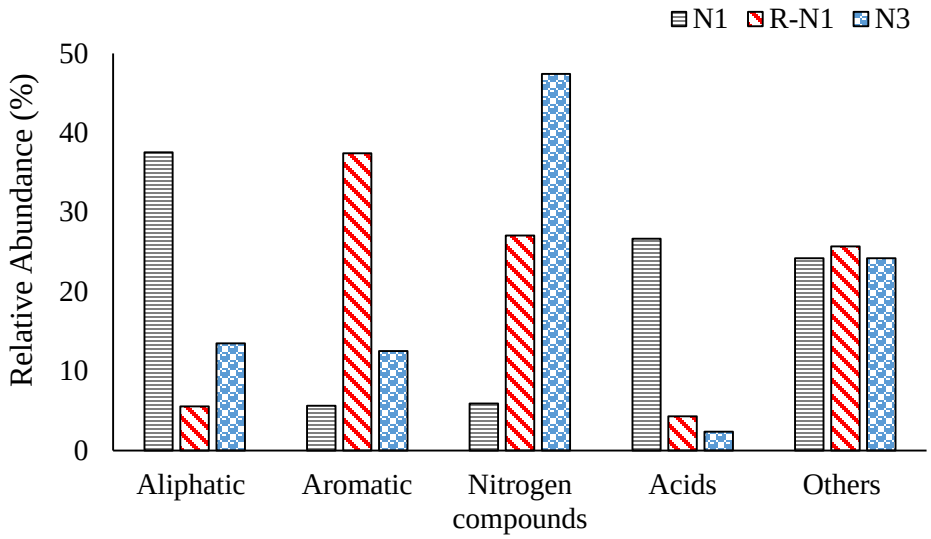

Figure 3.5. Distribution of main compounds in pyrolytic bio-oils produced from *Scenedesmus obliquus* microalgae samples at 500 °C

Phenol is of great commercial importance and accounts for about 76.7% of the aromatic hydrocarbon in the bio-oil from R-N1, as shown in Table A3.1. Phenol and its derivatives were produced from the decomposition of carbohydrate during pyrolysis (Yang *et al.* 2019). The higher aromatic hydrocarbon content in the bio-oil from the residual algae (R-N1) is as a result of the higher carbohydrate content in the biomass. From fuel application point of view, the presence of aliphatic and aromatic hydrocarbons which are valuable components in the bio-oils can influence the oxidation stability and cold flow property of the bio-oil produced (Mustapha and Isa 2020). The major components in microalgae are carbohydrate, protein and lipid, and the microalgae biomass composition variation could affect the produced pyrolytic bio-oil chemical composition. The main pyrolysis reactions involve dehydration, decarbonylation, decarboxylation, and deamination reactions (Wang, Sheng and Yang 2017). Specifically, the lipids content of the microalgae can undergo decomposition during pyrolysis

via decarbonylation, decarboxylation, and fragmentation of glyceride. At the same time, the primary reactions for carbohydrates during pyrolysis are dehydration, glycosidic bond cleavage, ring scission and rearrangement. The main reactions for protein decomposition during pyrolysis involves deamination and decarboxylation reactions. Most of the oxygen-containing compounds such as ketones, alcohols, and aldehydes were formed mainly due to the decomposition of carbohydrates and protein. Due to high protein content in the biomass, the pyrolytic bio-oil obtained from N3 biomass has the highest proportion to nitrogen-containing compounds when compared to N1 and R-N1.

The nitrogen-containing aliphatic compounds account for 2.20% while the nitrogen-containing aromatic compounds account for 3.72% of the bio-oil from N1 biomass (see Table A3.1). On the other hand, the nitrogen-containing aliphatic compounds account for 14.67% while the nitrogen-containing aromatic compounds account for 32.73% of the bio-oil from N3 biomass, as shown in Table A3.3. The major nitrogen-containing aliphatic compounds in the bio-oil from N3 biomass were 2-propen-1-amine (1.83%), acetamide (2.01%), pentanamide (2.94%) and butanamide (6.12%) while indole (10.26%) and 2-piperidinone (4.23%) were the most prominent among the nitrogen-containing aromatic compounds. The total proportion of nitrogen-containing compounds in the pyrolytic bio-oil from N3 was found to be 47.4 % but significantly reduced to 5.92% with the nutrient-stressed microalgae biomass (N1) at 500 °C. This further confirms the suitability of nutrient stressed approach for denitrogenation to enhance the quality of bio-oil produced from the pyrolysis of microalgae biomass.

3.3.4 Predictive Modelling of Bio-oil Yield

The model used to predict the yield of pyrolytic bio-oil was developed in relation to microalgae biomass composition and pyrolysis reaction temperature. A total of 70 data sets were generated from the pyrolysis experiments of 10 different microalgae biomass composition carried out between 400 to 700 °C at an interval of 50 °C. The desired model produced was based on 70% for (training), 15% (validation), while the remaining 15% was used for validating the consistency of the model. The optimum number of neurons was found to be 10 for the hidden layer and the ANN framework used to predict the yield of bio-oil is shown in Figure 3.6.

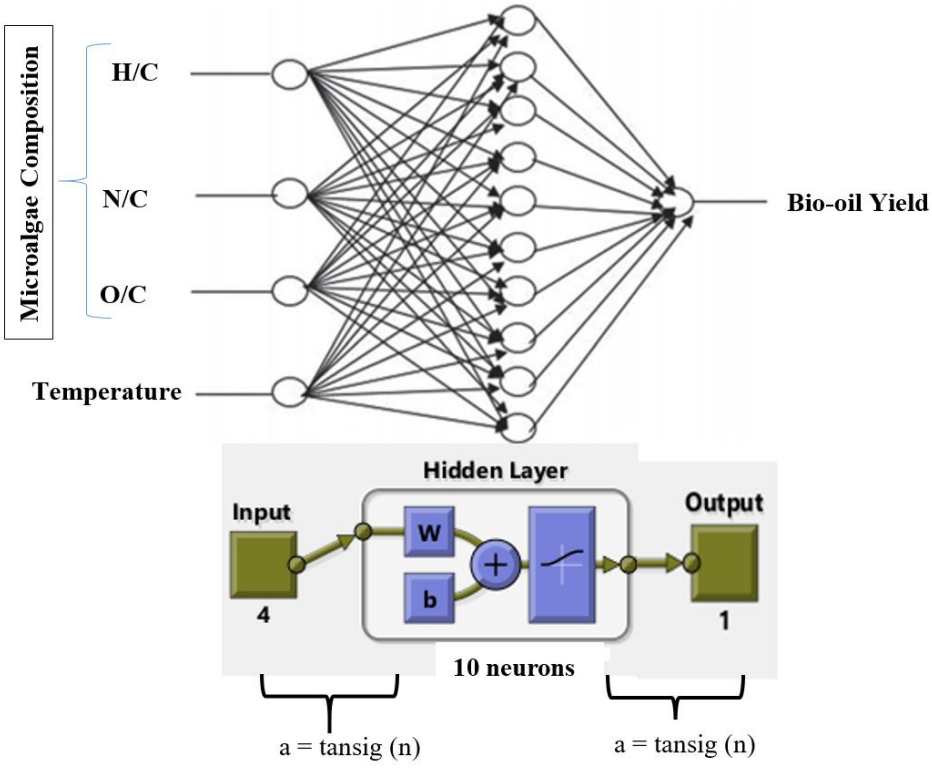

Figure 3.6. ANN architecture used for the prediction of the bio-oil yield

The regression plots in Figure 3.7 represent data for training, testing, and validation. A satisfactory coefficient of correlation of 0.9987 and 0.9812 was obtained for the training and the validation, which is an indication of high precision and accuracy of the developed ANN model. When the model was tested with data sets outside those used for training, a good correlation coefficient (0.9569) was obtained, which also confirm the developed ANN model was reliable. Overall, the plot of the yield of bio-oil obtained from predicted versus the experimental gave a correlation coefficient of 0.9849. The closeness of this value to 1 implies the predicted yield of bio-oil from ANN model agrees well with experimental values. Thus, the ANN model can be recommended to predict yield of pyrolytic bio-oil from microalgae biomass at any given biomass composition and pyrolysis temperature within the design space. Application of this model could help to save time and resources and also aid further optimization studies on producing pyrolytic bio-oils from microalgae

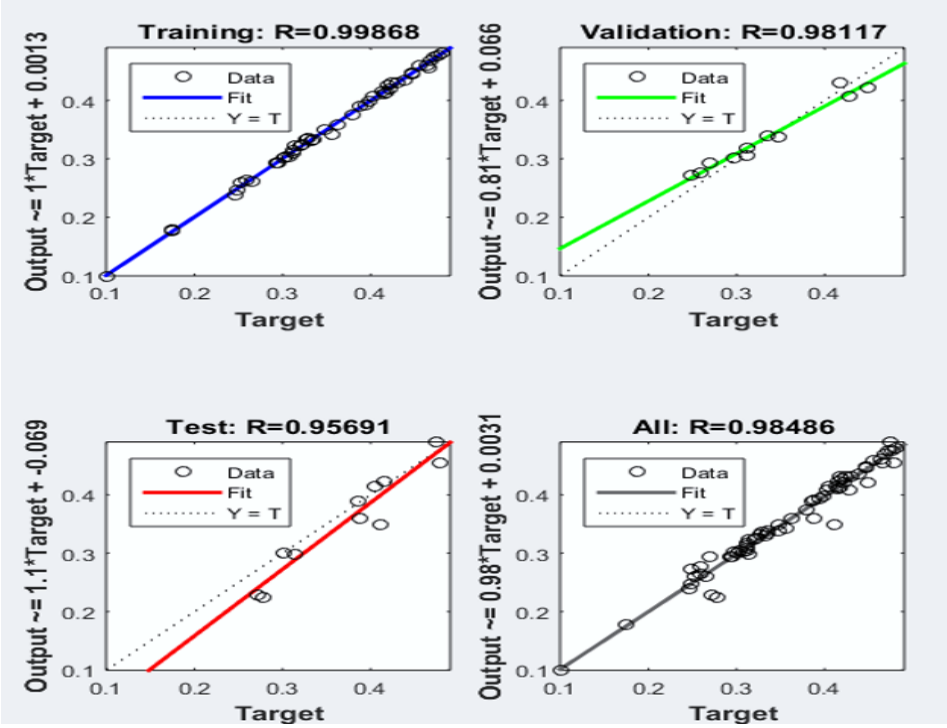

Figure 3.7: Regression plots of predicted versus experimental bio-oil yield for the ANN model

3.4 Conclusion

The pyrolytic bio-oil yield from the nutrient stressed biomass (N1) was higher than R-N1 and N3 in all the experimental conditions. The nitrogen content of bio-oil from the N3 biomass (8.84 wt%) with a reduction to 5.46 wt% haven been realized when nutrient-stressed biomass (N1) was used. Also, the nitrogen content of pyrolytic bio-oils was dependent more on feedstock composition than temperature. The quantity of aliphatic hydrocarbons and acids in bio-oil from N1 biomass was higher when compared to R-N1 and N3. Phenol which is of great commercial importance accounts for about 76.7% of the aromatic hydrocarbon in the residual algae (R-N1) bio-oil. The pyrolytic bio-oil from unstressed algae (N3) has the highest number of nitrogenous- compounds compared to N1 and R-N1. The proportion of nitrogenous compounds in bio-oil from N3 was 47.4% which decreased to 5.92% for the nutrient-stressed microalgae biomass (N1). These findings from present study confirm the suitability of nutrient stressed approach to enhance the quality of bio-oil produced through pyrolytic reaction of microalgae biomass.

CHAPTER 4

CATALYTIC PYROLYSIS OF NUTRIENT-STRESSED MICROALGAE FOR HIGH-QUALITY BIO-OIL PRODUCTION

4.1 Introduction

Microalgae have been proposed as a novel resource with the capacity to produce large quantities of lipids, proteins and carbohydrates that can be converted into biofuels and other valuable co-products (Sambusiti *et al.* 2015; Chew *et al.* 2017). Pyrolysis, as a method of converting microalgae into biofuels, has received much attention because of its low investment costs coupled with its potential to be applied to whole microalgae and not just the lipids (Ly *et al.* 2016; Huang *et al.* 2017). Biofuels produced from microalgae via thermal degradation are still far from the desired fuel quality. The major challenges associated with bio-fuel produced from pyrolysis of microalgae include high nitrogen content, high oxygen content resulting to low calorific value, high acidity, as well as high viscosity (Thangalazhy-Gopakumar *et al.* 2012; Bennett *et al.* 2017). These limitations affect the stability of the pyrolytic bio-oils and make it unfit to be used directly as transportation fuels (Liang 2013). Research efforts to address this obstacle are ongoing, and the use of catalyst have been proposed as possible options.

Pyrolysis in the presence of a catalyst is an approach widely used to impriove the quality of microalgal bio-oils and higher yield of bio-oils with less oxygen content has been demonstrated (Andrade *et al.* 2018). Thangalazhy-Gopakumar *et al.* (2012) studied the catalytic pyrolysis of *Chlorella vulgaris* at 650 ^{o}C using catalyst to biomass ratio of 1:1. The researchers found the use of HZSM-5 catalyst promoted the removal of oxygenated compounds but with little potential for the removal of nitrogenated compounds from

microalgal bio-oil. In another study, the catalytic pyrolysis of *Tetraselmis suecica* was investigated by Zainan, Srivatsa and Bhattacharya (2015) at 400 ^{o}C and catalyst to biomass ratio of 5:1. The authors also found decrease in oxygenated compounds as a result of the use of HZSM-5 catalyst but no change in the nitrogen content of pyrolytic bio-oil was observed. Chagas *et al.* (2016) also observed little effect on nitrogen content of pyrolytic bio-oil when HZSM-5 catalyst was added during the pyrolysis of Spirulina sp. at 450 ^{o}C. Other catalysts that have reportedly been used in the pyrolysis of microalgae include metal oxides (Bennett *et al.* 2017), nickel supported zeolite (Zainan *et al.* 2018; Srivatsa, Li and Bhattacharya 2019), titania-based (Aysu *et al.* 2017), and ceria-based (Aysu and Sanna 2015) catalysts. Nickel-based catalysts are reported to promote decarboxylation and decarbonylation reactions resulting in a higher amount of hydrocarbons (Zainan *et al.* 2018). The pyrolysis of *Pavlova* sp. in the presence of alumina-supported catalysts ($MgCe/Al_2O_3$, $NiCe/Al_2O_3$, and Ce/Al_2O_3) showed that all the catalysts greatly decreased the oxygen content in bio-oil and the yield of the bio-oil was also enhanced (Aysu and Sanna 2015). Also, silica-supported magnetite nanoparticle catalyst (Fe_3O_4/SiO_2) have been shown to promote acid ketonization during pyrolysis bio-oil upgrading (Bennett *et al.* 2017). So far, catalytic pyrolysis of microalgae have not received sufficient attention, and the search for catalyst with better activity for microalgae conversion is still ongoing. Among the few catalysts, HZSM-5 have shown good catalytic performance in promoting aromatization and deoxygenation of pyrolytic bio-oils with little or no effect on denitrogenation of the bio-oils. Metals oxides such as iron oxide (Fe_3O_4), and cerium oxide (CeO_2) have been shown with selective properties in promoting ketonization of acids and deoxygenation to produce bio-oil with low acidity. Incorporation of metal promoters such as W, Zr, Co or Mo on support material could also improve catalyst efficiency (Galadima

and Muraza 2018). Exploring catalysts with multifunctional capabilities to find a better catalyst for the improvement of the quality of pyrolysis bio-oils will be a major advancement towards developing sustainable and efficient thermal conversion of microalgae biomass.

Previous studies revealed that the most notable changes under nitrogen stressed condition during cultivation involve the enhancement of carbohydrates and/or lipids (high-energy storage compounds), coupled with a reduction of protein content (Griffiths, van Hille and Harrison 2012; Huang *et al.* 2013b; Depraetere *et al.* 2015; Liu *et al.* 2016). The increase in the stored high-energy compounds was linked to changes in metabolic processes following decline of needed nutrient (Sajjadi *et al.* 2018). The amount of nitrogen nutrient used during cultivation may have a direct effect on the protein content since protein accounts for the major intracellular nitrogen pools in microalgae and most of the nitrogen in the product bio-oils probably originates from the protein content of the microalgae (Sajjadi *et al.* 2018). Hence, the nutrient-stressed approach can be used to alter microalgae composition especially for high protein microalgae such as *Scenedesmus obliquus* towards improving quality of microalgal bio-oils produced via pyrolysis.

So far, catalytic pyrolysis of microalgae have not received sufficient attention, and the search for catalyst with better activity for microalgae conversion is still ongoing. Among the few catalysts, HZSM-5 have shown good catalytic performance in promoting aromatization and deoxygenation of pyrolytic bio-oils with little or no effect on denitrogenation of the bio-oils (Thangalazhy-Gopakumar *et al.* 2012). Metals oxides such as iron oxide (Fe_3O_4), and cerium oxide (CeO_2) have been shown with selective properties in promoting ketonization of acids and deoxygenation to produce bio-oil with low acidity. Incorporation of metal promoters such as W, Zr, Co or Mo on support material could also improve catalyst efficiency (Galadima

and Muraza 2018). Exploring catalysts with multifunctional capabilities to find a better catalyst for the improvement of the quality of pyrolysis bio-oils will be a major advancement towards developing sustainable and efficient thermal conversion of microalgae biomass.

4.2 Materials and Method

4.2.1 Feedstocks

The microalgae sample, *Scenedesmus obliquus,* grown under nitrogen stressed condition (N1) was collected from the Institute of Water and Wastewater Technology, Durban University of Technology, Durban, South Africa. The cultivation of algae was done in a 3000-litre capacity open raceway pond using a modified BG 11 media with reduced nitrogen (150 mg/L). The dried samples were crushed using a stainless steel laboratory grinder, sieved to a particle size of <125 µm and stored for further use. The lipid, carbohydrate and protein of the microalgae sample were 21.62%, 42.55% and 22.08% respectively. The ash content and volatile matter content were determined to be 10.17% and 81.77% respectively. The C, H, N, S and O content were determined to be 45.03%, 7.50%, 3.59%, 0.98% and 42.90%, respectively. The nitrogen gas (99.995%, purity) used during the pyrolysis process was obtained from Afrox®. Ammonium-ZSM-5 powder (SiO_2/Al_2O_3 mole ratio: 50:1, CBV5524G) was obtained from Zeolyst International. Analytical grade chemicals, requiring no further purification, were used in this study.

4.2.2 Preparation of Catalyst and Characterization

HZSM-5 was obtained from the calcination of ammonium ZSM-5 (NH_4-ZSM-5) at 550 °C for 5 h (Shakya *et al.* 2017a). Magnetite (Fe_3O_4) was prepared by the modified co-precipitation method reported by Hu *et al.* (2011). Briefly, 1:2 molar ratios of $FeCl_3 \cdot 6H_2O$:

$FeCl_2 \cdot 4H_2O$ was vigorously mixed in 50 mL of deionized water using ultrasonic sonicator operated at 15 kHz for 2 h. Subsequently, the pH of solution was adjusted to 12 using 2M solution of NaOH, and the solution was allowed to age for 60 min, it was then followed by centrifugation for separating the black solid from resulting mixture. The black solid was later dried in the oven at 105 °C overnight, ground then sieved to obtain homogeneous powdered material. Fe_3O_4-HZSM-5 support with weight ratio (1:4) of Fe_3O_4 and HZSM-5 was prepared by an impregnation method. The supported metal catalysts (M/Fe3O_4-HZSM-5) were prepared by doping the various transition metals (M = Zr, W, Co and Mo) on the HZSM-5/Fe_3O_4 support. The metal nitrates [Zr $(NO_3)_4$, W $(NO_3)_6$, Co $(NO_3)_2$, and Mo $(NO_3)_3$] of 10 wt% loadings were mixed with 20 g each of Fe_3O_4/HZSM-5 support, followed by vigorous ultrasonic treatment with the following applied conditions (SONIC – 150W @ 20 kHz ultrasonic homogenizer) for 2 hours. Then, the solution was oven-dried at 105 °C overnight, followed by heating at furnace temperature of 500 °C for 8 hours to obtain M/Fe_3O_4-HZSM-5 catalysts, where M = Zr, W, Co and Mo.

The crystalline phase composition of the synthesized catalysts was identified by X-ray diffraction using PANalytical-Empyrean X-ray diffractometer equipped with a Cu Kα radiation source (λ=0.1541 nm) at a scanning step size of 0.05°. The data were collected under atmospheric pressure over the scanning angle range of 5 to 90° in 2θ. The morphology of the synthesized catalysts was determined using high-resolution scanning electron microscopy (HRSEM) and the energy dispersive spectroscopy (EDS) analysis was done on the samples to investigate their elemental composition. Thermogravimetric analysis (TGA) was performed on the synthesized catalysts using TA instrument (SDT Q600). The heating was done under N_2 atmosphere from 30 to 800 °C at 10 °C/min.

4.2.3 Catalytic Pyrolysis Experiments

Experiments were conducted with a reactor made of stainless steel (outer diameter = 12.7 mm, inner diameter = 10.6 mm and length = 450 mm), heated by an electric furnace with the temperature measured using K type thermocouple placed inside the reactor. Oven-dried samples were used for all pyrolysis runs. The non-catalytic tests used 1g each of the dried microalgae sample while the catalytic tests used a mix of microalgae sample with catalyst (1:1 g/g). The whole reactor system was purged using pure N_2 at 30 mL/min to create an inert atmosphere. The pyrolysis tests were conducted by heating the reactor at 10 ^{o}C/min to the set temperature of 500 $^{\circ}$C. The reaction temperature was held for 1 hr while the sweeping gas was allowed to continue to flow. The vapour containing the bio-oils from the reactor was condensed into a glass flask at 0 ^{o}C while the residual solid (biochar) remained in the reactor. After cooling, the solids left in the reactor was recovered, and the flask and connectors were washed with acetone to collect the bio-oil. Thereafter, the acetone solvent was evaporated overnight at 60 ^{o}C, and the bio-oil obtained was measured gravimetrically. The bio-oil and biochar yield (after subtracting catalyst weight from the weight of solid recovered) was determined as a percentage of bio-oil and biochar recovered from a known weight of the dry biomass. The non-condensable gases with any other losses were calculated by difference (gas yield = 100 – (bio-oil yield + biochar yield)). The energy recovery in bio-oil was determined using equation 4.1 (Aysu, Fermoso and Sanna 2018). All the pyrolysis experiments were repeated at least two times, and the average values reported.

$$Energy\ recovery\ (\%) = \left(\frac{HHV\ of\ bio{-}oil * amount\ of\ bio{-}oil\ produced}{HHV\ of\ algae * amount\ of\ algae}\right) * 100 \qquad (4.1)$$

4.2.4 Bio-oil Analysis

The elemental composition of the bio-oils produced from the pyrolysis experiments was measured using an elemental analyzer (Vario EL-II Elementar Analysensysteme GmbH, Hanau, Germany) and the Dulong correlation (Yan *et al.* 2017) (Equation 4.2) was used in estimating the HHV of the produced pyrolytic bio-oil. The compounds in the pyrolytic bio-oils were analyzed using an Agilent 7890-5975C gas chromatography / mass spectrometer (GC-MS) under the following conditions: helium as carrier gas at flow rate of 1.76 mL/min; 1 µL injection size; and 1: 60 split ratio. Starting GC oven temperature was kept at 42 °C for 1 min; then the temperature was increased to 300 ºC at a rate of 5.5 ºC/min and held for 10 min; Scan mode (35.00 to 550.00 m/z); injector and detector temperature of 220 ºC and 250 ºC respectively. The compounds were identified using the National Institute of Standards and Technology (NIST) mass spectral data library.

$$HHV\left(\frac{MJ}{kg}\right) = 0.338C + 1.428\left(H - \frac{O}{8}\right) + 0.095S \quad (4.2)$$

where C, H, O, and S are weight percentage of carbon, hydrogen, oxygen, and sulphur in the bio-oils, respectively.

4.3 Results and Discussion

4.3.1 Catalysts Characterization

Fig. 4.1 shows the XRD patterns of the synthesized catalysts. The XRD patterns exhibited characteristics of HZSM-5 crystallites with the presence of diffraction peaks at 2θ = 7.9, 8.8, 23.2, 23.9 and 24.4° in all the catalysts (Zhang *et al.* 2009). The peak at 2θ = 35° confirmed the presence of crystalline phase of magnetite (Fe_3O_4) in the XRD patterns of Fe_3O_4-HZSM-5 and all the supported metal catalysts (Wardani *et al.* 2019). Due to the agglomeration of Fe_3O_4, the

pattern of Fe_3O_4-HZSM-5 showed an overall decrease in the peaks intensity when compared to HZSM-5. The peaks at 2θ = 30.2, 31.5 and 40.78° were attributed to XRD peaks of a monocyclic ZrO_2 present in the Zr/Fe_3O_4-HZSM-5 catalyst (Mangla and Roy 2018). The diffraction peaks at 2θ = 28.8, 33.4 and 34.1° were attributed to XRD peaks of a monocyclic WO_3 present in the W/Fe_3O_4-HZSM-5 catalyst (Thummavichai *et al.* 2018). The XRD patterns of Mo/Fe_3O_4-HZSM-5 catalyst exhibit peaks at 2θ = 32.2° and 36.1° attributed to orthorhombic molybdite phase of α-MoO_3 and monoclinic phase of β- MoO_3 respectively (Mitran *et al.* 2019). The XRD patterns of Co/Fe_3O_4-HZSM-5 catalyst exhibit peaks at 2θ = 31.19, 36.75 and 38.25° attributed to the cobalt oxide crystalline phase. These diffraction peaks agree with values reported for Co_3O_4 nanoparticles (Al-Senani, Deraz and Abd-Elkader 2020).

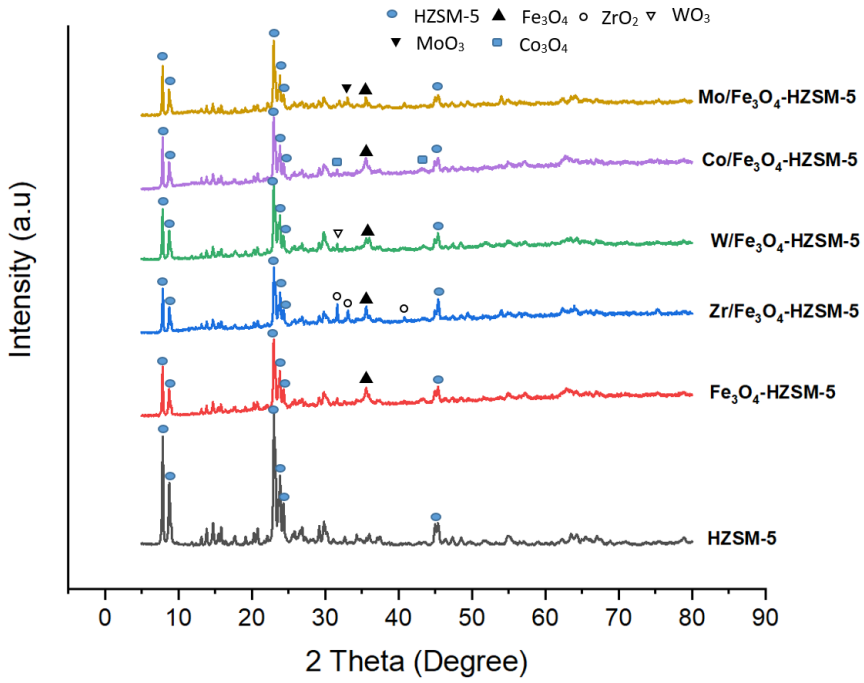

Figure 4.1. XRD patterns of the synthesized catalysts

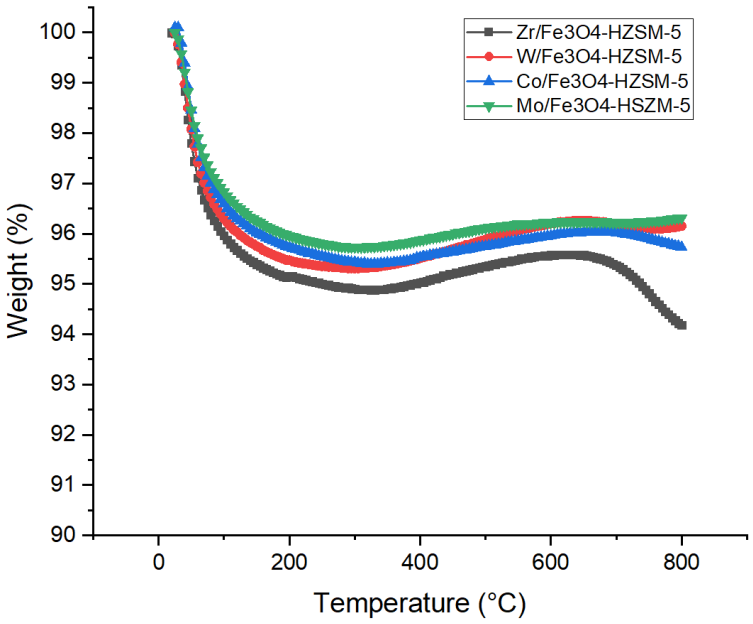

Figure 4.2. Thermogravimetric analysis (TGA) of the synthesized catalysts

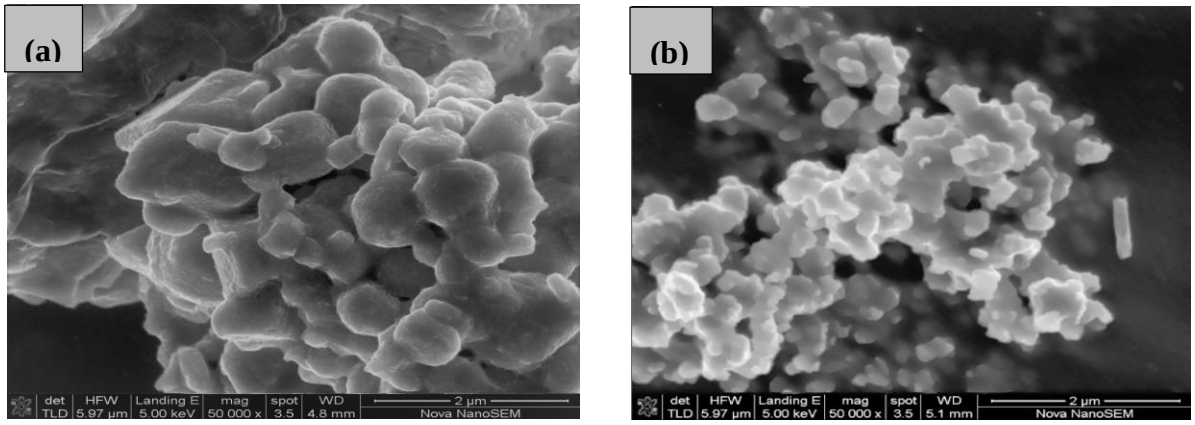

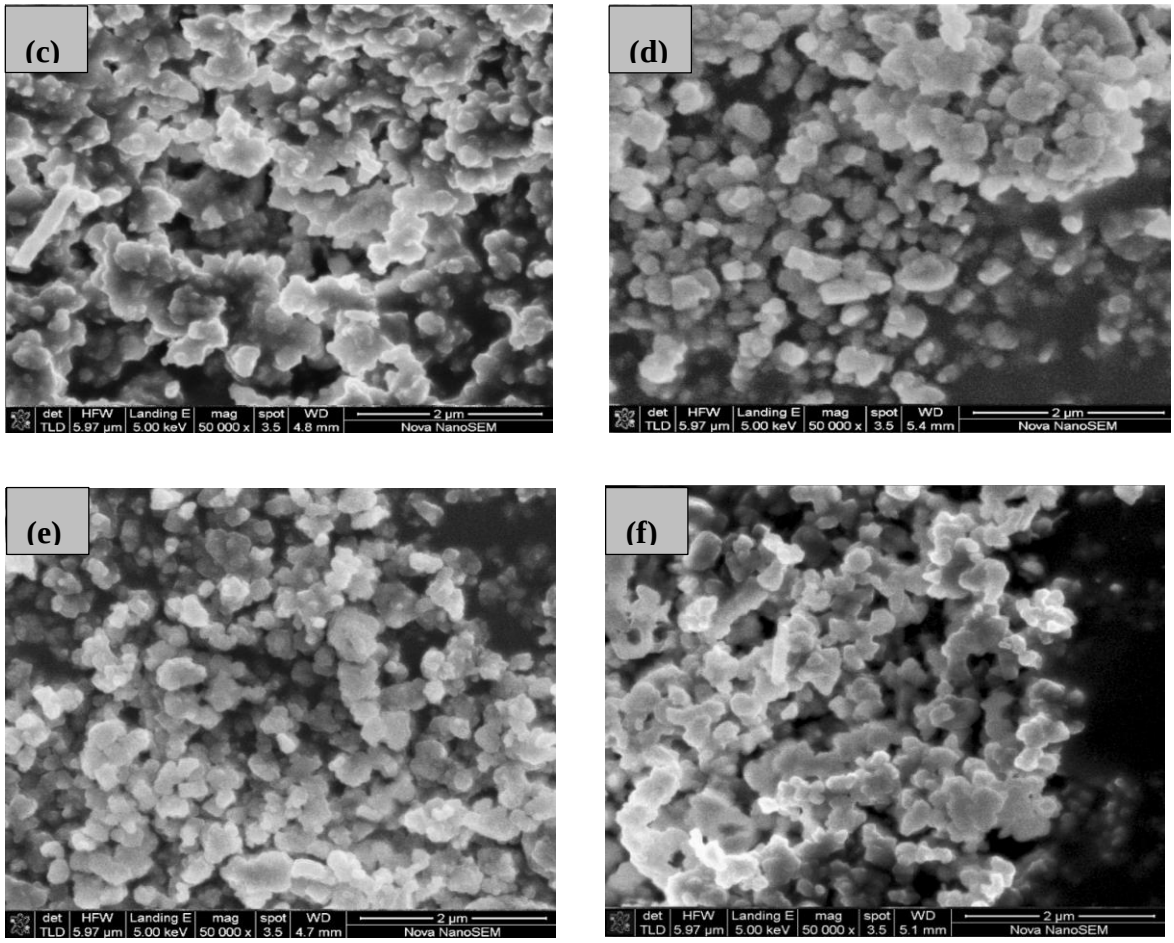

Figure 4.3. SEM image of (a) HZSM-5 (b) Fe_3O_4-HZSM-5 (c) W/Fe_3O_4-HZSM-5 (d) Zr/Fe_3O_4-HZSM-5 (e) Co/Fe_3O_4-HZSM-5 (f) Mo/Fe_3O_4-HZSM-5

The TGA profile of the synthesized supported metal catalysts is shown in Fig. 4.2. The TGA curves for all the synthesized catalysts showed a slight weight loss of between 3 - 5% indicating losses of moisture content within the temperature range of 30 to 150 ºC. Above this temperature up to temperature range considered for pyrolysis (400 - 700 ºC), the synthesized catalysts were considerably stable. Fig. 4.3 (a-f) shows the morphologies of the synthesized catalysts. The SEM image of HZSM-5 and Fe_3O_4-HZSM-5 (see Fig. 4.3 (a-b)) showed aggregate of particles and the HZSM-5 have an elongated prismatic shape (Kostyniuk, Key and Mdleleni 2019). The

SEM images of the synthesized supported metal catalysts are shown in Fig. 4.3 (c-f). The elemental composition from the EDS showed that the metal species (W, Zr, Co and Mo) were well dispersed on the Fe_3O_4-HZSM-5 supports (see Fig B4.1).

4.3.2 Pyrolysis of *Scenedesmus obliquus*

The products yield from the pyrolysis of nutrient-stressed *Scenedesmus obliquus* is presented in Fig. 4.4. The effect of various supported metal catalysts (Mo/Fe_3O_4-HZSM-5, Zr/Fe_3O_4-HZSM-5, W/Fe_3O_4-HZSM-5, and Co/Fe_3O_4-HZSM-5) on pyrolysis product yields was investigated at 500 °C using catalyst-to-biomass ratio 1:1. Fig. 4.4 shows that the pyrolytic bio-oil yield dropped from 46.37 wt% (without catalyst) to 11.07 – 17.73 wt% (catalytic). Excessive cracking activity of the acid sites of the catalysts might be responsible for the sharp decline observed in bio-oil yield (Aysu, Fermoso and Sanna 2018). A series of reactions which occurred during pyrolysis like dehydration, decarbonylation, decarboxylation, and deamination could be promoted by the catalyst surface acid sites thereby increasing cracking to produce more gaseous products (Rahman, Fermoso and Sanna 2018). This is supported by experimental data from this study which showed an increase in the yield of gas product from 22.05 wt% (without catalyst) to 50.32 – 61.11 wt% with the use of catalysts. As shown in Fig. 4.4, Co/Fe_3O_4-HZSM-5 catalyst gave the lowest biochar yield (22.27 wt%) which suggests this catalyst had the highest conversion among the supported metal catalysts and ~ 30% reduction in biochar yield was achieved when compared to non-catalytic process. Also, Co/Fe_3O_4-HZSM-5 produced highest pyrolytic bio-oil yield (17.73 wt%) while lowest bio-oil yield (11.07 wt%) was produced with W/Fe_3O_4-HZSM-5. In terms of gas yield, the highest gas yield (61.11 wt%) was achieved with Zr/Fe_3O_4-HZSM-5 catalyst while Mo/Fe_3O_4-HZSM-5 produced the lowest gas yield (50.32 wt%). The ranking order for the catalysts based on bio-

oil yield was Co/Fe_3O_4-HZSM-5 > Zr/Fe_3O_4-HZSM-5 > Mo/Fe_3O_4-HZSM-5 > W/Fe_3O_4-HZSM-5 whereas ranking order for the gas yield was Zr/Fe_3O_4-HZSM-5 > Co/Fe_3O_4-HZSM-5 > W/Fe_3O_4-HZSM-5 > Mo/Fe_3O_4-HZSM-5. This is an indication that the doping of various metals on the Fe_3O_4-HZSM-5 support modified the activity of the catalysts. Previous studies by Rahman, Fermoso and Sanna (2018) investigated the pyrolysis of *Isochrysis* sp. microalgae in the presence of Li-LSX-zeolite and micro-silica catalysts, and non-catalytic tests at 500 ^oC was compared. The authors observed reduction in the pyrolytic bio-oil yield from 37 wt% to 28 – 29 wt% while the produced gas yield was significantly increased from 28 wt% to ~ 36 wt% when the non-catalytic test was compared to catalytic tests.

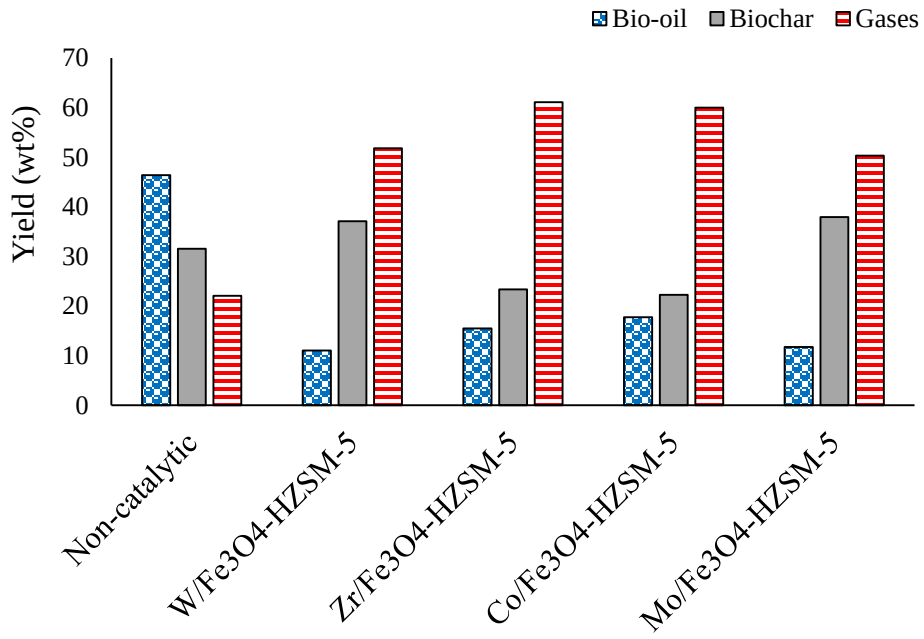

Figure 4.4. Product yields during the catalytic and non-catalytic pyrolysis of *S. obliquus* microalgae (temperature: 500 °C, catalyst to biomass ratio of 1:1)

The elemental analysis, atomic ratios, and HHV of the pyrolytic bio-oils produced from nutrient-stressed *Scenedesmus obliquus* microalgae over supported metal catalysts at 500 °C

are presented in Table 4.1. From the table, an enrichment of between 1 and 7% was seen in the carbon content of pyrolytic bio-oils produced with addition of supported metal catalysts when compared to bio-oil produced without catalyst. Also, enrichment of H/C ratio was observed for the catalytically produced pyrolytic bio-oils when compared to non-catalytic except for W/Fe_3O_4-HZSM-5 catalyst which showed downward trend. It can also be deduced that the presence of the supported metal catalysts promoted deoxygenation of the pyrolytic bio-oils when compared to non-catalytic process. Several reactions, like dehydration, decarboxylation, and decarbonylation are responsible for oxygen removal during pyrolysis (Rahman, Fermoso and Sanna 2018). The bio-oils produced in this study from nutrient-stressed *S. obliquus* microalgae contains significantly less oxygen content (11.84 wt% for non-catalytic, and 6.57 – 10.37 wt% for catalytic) compared to pyrolytic bio-oils produced from typical plant-based biomass (20 – 40 wt% and 30 – 45 wt% with and without catalyst, respectively) (Aysu, Fermoso and Sanna 2018). Pan *et al.* (2010) studied the pyrolysis of *Nannochloropsis* sp and found that oxygen composition in bio-oil reduced from 30.0 wt% (non-catalytic) to 19.5 wt% with the addition of HZSM-5. Pyrolysis of nutrient stressed *S. obliquus* microalgae with addition of catalysts in this study produced bio-oils with oxygen content far less than oxygen content from non-catalytic process and those from catalytic pyrolysis by Pan *et al.* (2010). In terms of nitrogen content, all the supported metal catalysts except for W/Fe_3O_4-HZSM-5 enhanced the quality of pyrolytic bio-oils by reducing nitrogen content in the product. The same trend was observed in terms of N/C. The amount of nitrogen compounds in bio-oil possibly obtained from microalgae protein and chlorophyll composition decreased from 5.46 wt% (without catalyst) to 4.77 wt% with Co/Fe_3O_4-HZSM-5 catalyst. Additionally, the use of catalysts resulted in lower O/C, which contributed to the higher HHV values observed. The

HHV was increased from 38.27 MJ/kg (non-catalytic) to 39.70 – 40.78 MJ/kg for the catalytic pyrolysis. Among the supported metal catalyst, Co/Fe_3O_4-HZSM-5 was the most efficient to enhance the quality of the pyrolytic bio-oil with the highest HHV (40.78 MJ/kg) and lowest nitrogen content (4.77 wt%). In terms of energy recovery, Co/Fe_3O_4-HZSM-5 gave the highest energy recovery in bio-oil of ~40%, followed by Zr/Fe_3O_4-HZSM-5 with 33.5% energy recovery in bio-oil and the least performing catalyst was with W/Fe_3O_4-HZSM-5 which gave 24.18% energy recovery in bio-oil. These findings further confirmed that the doping of various metals on the Fe_3O_4-HZSM-5 support altered the activity of the catalysts produced.

Table 4.1. Elemental analysis, atomic ratios and HHV of Pyrolytic bio-oil at 500 ˚C

Condition	Elemental analysis					Atomic ratios			HHV (MJ/kg)
	C (%)	H (%)	N (%)	S (%)	O (%)	H/C	N/C	O/C	
Non-catalytic	70.77	11.50	5.46	0.43	11.84	1.95	0.07	0.13	38.27
W/Fe_3O_4-HZSM-5	75.98	10.89	5.89	0.67	6.57	1.72	0.07	0.06	40.12
Zr/Fe_3O_4-HZSM-5	71.99	12.03	5.19	0.42	10.37	2.01	0.06	0.11	39.70
Co/Fe_3O_4-HZSM-5	73.00	12.42	4.77	0.43	9.38	2.04	0.06	0.10	40.78
Mo/Fe_3O_4-HZSM-5	71.47	12.61	5.25	0.35	10.33	2.12	0.06	0.11	40.35

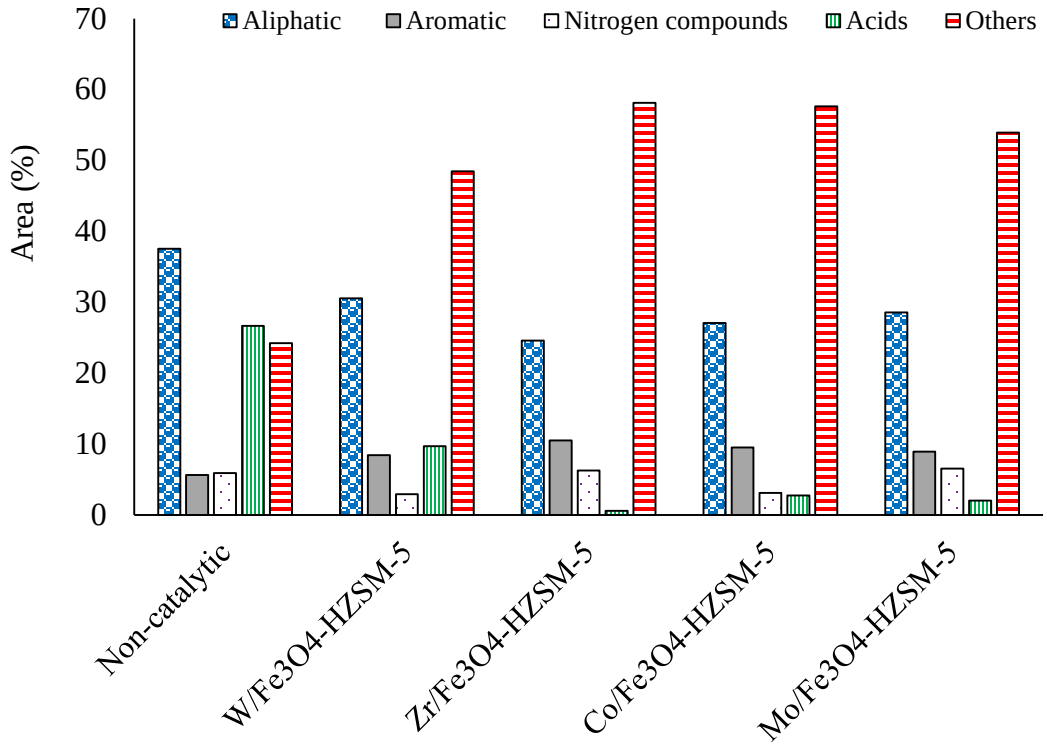

Figure 4.5. Distribution of main compounds in catalytic and non-catalytic pyrolytic bio-oils from *S. obliquus* microalgae (temperature: 500 °C, catalyst : biomass ratio 1:1)

The chemical composition of the bio-oils produced from the pyrolysis of *S. obliquus* microalgae with and without catalysts at 500 °C were analyzed by gas chromatography / mass spectrometer (GC-MS). The identified compounds present in the produced pyrolytic bio-oils were grouped into aliphatic and aromatic hydrocarbons, nitrogen-containing compounds (nitrogen-containing aliphatic and aromatics), acids, and others (such as ketones, aldehyde, alcohol, esters and ethers). The main compounds distribution based on the classification above is presented in Fig. 4.5. The relative abundance of the individual chemical compounds are presented in Table B4.1 – B4.5. As shown in Fig. 5, catalytic pyrolysis promotes the production of more aromatic compounds whilst the aliphatic compounds were decreased. The proportion

of aromatic compounds increased from 5.62% (for non-catalytic) to 8.42 – 10.48% with addition of supported metal catalysts.

A proposed reaction mechanism to produce aromatic and polyaromatic compounds from microalgae (lipid, carbohydrate and protein) was reported by Kumar *et al.* (2017a). The protein undergoes decomposition via deamination and decarboxylation reactions during pyrolysis to produce aromatics which can further be polymerized to form polycyclic aromatic hydrocarbons (PAH). Carbohydrates undergo deoxygenation (dehydration, decarboxylation, and decarbonylation) to smaller compound such as alcohols, aldehydes, ethers, and ketones. These compounds can be cracked into olefins; which can then be converted to different aromatics compounds through a series of aromatization reactions. The lipids content of the microalgae can undergo decomposition during pyrolysis via dehydration, decarboxylation, decarbonylation to produce heavy hydrocarbon which can then be cracked into olefins and subsequently converted into aromatics via secondary reactions.

The increase in aromatic compounds observed with the addition of supported metal catalysts is attributable to deoxygenation of oxygenated aromatic compounds and secondary reactions based on Diels-alder mechanism (Horne and Williams 1996). The incorporation of HZSM-5 in all the catalysts promote the aromatization of the bio-oils produced as seen in this study. Past work also revealed HZSM-5 catalyst could enhance aromatics formation and also reduced oxygen content in bio-oils (Wang and Brown 2013; Naqvi *et al.* 2017). As shown in Table B4.1 – B4.5, the aromatics compounds found in all the pyrolytic bio-oils include phenol, benzene, naphthalene and their derivatives. Both W/Fe_3O_4-HZSM-5 and Co/Fe_3O_4-HZSM-5 were found to promote denitrogenation reactions whereby the nitrogen compounds in pyrolytic bio-oils reduced from 5.92% (without catalyst) to 2.94% and 3.11%, respectively. The

proportion of acids found in the bio-oil produced from non-catalytic pyrolysis was relatively high (26.68%) as shown in Fig. 4.5, which might become critical with regards to the performance of the bio-oil. The high acid content in bio-oils which suggests high acidity could lead to corrosion problems and renders the bio-oils to be thermo-chemically unstable during transportation and storage (Bennett *et al.* 2017; Aysu, Fermoso and Sanna 2018). The total amounts of acids in the pyrolytic bio-oil decreased from 26.68% (non-catalytic) to 0.58 – 9.68% with supported metal catalysts. Addition of catalysts significantly lowers the acidity in pyrolytic bio-oils produced from *S. obliquus* microalgae which is a vital boost to the bio-oil quality. Among the oxygen-containing compounds, 2-pentanone was found to be the most prominent in all the pyrolytic bio-oils produced with or without catalysts, as shown in Table B4.1 – B4.5. The amount of 2-pentanone increased from ~10% (non-catalytic) to 27.36 – 53.90% (catalytic). Clearly, our findings revealed that the presence of all the supported metal catalysts promotes acid ketonization in the bio-oils, thereby lowering the acidity and enhancing the stability of the pyrolytic bio-oils. The incorporation of Fe_3O_4 in the catalysts system could be primarily responsible for promoting acid ketonization in this study. Ketonic-rich bio-oils are found to be suitable for producing gasoline, diesel and jet fuels (Wang *et al.* 2012). Previous research has also demonstrated iron oxide (Fe_3O_4) catalyst as effective for acids ketonization (Bennett *et al.* 2017). The catalytic pyrolysis of *Scenedesmus obliquus* over supported metal catalysts enhanced the quality of bio-oils with high stability and low acidity. The synergies between the doped metals and Fe_3O_4-HZSM-5 support could better-described the activity of the supported metal catalysts. Overall, among the catalysts, the Co/Fe_3O_4-HZSM-5 catalyst performed better in enhancing the pyrolytic bio-oil quality with highest HHV (40.78 MJ/kg), and also gave the highest bio-oil yield (17.73 wt %). Hence, the effect of

temperature and catalyst to biomass ratio on the product yield was further investigated using this catalyst.

4.3.3 Effect of Temperature

To assess the influence of temperature on the yield of products obtained when *Scenedesmus obliquus microalgae* was pyrolysed in the presence of Co/Fe_3O_4-HZSM-5 (catalyst: biomass ratio of 1:1), temperature between the range of 400 and 700 °C was varied. The results obtained are presented in Fig. 4.6. As the temperature was increased from 400 to 500 ^oC, the gas yield increased significantly from 44.81 wt% to 60 wt% at the expense of bio-oil yield which decreased from 24.97 wt% to 17.73 wt %. But also, due to increased cracking activity as a result of temperature increase to 500 °C, biochar yield reduced from 30.22 wt% to 22.27 wt%. This suggests higher conversion with increase in temperature to 500 °C. Again as temperature was increased from 500 to 700 °C, gas yield slightly increased from 60 wt% to 62.57 wt% with a decline in pyrolytic bio-oil yield from 17.73 wt% to 15.43 wt%. At higher temperature, the effect of secondary cracking reactions on the pyrolysis vapours could lead to higher gas yield. Above the temperature of 500 °C, little or no change was observed in the biochar yield suggesting highest conversion was attained at 500 °C. In summary, an increase in temperature favours production of more gas products. The highest conversion was attained at 500 °C while highest bio-oil yield was obtained at temperature of 400 °C. Catalytic pyrolysis of *Pavlova* sp. using ceria-based catalysts also reported similar findings; however, the authors obtained optimum bio-oil yield at 500 °C possible due to the difference in the microalgae composition and the type of catalyst employed (Aysu, Fermoso and Sanna 2018).

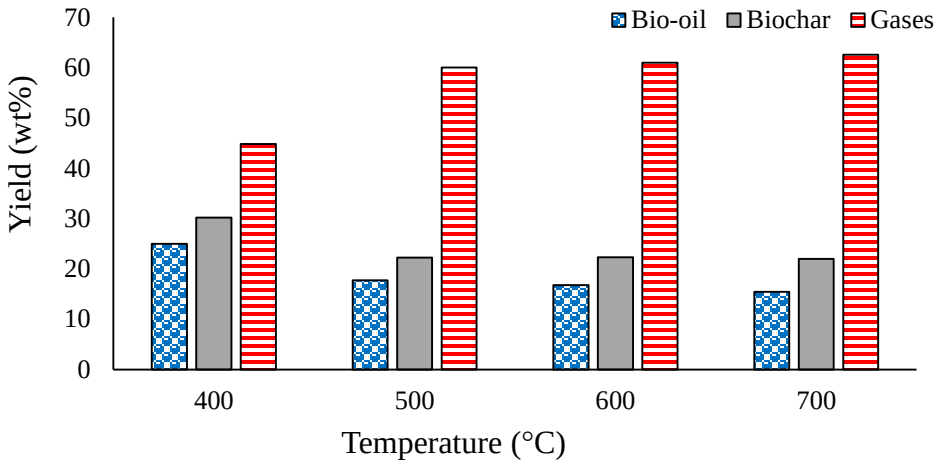

Figure 4.6. Effect of temperature on product yields obtained from pyrolysis of *S. obliquus* over Co/Fe_3O_4-HZSM-5 catalyst (catalyst to biomass ratio of 1:1)

4.3.4 Effect of Catalyst to Biomass (C:B) Ratio

The influence of catalyst-to-biomass (C:B) ratio (0.25:1, 0.5:1 and 1:1 g/g) at 500 °C on the yield of pyrolysis products using Co/Fe_3O_4-HZSM-5 was investigated, and result presented in Fig. 4.7. The bio-oil yield from pyrolysis test without catalyst was 46.37 wt% but significantly reduced to 28.92 wt%, 26.86 wt% and 17.73 wt% with the addition of Co/Fe_3O_4-HZSM-5 catalyst using C:B ratio of 0.25:1, 0.5:1 and 1:1 respectively. In contrast, the gas yield gradually accumulate as C:B ratio was increased and highest gas yield of 60 wt% was obtained using C:B ratio 1:1. A higher C:B ratio will ensure a longer time of exposure between the catalyst and pyrolysis vapours leading to an increase in the cracking of the vapours to favour the production of more gaseous products to the detriment of bio-oil product (Hernando *et al.* 2016). Although higher bio-oil yield was produced using C:B ratio of 0.25:1, however, the conversion was much higher with C:B ratio of 1:1 having lowest biochar yield (22.27 wt %) when

compared to biochar yields of the non-catalytic test (31.58 wt%) and catalytic using C:B ratio of 0.25:1 (36.88 wt%), and 0.5:1 (33.13 wt%).

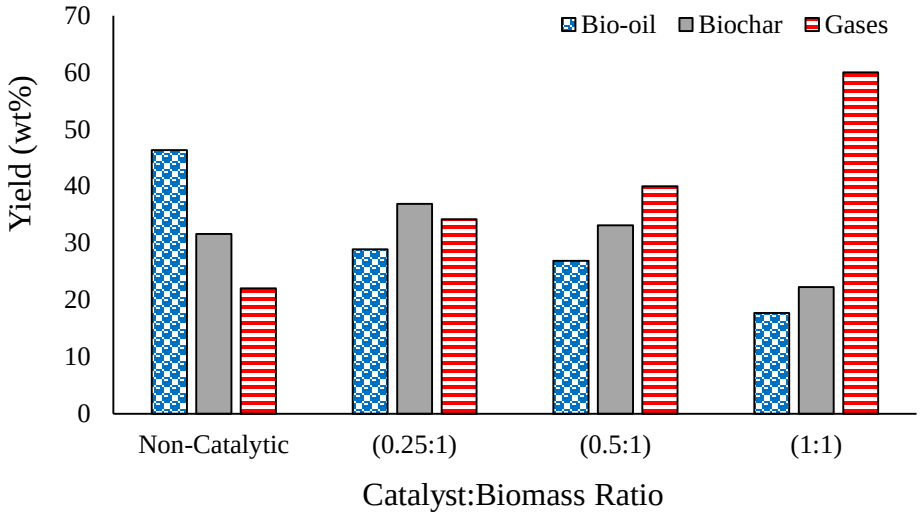

Figure 4.7. Effect of catalyst to biomass ratio on product yields obtained from pyrolysis of *S. obliquus* over Co/Fe_3O_4-HZSM-5 catalyst at 500 ^oC

4.4 Conclusion

The pyrolysis of *S. obliquus* microalgae in the presence of supported metal catalysts promotes deoxygenation, denitrogenation, aromatization and acid ketonization producing high-quality bio-oils with high stability and low acidity. The highest yield of pyrolytic bio-oil was attained at 400 °C while optimum conversion was achieved at 500 °C. The bio-oil yield was reduced while gas yield was promoted when the non-catalytic test was compared to catalytic tests. Among the catalysts, the Co/Fe_3O_4-HZSM-5 catalyst gave the maximum yield of bio-oil (17.73 wt%) while lowest yield of bio-oil (11.07 wt%) was obtained using W/Fe_3O_4-HZSM-5. Also, the produced pyrolytic heating values was found to increase from 38.27 MJ/kg (non-catalytic) to 39.70 – 40.78 MJ/kg with addition of supported metal catalysts. Overall, the Co/Fe_3O_4-HZSM-5 catalyst was the most effective for production of high-quality pyrolytic

bio-oil from nutrient-stressed *Scenedesmus obliquus* microalgae with properties close to that of crude petroleum.

CHAPTER 5

CATALYTIC HYDROTHERMAL LIQUEFACTION OF NUTRIENT-STRESSED MICROALGAE FOR PRODUCTION OF HIGH-QUALITY BIO-OIL

5.1 Introduction

Hydrothermal liquefaction (HTL) is considered to be a preferable thermal conversion method for production of bio-oil from aquatic biomass such as microalgae because biomass drying-step is not required, thus avoiding the high energy costs associated with biomass drying (Barreiro *et al.* 2013b; Lu *et al.* 2021). Besides, HTL is an interesting technique that utilises wet microalgae biomass for bio-oil production with low energy consumed in comparison to pyrolysis (Guo *et al.* 2015; Shakya *et al.* 2017b). Consequently, HTL has attracted growing interest as a promising technique to produce biofuels from microalgae. Despite the above-stated advantages, maximising the yield and quality of bio-oil product from the HTL of microalgae has been a challenge. For instance, due to the high nitrogen and oxygen content found in HTL bio-oils, there is the need for the bio-oils to be further processed before usage as fuel (Gollakota, Kishore and Gu 2017).

One of the most widely investigated approaches employed as a control strategy for addressing the problem of yield and quality of HTL bio-oils is the utilisation of various catalysts which improve the hydrothermal liquefaction process. Catalysts played an essential role in improving the quality and yield of bio-oil produced from HTL of microalgae (Vlaskin *et al.* 2017; Galadima and Muraza 2018). Past studies have reported a beneficial effect from the utilisation of catalysts in reducing the oxygen composition in bio-oil product as well as improving the yield of bio-oil (Xu *et al.* 2014; Ma *et al.* 2019). Majority of the earlier works were focusing on homogeneous catalyst using alkali or metallic salts for the generation of bio-

oils from the HTL conversion of microalgae (Ross *et al.* 2010; Jena, Das and Kastner 2012). Very recently, researchers have explored the use of heterogeneous catalysts because they are easy to separate, reusability and selectivity (Arun *et al.* 2020; Lu *et al.* 2020; Ma *et al.* 2020; Brindhadevi *et al.* 2021; Lu *et al.* 2021). Due to their high selectivity and activity, zeolitic based catalysts have been given priority above other heterogeneous catalysts for HTL and bio-oil upgrading. For example, Xu *et al.* (2014)) found increased yield of bio-oil (from 32% to 38%) with HZSM-5 as catalyst in the HTL of *Chlorella pyrenoidosa.* The authors further studied the effect of doping cerium on HZSM-5 (Ce/HZSM-5 catalyst) and found significant improvement in the yield of bio-oil (52%) when compared to the use of HZSM-5 alone (38%). Previous study by Ma *et al.* (2019)) investigated the HTL of *Ulva prolifera* with three different zeolites catalysts (Mordenite, Y-Zeolite and ZSM-5) and it was found that ZSM-5 catalyst showed superior performance in comparison to the other zeolite catalyst having the highest bio-oil yield (29.3 wt %). The authors also found that the oxygen content in HTL bio-oil was greatly reduced with the addiiton of ZSM-5 when in comparison to the use of mordenite and Y-zeolite as catalysts for the liquefaction process.

Based on this background, zeolites as catalysts have shown to be promising for enhancing the quality and yield of HTL bio-oil derived from microalgae, and also some studies have shown that the chances of making fuel-grade bio-fuels could be enhanced with zeolite catalysts especially with HZSM-5 (Dimitriadis and Bezergianni 2017). However, there is likelihood of catalyst deactivation during the HTL process because of decrement in the number of active sites related to the zeolite frameworks (Yeh *et al.* 2013). Also, the zeolitic framework degradation resulting from the synergistic impact of water and heat during hydrothermal conditions and the blockage of pores by carbonaceous deposits have been identified as possible

challenges that could affect the efficiency of the catalyst (Yeh *et al.* 2013). To address these challenges, some approaches have been suggested, which include the incorporation of metals in the catalyst or the use of fluoride media in the zeolite preparation (Galadima and Muraza 2018). For instance, the role of metal promoters (such as Ni, Zr or Ru) and incorporating support material like ZrO_2 could improve catalyst efficiency (Galadima and Muraza 2018).

Another approach yet to be explored with the thermal conversion process may involve the use of nitrogen stressed condition to alter the biomass feedstock composition for improved bio-oil product yield and quality. Microalgae have variable composition that depend largely on the species types, growth and environmental conditions (Xu *et al.* 2011). Studies have shown that the most notable changes under nitrogen limitation condition involve the accumulation of carbohydrates and/or lipids and degradation of proteins (Depraetere *et al.* 2015; Ikaran *et al.* 2015; Li *et al.* 2016; Liu *et al.* 2016). The yield and quality of bio-oil product derived from microalgae have been shown to be dependent on the microalgae's biochemical composition (Barreiro *et al.* 2013b). It is believed that the initial protein content of the microalgae feedstock significantly influences product quality as most of this nitrogen ends up in the liquefaction product (Saber *et al.* 2016). Thus, nitrogen alteration is seen as an approach that could provide the needed solution towards developing efficient and sustainable HTL process for quality biofuel production from various species of microalgae.

Scenedesmus obliquus microalgae was chosen in this study because of its high protein composition (Chen *et al.* 2014; Koley *et al.* 2018) and to stand in as baseline for high-quality HTL bio-oil production from high protein microalgae. Till date, very few studies are available for the catalytic HTL of *S. obliquus* microalgae (Koley *et al.* 2018; Kohansal, Tavasoli and Bozorg 2019; Arun *et al.* 2020). Recently, Kohansal, Tavasoli and Bozorg (2019)) and Arun

et al. (2020)) reported the use of heterogeneous catalysts such as Ni/AC, Ni/CeO_2, Ni/AC-CeO_2 and clamshell derived catalyst for the HTL of *S. obliquus* into bio-oil. The major finding from both works was higher bio-oil yield, but high nitrogen composition in the biofuel product remained a challenge, thereby affecting the quality of bio-oil produced. Hence, further research efforts are needed to identify better heterogeneous catalysts that can improve the quality of HTL bio-oil by simultaneously reducing oxygen and nitrogen content of the bio-oil product to meet desirable standard. To the best of the authors' knowledge, no previous work has documented the use of the zeolite-based catalyst for the HTL of *S. obliquus* microalgae.

5.2 Materials and Methods

5.2.1 Materials

Two different dry samples of *Scenedesmus obliquus* microalgae grown under different conditions were collected from the Institute of Water and Wastewater Technology, Durban University of Technology, Durban, South Africa. The first sample was grown under nitrogen stressed (150 mg/ml) BG 11 media (NSM) while the other sample was produced under the unstressed BG 11 media as the control sample (CM). A laboratory grinder was used for size reduction of the dry microalgae sample and sieved to <150 µm, and a desiccator was used to store the powder for further use. Analytical grade chemicals requiring no further purification were used in this study.

5.2.2 Microalgae Biomass Characterization

The Bligh and Dyer (1959)) procedure was used for total lipid extraction and analysis while the procedure detailed by Lowry *et al.* (1951)) was used for the determination of protein content. Carbohydrate analysis was done as per the procedure by Dubois *et al.* (1956)). The

moisture, volatile matter and ash content of the microalgae samples were estimated in line with ASTM standards (D1102, E-871 and E872). The elemental compositions of the samples were determined using an elemental analyser (Vario EL-II Elementar Analysensysteme GmbH, Hanau, Germany). The Dulong correlation (equation 5.1) was used to determine the HHV of the microalgae biomass (Saber *et al.* 2016). All tests and measurements were done in duplicates and the mean value was reported.

$$HHV\left(\frac{MJ}{kg}\right) = 0.338C + 1.428\left(H - \frac{O}{8}\right) + 0.095S \quad (5.1)$$

where C, H, O, and S represent percentage by weight of carbon, hydrogen, oxygen, and sulphur in the microalgae biomass, respectively.

5.2.3 Catalyst Preparation and Characterisation

Ammonium ZSM-5 (NH_4/ZSM-5) zeolite powder (SiO_2/Al_2O_3 mole ratio: 50:1, CBV5524G) was purchased from Zeolyst International, and HZSM-5 was obtained from the calcination of NH4/ZSM-5 at 550 °C for 5 h (Shakya *et al.* 2017a). Then, impregnation method was used to prepare the zirconium doped HZSM-5 (Zr/HZSM-5) catalyst. 20g of HZSM-5 powder was added into zirconium nitrate solutions (10 wt% loading) and mixed thoroughly using a homogeniser for 2 h at 80 °C. After that, the mixture was oven-dried at 105 °C overnight and allowed to be cooled, ground and finally screened through a 75 μm sieve. The obtained samples were calcined at 500 °C for 8 h and stored in a desiccator for further use.

The XRD pattern and crystalline nature of the synthesised catalyst were examined at a scanning angle range of 5 to 90° using PANalytical-Empyrean XRD equipped with a Cu Kα radiation source (λ=0.1541 nm). HRSEM was employed to study the morphology of the synthesised catalyst. Thermogravimetric analysis was carried out on the prepared catalysts

using TA instrument (SDT Q600) to analyse its thermal behaviour and stability. The programmed heating was done under N_2 atmosphere from 30 to 800 °C at 10 °C/min.

5.2.4 Hydrothermal Liquefaction Experiments

HTL Experiments were carried out using stainless autoclave of 50 mL capacity. An external electrical furnace was used to heat the autoclave, and a thermocouple was used to measure the temperature-controlled to ±1 K. For each sample of the *Scenedesmus obliquus* microalgae prepared as explained in the earlier section 5.2.1 (nutrient-stressed microalgae - NSM and control microalgae - CM), 2 g of the biomass sample with 18 ml of de-ionised water was placed into the autoclave reactor. For the catalytic experiments, 0.4g of the synthesised catalyst was mixed with the biomass and the reactor system was purged three times with pure N_2 (99.999%) to displace the air inside the system and then sealed. Thereafter, the reaction temperature was raised to the desired values (250 °C, 300 °C, or 350 °C), and the temperature was kept for 60 min. When the reaction time was completed, cooling water at room temperature was used to cool the autoclave rapidly. After that, separation of products from the liquefaction process consisting of the organic phase, water-soluble phase, solid residue, as well as the gaseous products was carried out. The non-condensable gas was vented, and separation of the solid-liquid mixed-phase was carried out using solvent-based phase separation. The autoclave wall and the liquid product fraction were washed with 20 mL of dichloromethane (DCM) (Sigma-Aldrich, 99% purity). Then, 20 mL of water was put in the mixture, and the separation of the two phases was done. The organic phase made up of bio-oils, and the water-soluble phase consisting of the aqueous products were collected independently. The filtration of the organic phase was done, and the residual solid material left on the filter paper was collected and dried at 105 °C for 24 h. The evaporation of dichloromethane solvent from the organic

phase was conducted to attain the actual bio-oil. Gravimetric methods, using equations 5.2 and 5.3, were employed to determine the bio-oil and biochar yield respectively. The weight difference (equation 5.4) was used to determine the total amount of the discarded products which include gases together with water-soluble products and possible losses due to experimental errors referred to as "gas + loss" in this study. The non-catalytic and catalytic experiments under the same liquefaction conditions were repeated twice, and the average result was used to determine the liquefaction product yield according to the following formula reported in Xu *et al.* (2014)).

$$Bio-oil\ yield\ (wt\%) = \frac{Weight\ of\ the\ boi-oil}{Weight\ of\ biomass} * 100 \quad (5.2)$$

$$Solid\ residue\ yield\ (wt\%) = \frac{Weight\ of\ the\ solid\ residue}{Weight\ of\ biomass} * 100 \quad (5.3)$$

$$(Gas + loss)\ (wt\%) = 100 - bio - oil\ yield(wt\%) - solid\ residue\ (wt\%) \quad (5.4)$$

5.2.5 HTL Bio-oil Analysis

The compounds in the bio-oil produced from the HTL reaction were analysed with GC-MS (Agilent 7890-5975C) using DB-1701 column (30m×0.25mm×0.25 μm). Helium was used as carrier gas at flow rate of 1.5 mL/min; 1 μL injection size; and 1: 60 split ratio. Starting GC oven temperature was kept at 40 °C for 3 min; then increased to 300 °C at a rate of 5.5 °C/min and held for 5 min; injector and detector temperature of 230 °C and 250 °C respectively. The compounds were identified using National Institute of Standards and Technology (NIST) mass spectral data library. The elemental composition and HHV of the HTL bio-oils were measured by adopting the technique outlined in section 5.2.2. The functional groups present in the HTL bio-oils were identified with Spectrum 100 FTIR (PerkinElmer Co.) using the KBr

pellet method. The scans were performed with a resolution of 4 cm^{-1} over a range of 400 to 4000 cm^{-1}.

5.3 Results and Discussion

5.3.1 Characterisation of *Scenedesmus obliquus* Microalgae Biomass

The proximate, ultimate and biochemical composition of the *Scenedesmus obliquus* microalgae grown under varied growth conditions is given in Table 5.1. The proximate analysis showed that the nutrient-stressed microalgae (NSM) have a moisture content (4.38%), ash content (10.17%), and volatile content (81.77%) while control microalgae (CM) has a moisture content (10.05%), ash content (14.91%), and volatile content (73.26%). The variation in the proximate analyses is a strong indication that nutrient stressing during microalgae cultivation could alter the microalgae composition. Table 5.1 shows that under nutrient-stressed condition, the protein content was greatly reduced from 42.35% to 22.08% and both carbohydrate and lipid content was increased from 25.36% to 42.55% and 17.16% to 21.62% respectively. The reduction in protein content observed with the NSM may be as a result of lower nitrogen resulting from nitrogen stress condition since protein accounts for the major intracellular nitrogen pools in microalgae. In the same vein, the decline in nitrogen could cause some metabolic processes resulting in the production and accumulation of high-energy compounds as neutral lipids, and/or carbohydrates (Lamers *et al.* 2012; Sajjadi *et al.* 2018). Some previously conducted research work has indicated that the microalgae composition could vary under different growth conditions. Xu *et al.* (2011) cultivated *Chlorella vulgaris* under standard nitrogen nutrient (0.150 kg/m^3) and low nitrogen (0.049 kg/m^3) nutrient condition. Under the nutrient-stressed condition, a reduction from 29 wt % to 6 wt % was observed for the protein content in the microalgae. In contrast, a significant increase from 19.70 wt % to 51

wt % was observed for the carbohydrate content. The reduction in the protein with increasing carbohydrate and lipid content observed under the nutrient-stressed environment is an important alteration in the biomass composition that could influence the biofuel product yield and quality.

Table 5.1. Properties of the *Scenedesmus obliquus* microalgae samples

	Nitrogen stressed microalgae (NSM)	Control microalgae (CM)
Biochemical composition (%)		
Lipid	21.62	17.16
Protein	22.08	42.35
Carbohydrate	42.55	25.36
Proximate Analysis (%)		
Moisture	4.38	10.05
Ash	10.17	14.91
Volatile matter	81.77	73.26
Fixed carbon (by difference)[a]	3.68	1.78
Ultimate Analysis (%)		
C	45.03	43.25
H	7.50	8.46
N	3.59	6.83
S	0.98	0.63
O (by difference)[b]	42.90	40.83
H/C	2.00	2.35
N/C	0.07	0.14
O/C	0.71	0.71
Heating value (MJ/kg)		
HHV	18.37	19.47

[a] Fixed carbon content (%)= 100% - (%moisture content + %Ash + % volatile matter)

[b] O composition (%) = 100% - %C + %H + %N + %S

It is believed that the starting composition of nitrogen will have a great influence on product quality, and most of the nitrogen in the HTL bio-oil product are attributed to the protein content of the microalgae feedstock. As shown in Table 5.1, the biochemical composition also indicated that *Scenedesmus obliquus* is a high protein microalgae under the unstressed BG11 growth condition referred to as the control microalgae in this study. High protein content (56.1%) was also reported by Koley *et al.* (2018)) for *Scenedesmus obliquus* microalgae. Table 5.1 also revealed the elemental composition of the *S. obliquus* microalgae with the control microalgae (CM) having high nitrogen content (6.83%) compared to nutrient-stressed microalgae (NSM) with a nitrogen content of 3.59%. The sulphur content in both microalgae samples was found to be < 1%. Previous studious have also reported the sulphur content of different microalgae strain, including *S obliquus* to be < 1% (Brown, Duan and Savage 2010; Shakya *et al.* 2015; Koley *et al.* 2018). To provide more meaningful comparison basis for different biomass samples, the characteristics of the biomass as a function of fuel efficiency and quality could be examined based on the elemental ratio such as N/C, H/C, and O/C. As shown in Table 5.1, the N/C value was significantly reduced to about 50% due to the effect of nutrient stressing on the microalgae. Nutrient stressing tend to increase the carbohydrate content leading to an increase the carbon content, as shown in Table 5.1. Thus a slightly higher H/C value was observed with the control microalgae because of lower carbon composition present in CM. Since the hydrogen content is lower to the carbon content of microalgae, variation in carbon content have a more pronounced effect on the microalgae composition than hydrogen content. Table 5.1 further shows that CM has a slightly higher HHV of 19.46 MJ/kg compared to the nutrient-stressed microalgae with HHV of 18.37 MJ/kg possible owing to lower oxygen composition present in CM. Previous studies have also shown that material with

lower O/C has higher HHV (López-González *et al.* 2014; Zainan *et al.* 2018). Our findings from the characterization of biomass considered in this study revealed that nutrient stressing during cultivation altered the microalgae biomass composition, especially the reduction of protein content and enhancement of carbohydrate and lipids content.

5.3.2 Catalyst Characterisation

Fig. 5.1(a) shows the XRD patterns of HZSM-5 alone and the zirconium doped HZSM-5 catalyst. The presence of diffraction peaks at 2θ = 7.9, 8.8, 23.2, 23.9 and 24.4° on both samples confirms the doped catalyst (Zr/ HZSM-5) retains the skeletal structure of HZSM-5 zeolites (Zhang *et al.* 2009). This is an indication that doping of zirconium did not affect or destroy the HZSM-5 zeolite framework. The peaks at 2θ = 31.5 and 37.5° were attributed to XRD peaks of a monocyclic ZrO_2 present in the doped HZSM-5 (Mangla and Roy 2018) which is an indication that zirconium species were dispersed on the HZSM-5 support. The relative crystallinity of the zirconium doped HZSM-5 (89.03%) was observed to be slightly lower than that of the undoped HZSM-5 (92.10%). The slight decrease observed could be as a result of the intermixing of the zirconium species with the HZSM-5 support. The TGA-DSC profile of the synthesised catalyst is shown in Fig. 5.1b. The TGA curve showed a slight weight loss of < 5% indicating loss of moisture content within the temperature range of 50 to 200 ºC. Above this temperature up to 600 ºC, the TGA curve showed the synthesised catalyst was stable, which further confirm the thermal stability of the synthesised catalyst. The morphology of the doped and undoped HZSM-5 was determined using SEM and compared (see Fig. 5.1c and 5.1d). The HZSM-5 alone showed an elongated prismatic-like agglomerative morphology and dispersion of the zirconium species were observed on the doped HZSM-5. The agglomerating

tendency exhibited by the HZSM-5 with zirconium modification is also an indication it can be used for liquefaction (Arun *et al.* 2020).

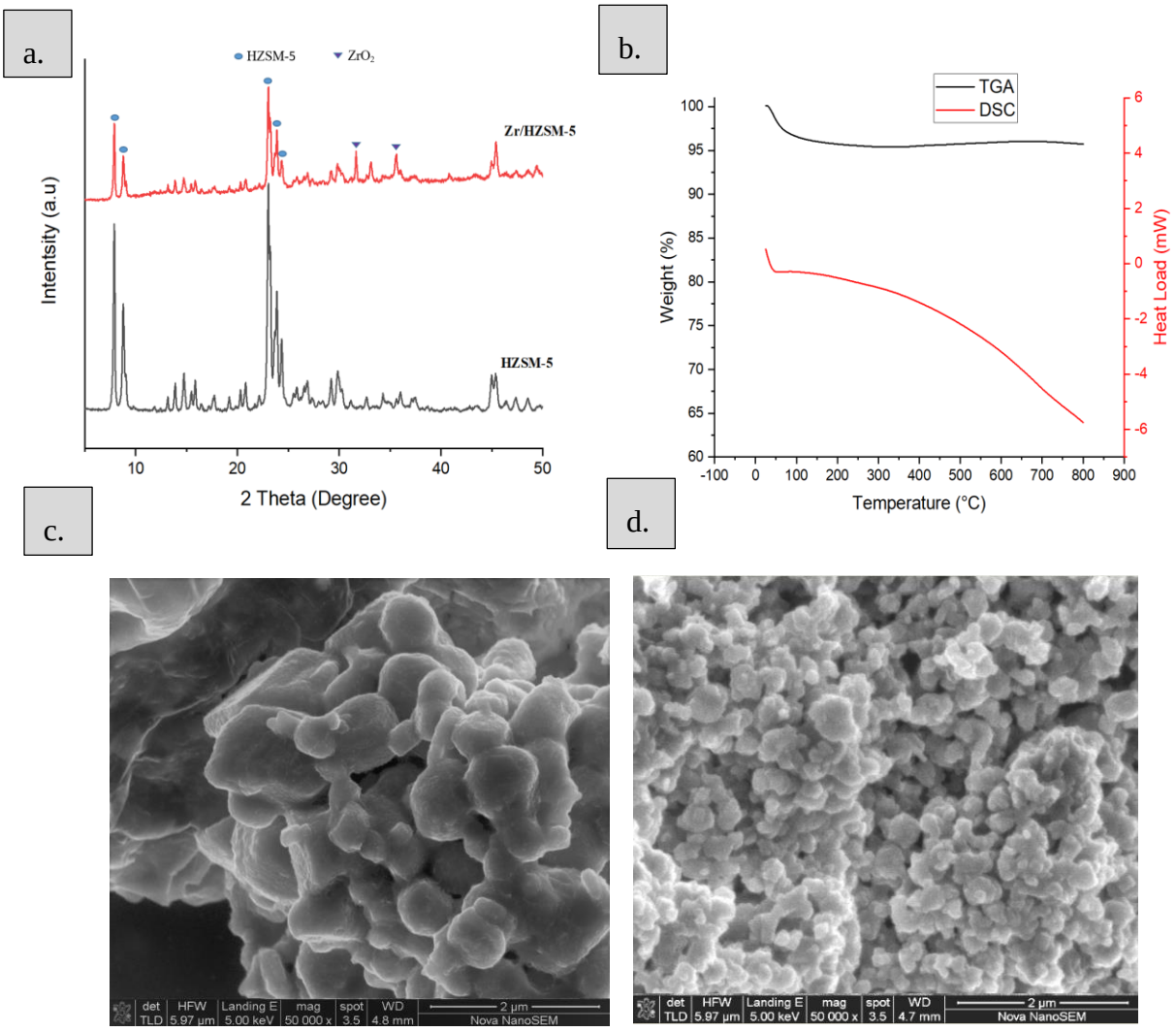

Figure 5.1 (a) XRD pattern (b) TGA/DSC (c) SEM image of HZSM-5 (d) SEM image of Zr/HZSM-5

5.3.3 Liquefaction Product Yields

The distribution and yield of products obtained from HTL of nutrient-stressed and unstressed *Scenedesmus obliquus* microalgae with and without catalyst are presented in Fig. 5.2. During

the non-catalytic HTL process, an increase in temperature result in higher bio-oil yield with the maximum yield of bio-oil recorded at 350 ºC for both samples of nutrient-stressed microalgae (NSM) and the unstressed control microalgae (CM). The NSM and CM showed the maximum bio-oil yield of 39.07 wt% and 17.19 wt% respectively at 350 ˚C. As shown in Fig. 5.2, both the bio-oil and gas yield increased while the biochar yield decreased as temperature was raised from 250 ˚C to 350 ˚C for both NSM and CM. At increased temperatures, the activation energy needed for bond dissociation is easily overcome with extensive decomposition/depolymerisation of the biomass resulting in higher bio-oil yield (Brown, Duan and Savage 2010). Lipids become hydrolysed into glycerol and fatty acids during the early stage of the HTL process. Fatty acids contribute to the generation of bio-oil, while the glycerol is responsible for the aqueous phase. However, at a higher temperature, the glycerol can be further hydrolysed and decomposed into smaller alcohols or aldehydes, thereby increasing the bio-oil yield. The HTL process can also result in the hydrolysis of carbohydrates to products that are soluble in the aqueous phase. At higher temperature, the glucose in the aqueous phase can then be converted into bio-oil, thereby increasing the bio-yield (Shakya *et al.* 2015). When compared to CM, the liquefaction of NSM at 350 °C gave higher bio-oil yield (39.07 wt%) possibly because of its high lipid and carbohydrate content. This shows that the yield of bio-oil was dependent on microalgae composition, and higher lipid and carbohydrate content in the biomass enhanced bio-oil yield. Some previous investigations on HTL of microalgae at different temperatures also observed similar trends in product yields (Shakya *et al.* 2017b; He *et al.* 2020).

Also, Fig. 5.2 shows that the yield of bio-oil was raised from 8.6 wt% to 17.19 wt% and 12.54 wt% to 39.07 wt% for CM and NSM, respectively as the temperature was increased

from 250 °C to 350 °C. The high protein content in the CM microalgae could be responsible for the lower yield of bio-oil (8.6 wt%) obtained at 250 °C. The peptide bonds in proteins are usually more stable than glycosidic bonds in carbohydrates at lower temperatures, and that may be responsible for slow hydrolysis of protein (Rogalinski *et al.* 2008). However, an increase in temperature usually enhanced hydrolysis of proteins and may be responsible for the rise in bio-oil yield observed with increase in temperature. This corroborated the results from GC-MS analysis shown in Fig. 5.4, which also revealed higher nitrogen-containing compounds with increase in temperature due to protein decomposition. A significant decrease in the yield of biochar (68 wt% to 31.47 wt%) was found with increase of temperature from 250 °C to 350 °C for CM. A similar trend was observed with the biochar yield from NSM. The decrease in biochar yield due to an increase in temperature may be ascribed to the severity of the conversion of volatile matter content in the microalgae to biofuel products. Most of the products passed through secondary decompositions (cracking) with increase in temperature, resulting in higher bio-oil and gas yields (Abu El-Rub, Bramer and Brem 2004).

With the addition of Zr/HZSM-5 catalyst during the HTL process, increase in temperature also increased the yield of bio-oil. The highest bio-oil yield of 52.8 wt% for NSM and 24.27 wt% for CM was obtained at a temperature of 350 °C, as shown in Fig. 5.2. This shows an increment of 35.14 % for NSM and 41.19 % for CM when compared to the bio-oil yield without catalyst under the same temperature condition. As stated earlier, composition of algal biomass could have a strong influence on the yield of bio-oil; lower lipid and carbohydrate content could be mostly responsible for the lower yield of bio-oil observed with the CM biomass. For all the temperature conditions studied, the catalytic group produced higher yield of bio-oil when compared with the non – catalytic group. This is an indication that

the use of Zr/HZSM-5 catalyst was beneficial and improved the bio-oil yield from the liquefaction of NSM and CM. The work of Xu *et al.* (2014)) also showed higher yield of bio-oil with the addition of Ce/HZSM-5 catalyst for the HTL of *C. pyrenoidosa*. Though much detail was not reported about the composition of *C. pyrenoidosa*, the findings from the study revealed that the use of HZSM-5 and Ce/HZSM-5 catalyst increased the yield of bio-oil from 33% (non-catalytic) to 34.02% and 49.87% respectively. This indicates that better catalytic effect on HTL bio-oil yield was induced by Ce modification on HZSM-5.

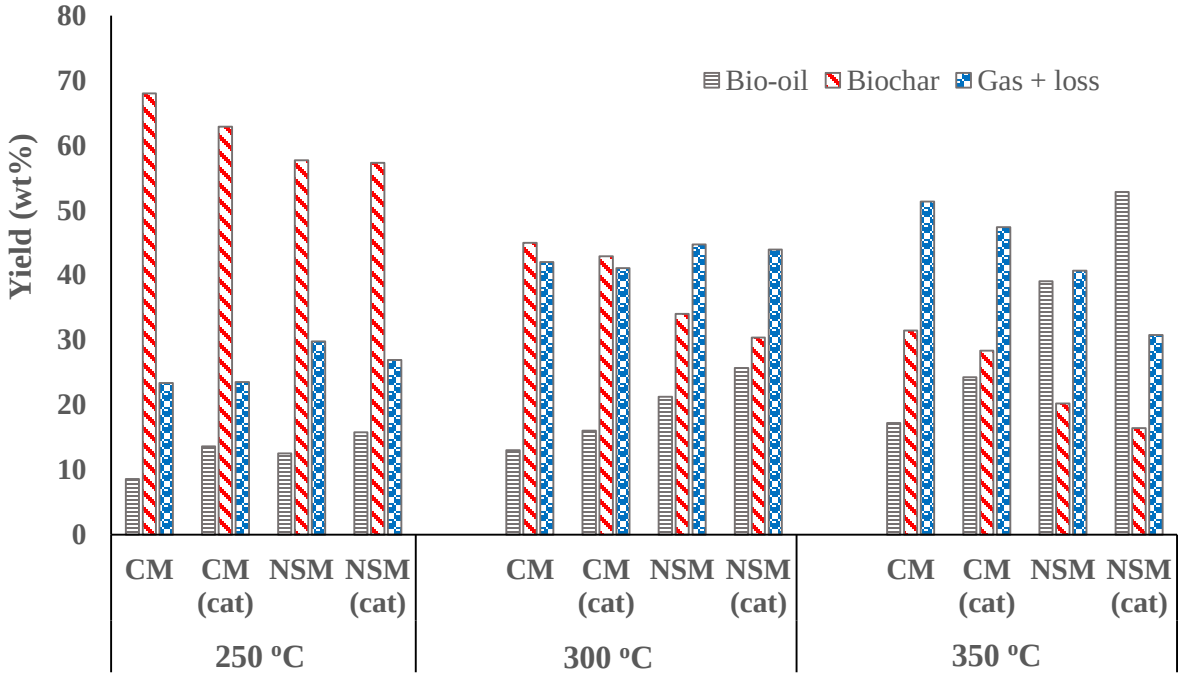

CM - Control microalgae, CM (cat)- Control microalgae with catalyst
NSM - Nutrient stressed microalgae, NSM (cat) - Nutrient stressed microalgae with catalyst

Figure 5.2. Product distribution from HTL of nutrient stressed and unstressed *Scenedesmus obliquus* microalgae with and without Zr/HZSM-5 catalyst

5.3.4 HTL Bio-oil Characterization

5.3.4.1 Elemental Analysis

The elemental composition, atomic ratios and HHV of the bio-oil produced from the HTL of NSM and CM at 350 °C with and without Zr/HZSM-5 catalyst are presented in Table 5.2. The characteristics of the raw microalgae before HTL and conventional petroleum crude are also shown for comparison with the produced HTL bio-oils. The hydrogen and carbon composition in the HTL bio-oil from NSM were 13.22 wt% and 70.56 wt% which translates to an increment of 76.27% and 56.70% for hydrogen and carbon, respectively when compared with the raw NSM. The use of catalyst further increased the carbon content to 73.68 wt% and hydrogen content to 14.38 wt% translating to an increment of 63.62% and 91.73% respectively when compared with the raw NSM. The hydrogen content in the bio-oils obtained from the HTL of NSM with and without catalyst was found to be in the range specified for petroleum crude (10 -14 wt%), but, the carbon content is slightly lower to that of petroleum crude as shown in Table 5.2.

A similar trend was observed with the CM where the carbon and hydrogen content significantly increased when compared to the raw CM, and it further increased with the addition of catalyst. However, higher carbon and hydrogen content resulting in higher HHV was found with bio-oil from NSM when compared to CM with or without the use of catalyst. Interestingly, the nitrogen content of the raw *S. obliquus* microalgae decreased from 6.83 wt% to 3.59 wt% under the nutrient-stressed condition. Before the liquefaction process, a significant reduction of 47.43 wt% in the nitrogen content was achieved with nutrient stressing during the microalgae cultivation. After the liquefaction process, the nitrogen composition for NSM bio-oil without catalyst was 1.99 wt% and further reduced to 1.40 wt% in the presence of catalyst.

These values were found to be within the specified value for nitrogen content of petroleum crude (0.1 – 2 wt%).

On the other hand, the case of CM with high protein content showed a contrary trend. The nitrogen content in the HTL bio-oil without catalyst was found to be 8.55 wt% and slightly reduced to 7.78 wt% in the presence of catalyst. This shows that the bio-oil products from CM have high nitrogen content and will be required to be processed further before being used as fuel. At higher temperature close to the subcritical temperature, protein easily gets hydrolysed leading to higher bio-oil yield with a relative abundance of nitrogenous compounds (Shakya *et al.* 2017b).

Table 5.2. Elemental analysis, atomic ratios and HHV of HTL bio-oil from *Scenedesmus Obliquus* microalgae at 350 °C

Condition	Elemental analysis					Atomic ratios			HHV (MJ/kg)
	C (%)	H (%)	N (%)	S (%)	O (%)	H/C	N/C	O/C	
Raw NSM	45.03	7.50	3.59	0.98	42.90	2.00	0.07	0.71	18.37
Non-catalytic NSM	70.56	13.22	1.99	0.35	13.88	2.25	0.02	0.15	40.28
Catalytic NSM	73.68	14.38	1.40	0.01	10.54	2.34	0.02	0.11	43.56
Raw CM	43.25	8.46	6.83	0.63	40.83	2.35	0.14	0.71	19.47
Non-catalytic CM	65.61	11.01	8.55	0.59	14.24	2.01	0.11	0.16	35.41
Catalytic CM	71.13	12.12	7.78	0.33	8.64	2.04	0.09	0.09	39.84
Petroleum crude	83 - 87	10 - 14	0.1 - 2	0.1 - 1.5	0.5 - 6	-	-	-	42.25 - 48.47

It is evident from the elemental analysis (see Table 5.2) that nutrient-stressed microalgae with the use of catalyst (Zr/HZSM-5) drastically reduced the nitrogen content of HTL bio-oil obtained from a high protein *S. obliquus* microalgae to acceptable limits recommended for petroleum crude. Also, addition of catalyst during the HTL greatly reduced the oxygen content of the produced bio-oils. From all the temperature conditions studied, the sulphur content was found to be < 1 wt% and fall within the range of 0.1 to 1.5 wt% for petroleum crude (Saber *et al.* 2016). The HHV of the bio-oils from NSM were higher than those of CM for all conditions due to their higher carbon and hydrogen content, and lower oxygen content. The highest HHV (43.56 MJ/kg) was found for bio-oil derived from catalytic HTL of NSM and this value compared well within the specified range (42.25 – 48.47 MJ/kg) for petroleum crude (Saber *et al.* 2016). The atomic ratio H/C increased from 2.00 to 2.25 in the bio-oil from non-catalytic NSM and further increased to 2.34 in the presence of catalyst.

On the other hand, a decline in H/C from 2.35 to 2.01 was observed with the bio-oil from CM. As shown in Table 5.2, a reduction in O/C value was observed for both NSM and CM bio-oil due to the decrease in oxygen content and an increase in the carbon content. The use of NSM resulted in a very low N/C ratio (0.02) for both catalytic and non-catalytic process. The low N/C value is attributable to the low nitrogen content present in the NSM bio-oil. Although the N/C ratio of CM bio-oil reduced from 0.14 to 0.11 without catalyst and further reduced to 0.09 in the presence of catalyst, these values obtained are still very high when compared to those obtained for NSM. This confirms the suitability of nutrient-stressed approach towards enhancing the quality and yield of HTL bio-oil derived from microalgae.

5.3.4.2 FTIR Analyses

Fig. 5.3 shows the comparism of the FTIR spectra of the bio-oils from HTL of NSM and CM with and without Zr/HZSM-5 catalyst at a temperature of 300 °C and 350 °C. The assignments and interpretation of spectral peaks was made based on literature (Gai *et al.* 2014; Shakya *et al.* 2017b). The peaks observed at 2800 – 3000 cm^{-1} were attributed to C-H and O-H stretching, thus showing the presence of alkanes and alkyls. These peaks were more prominent at 350 °C than 300 °C for both NSM and CM. At 300 °C, the broad bands at 950 – 1300 cm^{-1} attributed to C-O and O-H bending indicated the presence of ethers, alcohols and esters in both NSM and CM bio-oils. With the use of catalyst, absorption bands at 700–950 cm^{-1} show the presence of aromatic compounds and their derivatives (Hadhoum *et al.* 2019). The work of Dimitriadis and Bezergianni (2017)) have also established that aromatics formation could be enhanced in the presence of zeolite catalyst, especially with HZSM-5. As shown in Fig. 5.3, due to the extensive decomposition/depolymerisation of the biomass taken place at 350 °C, more peaks were observed compared to those obtained at 300 °C. The intense peaks observed between 1690 – 1750 cm^{-1} for both NSM and CM bio-oil at 350 °C were linked to the carbonyl stretching C=O suggesting presence of carboxylic acids, aldehydes, amides, esters and ketones. Also, the absorption peak at 1377 – 1462 cm^{-1} attributable to the C-H bending vibration suggests the presence of esters and alkyls. The absorption peaks at 1525 – 1575 $cm^{-1,}$ which corresponded to N-H bending, indicated the presence of amide compounds and were more prominent in the high protein microalgae CM bio-oil compared to NSM bio-oil. This is an indication of the presence of more nitrogen compounds in CM relative to NSM and further corroborated the elemental composition analysis results. The FTIR analyses also agreed well with the results from GC-MS analysis shown in Fig. 5.4.

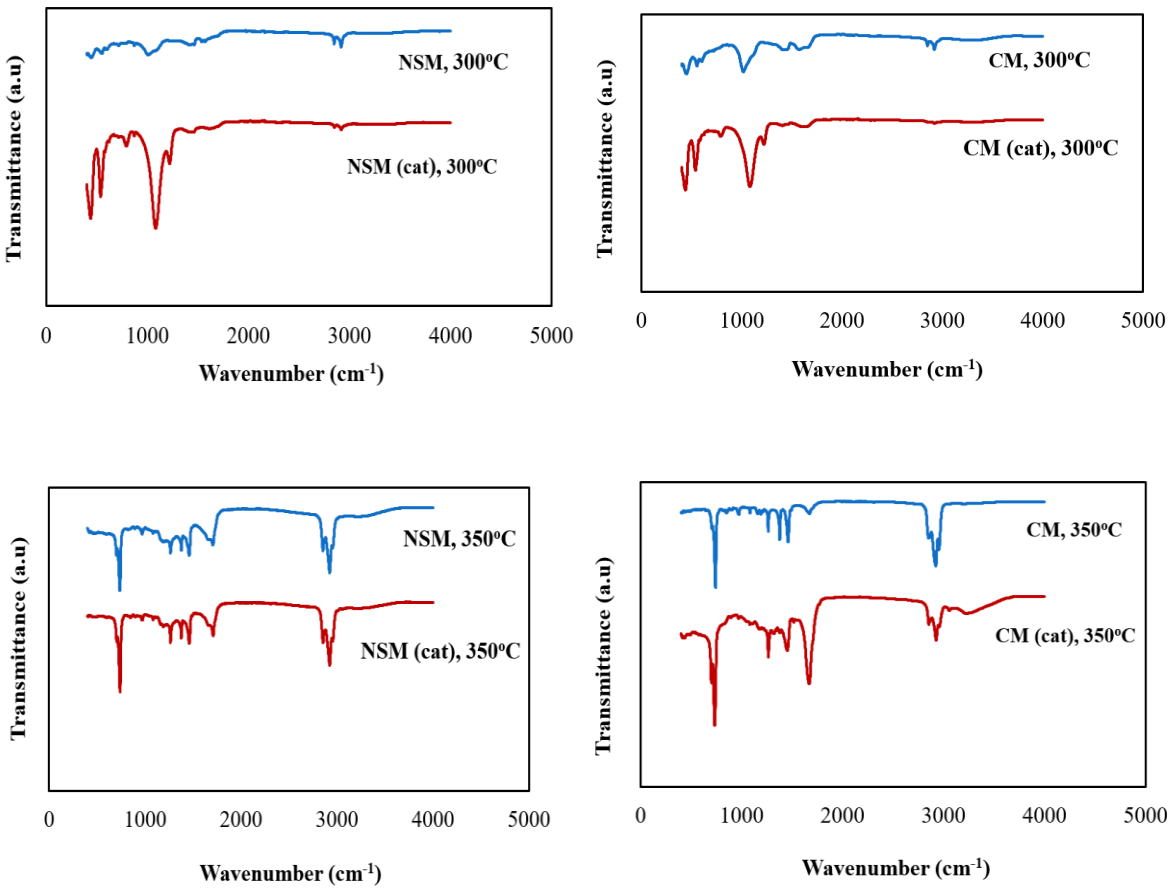

Figure 5.3. FTIR spectra of bio-oil produced from HTL of nutrient stressed and unstressed *Scenedesmus obliquus* microalgae with and without Zr/HZSM-5 catalyst at 300 ˚C and 350 ˚C.

5.3.4.3 GC-MS Analysis

The compounds present in the produced HTL bio-oils were identified using GC-MS. The main compounds identified and their distribution in bio-oils obtained from HTL of NSM and CM with and without catalyst at 300 ˚C and 350 ˚C are presented in Figure 5.4. The individual chemical compounds present in the HTL bio-oils and their relative abundance are presented in Table C5.1 – 5.8. The dominant mechanism at the early stage of liquefaction is hydrolysis followed by decomposition of the biomass via dehydration, decarboxylation, and deamination (Jena *et al.* 2015). As shown in Fig. 5.4 and Table C5.1 for NSM with high lipid

and carbohydrate content at 300 ºC, the most abundant compounds observed were fatty acids (52.01%) and oxygenated compounds (42.90%). Hydrolysis of lipids in subcritical water can lead to bio-oil containing high content of fatty acids while decomposition of carbohydrates and protein resulted in the formation of most of the oxygen-containing compounds. The most abundant fatty acid found in NSM bio-oil at 300 ºC was stearic acid. Other fatty acids like pentadecanoic acid, 9-octadecenoic acid and hexadecanoic acid were also observed. Among the oxygen-containing compounds present in the bio-oil, the most prominent was 9-octadecenal. The results also showed that the bio-oil contains nitrogen containing compounds like amides and alkanes/alkenes compound such as heptadecane and 1-decene. With the addition of catalyst to the HTL process at 300 °C, the resultant bio-oils comprises of combination of fatty acids, alkanes/alkenes, aromatic derivatives, nitrogen and oxygen containing compounds. As shown in Fig. 5.4 and Table C5.2, the reduction in the fatty acids was observed in the presence of catalyst when compared to the non-catalytic process. This could be a result of the formation of hydrocarbons from decarboxylated fatty acids. This is evident with the increase in the alkanes/alkenes derivatives and aromatic derivatives observed in the presence of catalyst relative to the non-catalysed process. The addition of catalyst at 300 °C showed that the nitrogen-containing compounds decreased while oxygenates were slightly increased.

In the case of the CM at 300 °C shown in Fig. 5.4 and Table C5.3, the fatty acid has 42.25%, which is less than 52.01% observed in NSM under the same condition. The fatty acids with the highest content are pentadecanoic acid and octadecanoic acid (see Table C5.3). As expected for high protein microalgae like CM, the bio-oil contains high nitrogen-containing compounds (13.57%) which are far greater than that obtained with NSM (4.13%) under the

same conditions. The degradation of proteins increased the bio-oil yields with a resultant increase in the nitrogen content of the product (He *et al.* 2020).

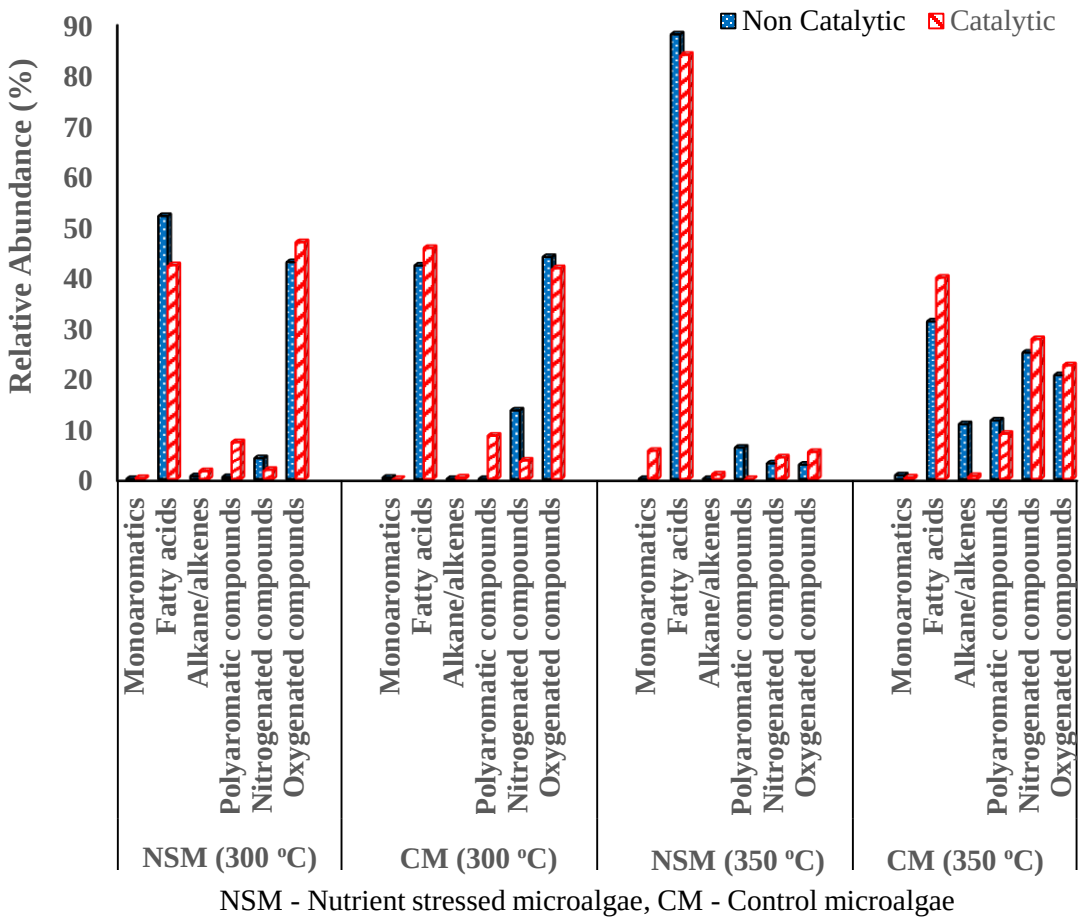

Figure 5.4. Distribution of main compounds in HTL bio-oils produced from nutrient stressed and unstressed *Scenedesmus obliquus* microalgae with and without Zr/HZSM-5 catalyst at 300 ˚C and 350 ˚C.

With the use of Zr/HZSM-5 catalyst on the HTL of CM, as shown in Fig. 5.4 and Table C5.4, the amount of nitrogen-containing compounds were significantly reduced with little or no difference in the oxygenates related compounds. Unlike the NSM, the use of catalyst

increases the fatty acid in the bio-oil derived from CM. This suggests that the addition of catalyst increases the hydrolysis of lipids to fatty acids. The amino acids present in the protein undergo decarboxylation and deamination reactions in the hydrothermal media to produce amides and organic acids (Shakya *et al.* 2017b).

As the temperature of the HTL process increases to 350 °C for NSM shown in Fig. 5.4 and Table C5.5, fatty acid was the most abundant with a reduction in the oxygen-containing compounds observed. The increase in the fatty acid content from 52.01% to 87.86% could be due to increase hydrolysis of lipid at a higher temperature. At 350 °C, the most abundant fatty acid in NSM was found to be cis-vaccenic acid (omega-7- fatty acid) reported to have great health benefit in reducing the prevalence rate of obesity, cancer and cardiovascular disease (Wang and Lee 2015). This could be explored for the possibility of extracting products of great value from the bio-oil for applications other than biofuels. Fig. 5.4 also showed that higher temperature resulted in lower nitrogen and oxygen compounds in the HTL bio-oil. The reduction in the oxygen and nitrogen compounds observed from GC-MS analysis corroborate with the elemental composition earlier discussed in section 5.3.4.1. Furthermore, the decarboxylation of fatty acids to form aromatic derivatives was also observed.

In the presence of catalyst for the HTL of NSM at 350 °C as shown in Fig. 5.4 and Table C5.6, more compounds such as benzene derivative, alkane/alkene, esters, phenol, amine, formamide, and other organics acids were observed indicating excessive degradation and decomposition of NSM. This is evident with the remarkable increase in the bio-oil yield obtained from HTL of NSM with use of catalyst when compared to without catalyst.

In the case of CM at 350 °C shown in Fig. 5.4 and Table C5.7, octadecanoic acid is the most abundant in the HTL bio-oil and other components such as N-containing compound,

alkane/alkene, esters, and aromatic derivative were also present. The hydrolysis of protein contributed to the high nitrogen-containing compounds like pyrazine, pyrrole, amine and amide present in the bio-oil. A broad spectrum of oxygen-containing compounds like phenols and its derivatives were produced from the hydrolysis of carbohydrate. With the use of catalyst at 350 °C for HTL of CM as shown in Fig. 5.4 and Table C5.8, a slight increase was observed in the fatty acid content, nitrogen-containing compound and the oxygen-containing compounds. Similar to the CM without catalyst, octadecanoic acid was found to be the most abundant compound present in the bio-oil. Other compounds such as N-containing compound, alkane/alkene, esters, and aromatic derivative were also present in the bio-oil. The presence of chlorophyll derivative such as phytol was observed, which can be as a result of the decomposition of chlorophyll present in the microalgae. The GC-MS results show that higher denitrogenation and deoxygenation was achieved with NSM with or without the use of catalyst when compared to CM. The use of Zr/HZSM-5 catalyst on both NSM and CM promoted the production of more aromatic derivative in the HTL bio-oil.

5.4 Conclusion

In summary, the effects of nutrient-stressed condition and the use of Zr/HZSM-5 catalyst on the hydrothermal liquefaction of high protein *Scenedesmus obliquus* microalgae at temperatures of 250 °C, 300 °C and 350 °C were investigated. The results showed that nutrient-stressed condition altered the microalgae compositions, especially the reduction of protein content and enhancement of the lipid and carbohydrate contents. The bio-oil yield and properties were dependent on feedstock composition and reaction conditions (temperature, catalytic or non-catalytic). The maximum yield of bio-oil (52.8 wt%) was produced from the HTL of nutrient-stressed microalgae (NSM) with addition of catalyst at 350 °C. Under this

condition, the nitrogen and oxygen content present in the produced HTL bio-oil was significantly reduced having high heating value (43.56 MJ/kg) which falls within the range specified for crude petroleum (42 – 48 MJ/kg). When compared with NSM, the unstressed *Scenedesmus obliquus* microalgae (CM) with or without catalyst produced bio-oils with lower yield and HHV as well as bio-oil products with high nitrogen content that will require further processing before being used as fuel. This study confirms the suitability of the nutrient-stressed *Scenedesmus obliquus* microalgae as hydrothermal liquefaction feedstock for high-quality bio-oil production.

CHAPTER 6

HYDROTHERMAL GASIFICATION OF MICROALGAE AND ITS DERIVATIVES: A THERMODYNAMIC STUDY USING ASPEN PLUS

6.1 Introduction

Hydrothermal gasification (HTG) also known as supercritical water gasification (SCWG) has been identified as a viable route for the production of high-quality methane and hydrogen-rich gas from wet algal biomass (Jiao *et al.* 2017; Duan *et al.* 2018). Hydrogen is a clean energy, and both hydrogen and methane are considered essential components of the world's future energy portfolio (Onwudili *et al.* 2013; Mathimani *et al.* 2019). HTG operates at relatively lower temperatures (400–700 ºC) and pressures (24–36 MPa) in the absence or presence of catalysts compared to that employed in the traditional air/steam gasification of dry biomass feedstocks (Liu *et al.* 2018; Atikah and Harun 2019). The traditional gasification of coal and other low ash lignocellulose biomass is widely known and has been commercialized (Chen *et al.* 2015; Bharath *et al.* 2018; Karatas and Akgun 2018; Lajili *et al.* 2018; Liu *et al.* 2018; Widjaya *et al.* 2018; Xiao *et al.* 2018). On the other hand, experimentally studies have been investigated on hydrothermal gasification of microalgae over the years and commercialization not yet accomplished (Stucki *et al.* 2009; Onwudili *et al.* 2013; Duan *et al.* 2018). For instance, the work of Stucki *et al.* (2009) demonstrated the possibility of achieving complete gasification of *Spirulina platensis* microalgae to methane-rich gas in supercritical water with ruthenium as a catalyst. Onwudili *et al.* (2013) studied the production of hydrogen from three different algae (*Chlorella vulgaris, Spirulina platensis and Saccharina latissima*) under supercritical water gasification conditions at 500 ºC, and 36 MPa. Among the different algae considered, *Saccharina*, a carbohydrate-rich macro-alga, gave the highest hydrogen gas

yield of 15.1 mol/kg. The variation in product distribution from the three algae samples were linked to their different biochemical compositions. Recently, Duan *et al.* (2018) studied the hydrothermal gasification of the *Chlorella pyrenoidosa* microalgae over a two-component catalyst mixture of Ru/C and Rh/C. The effect of temperature (380–600 ºC), water density (0–0.197 g/cm3), and catalyst loading (0–20wt %) on the yield, and composition of the gaseous products was examined. Higher gasification efficiency, gas yield and low tar were reported via this route. Till date, hydrothermal gasification of microalgae has not received sufficient attention. The effect of process factors such as biomass feedstock composition, biomass concentration, gasification temperature, gasification pressure, and residence time on gas products yield and selectivity needs to be well understood for the development of optimal processing technique.

Thermodynamic modelling approach is faster, economically more attractive and can be applied to determine the optimum experimental operating conditions with high accuracy (Adnan *et al.* 2017). The experimental works on hydrothermal gasification are time-consuming and expensive in terms of investment cost and consumable materials (Adnan and Hossain 2018a; Raheem *et al.* 2019). Hence, it is necessary to develop a reliable thermodynamic model to simulate the process behaviour to save time and resources. Previous studies on thermodynamic modelling have been carried out to investigate various aspects of traditional air/steam gasification of dry biomass feedstocks (Adnan *et al.* 2017; Adnan and Hossain 2018a; Atikah and Harun 2019). However, there is a scarcity of modelling work on hydrothermal gasification of microalgae using Aspen Plus or any other simulation software. We report here for the first time the thermodynamic modelling and simulation of the hydrothermal gasification performance of a *Scenedesmus obliquus* microalgae and its

derivatives (lipid and residual algal biomass) using Aspen Plus. This is an attempt to create a link between the experimental and modelling aspect of hydrothermal gasification processing of microalgae which highlight the usefulness and novelty of this study. The thermodynamic model analysis proposed will serve as a useful tool to design, simulate and optimize the hydrothermal gasification processing of microalgae.

6.2 Experimental

6.2.1 Feedstock Characterisation

Scenedesmus obliquus microalgae grown under BG 11 media was collected from the Institute of water and wastewater technology, Durban University of Technology, Durban, South Africa. The lipid content from the microalgae was extracted using the solvent extraction method reported by Bligh and Dyer (1959)). In this study, the whole algae biomass, lipids and the lipid extracted algae (LEA) are considered as feedstocks for the hydrothermal gasification process.

The proximate, ultimate and higher heating values (HHV) of the whole algae, lipid and LEA were determined using methods described by Saber *et al.* (2016)), and the data are presented in Table 6.1.

Table 6.1. Feedstock composition for the hydrothermal gasification process

	Whole algae	Lipid	Lipid extracted algae (LEA)
Proximate Analysis (%)			
Moisture	10.05	4.17	9.23
Ash	14.91	11.94	13.95
Volatile matter	73.26	76.29	70.46
Fixed carbon	1.78	7.60	6.36
Ultimate Analysis (%)			
C	43.25	54.19	42.37
H	8.46	10.12	8.16
N	6.83	2.81	7.28
S	0.63	0.02	0.57
O	40.83	32.87	41.62
Heating value (MJ/kg)			
HHV	19.47	26.89	18.60

6.2.2 Hydrothermal Gasification Process Modelling with Aspen Plus

6.2.2.1 Process Description

The hydrothermal gasification model based on Gibbs free energy minimisation was developed using Aspen Plus (Version 11). The simulation methodology reported by Atikah and Harun (2019)) was adopted with slight modifications. The list of components added to the simulation includes a non-conventional element (biomass and ash), conventional element (hydrogen, nitrogen, oxygen, sulfur, carbon monoxide, carbon dioxide, methane, water, ammonia, and hydrogen sulfide), and solid element (carbon). The non-conventional components are modelled by their proximate and ultimate analyses. The HCOALGEN and

DCOALIGT models were used to determine the enthalpy and density of both non-conventional components. The Peng-Robinson with Boston-Mathias function (PR-BM) property method was considered for this simulation as it provides good accuracy for gasification simulations (Fernandez-Lopez *et al.* 2017; Adnan and Hossain 2018a; Adeniyi *et al.* 2020).

Fig. 6.1 shows the Aspen plus flow sheet diagram for the simulation model and Table 6.2 provides a summary of the units used in the simulation model. A 10 kg/hr of biomass feedstock was used in all the simulation runs, and the hydrothermal gasification process was simulated using the RYield and RGibbs reactors. The RYield was used for modelling the decomposition of the biomass feedstock in which the non-conventional biomass was converted to conventional components (H_2, N_2, S, O, H_2O) and solid component (carbon and ash). An initial assumption was made for the yield of decomposer products in the RYield, and a calculator block was added to the Aspen simulation to calculate the actual yield based on the proximate and ultimate analysis of the biomass feedstock as given in the FORTRAN statement:

FACT = (100 – WATER)/100

H_2O = WATER/100

ASH = (ULT1/100)*FACT

C = (ULT2/100)*FACT

H_2 = (ULT3/100)*FACT

N_2 = (ULT4/100)*FACT

O_2 = (ULT5/100)*FACT

S = (ULT6/100)*FACT

From the FORTRAN statement, The ULT was defined as the ultimate analysis values of the feed on a dry basis. The variable WATER (percentage moisture content of feedstock obtained from its proximate analysis) was used to convert the ultimate analysis from dry basis to a wet basis. The ULT and WATER were then used to calculate the actual yield of the individual components (H_2O, ash, C, H_2, N_2, O_2, and S) in the product stream of decomposer unit (DECOMP) shown in Fig. 6.1. The calculator block was set to execute before the DECOMP unit operation.

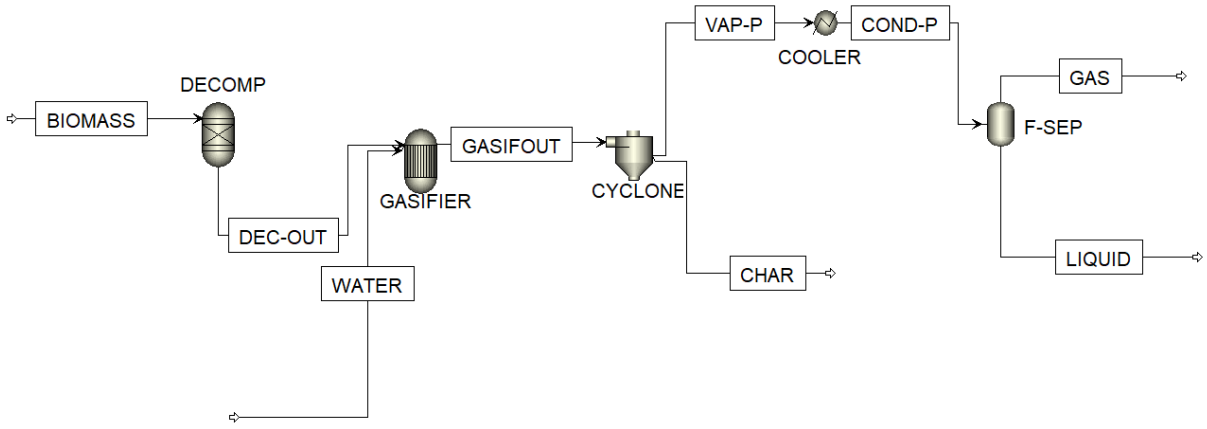

Figure 6.1. Aspen Plus flow diagram of the hydrothermal gasification model

The main hydrothermal gasification reaction was carried out in the RGibbs block referred to as GASIFIER in the simulation. The CYCLONE unit was used to separate the solids (char) from the vapour products leaving the GASIFIER. The vapour products were cooled to ambient temperature using the COOLER, and the F-SEP unit was used to separate the condensed liquid product from the gaseous product. The hydrothermal gasification process as described consists

of the following set of chemical reactions shown in equations 6.1 – 6.10 (Fernandez-Lopez *et al.* 2017; Adnan and Hossain 2018a)

Devolatilation $Biomass \rightarrow Char + gases(CO + CO_2 + H_2 + CH_4)$ (6.1)

Steam reforming $C + H_2O \leftrightarrow CO + H_2 \;\; \Delta H^o_{r(298)} = 131\ KJ/mol$ (6.2)

Water-gas shift $CO + H_2O \leftrightarrow CO_2 + H_2 \quad \Delta H^o_{r(298)} = -41.2\ KJ/mol$ (6.3)

Methanation $C + 2H_2 \leftrightarrow CH_4 \quad \Delta H^o_{r(298)} = -75\ KJ/mol$ (6.4)

Methanation $CO + 3H_2 \leftrightarrow CH_4 + H_2O \quad \Delta H^o_{r(298)} = -165\ KJ/mol$ (6.5)

Boudouard $C + CO_2 \leftrightarrow 2CO \;\; \Delta H^o_{r(298)} = 172\ KJ/mol$ (6.6)

Steam reforming of methane $CH_4 + H_2O \leftrightarrow CO + 3H_2 \;\; \Delta H^o_{r(298)} = 206.1\ KJ/mol$ (6.7)

Dry reforming of methane $CH_4 + CO_2 \leftrightarrow 2CO + 2H_2 \;\; \Delta H^o_{r(298)} = 247.3\ KJ/mol$ (6.8)

Hydrogen sulfide formation $H_2 + S \leftrightarrow H_2S$ (6.9)

Ammonia formation $0.5N_2 + 1.5H_2 \leftrightarrow NH_3$ (6.10)

Table 6.2. Description of Aspen plus unit operation blocks used in the simulation model

Aspen plus name	Block name	Description
RYield	DECOMP	It is used to convert the non-convention biomass to convention component based on the proximate and ultimate analyses of the feed.
RGibbs	GASIFIER	Calculation of phase and chemical equilibrium by minimisation the Gibbs free energy of the system
SSplit	CYCLONE	Separation of solid (char) from the vapour stream product
Heater	COOLER	Reduction of vapour stream temperature to induce condensation of liquid products
Flash2	F-SEP	Separation of the liquid product from the non-condensable gaseous product
Calculator	CONVERT	Calculation of RYield mass yields using FORTRAN statement

6.2.3 Process Model Assumptions

The following assumptions were made for the development of the hydrothermal gasification simulation model:

(i) The simulation model operates at steady-state and as such time-dependent functions such as heating rate are not considered;

(ii) The gaseous products from the gasifier were H_2, CH_4, CO, CO_2, H_2O, NH_3, and H_2S;

(iii) Methane is the only hydrocarbon gas considered;

(iv) Char consist of only carbon and ash;

(v) Ash is considered inert and did not take part in the chemical reaction;

(vi) No oxides of nitrogen or sulfur were formed;

(vii) All the reactions involved in the hydrothermal gasification reach the equilibrium.

6.2.4 Effect of Pressure, Temperature, Biomass Concentration and Feedstock Composition

The whole algae, lipid and residual biomass after lipid extraction of *Scenedesmus Obliquus* microalgae were considered as a feedstock for the hydrothermal gasification model with varying feedstock compositions as shown in Table 6.1. The effect of HTG temperature, pressure, biomass concentration and feedstock composition on the yield and composition of the gaseous product was studied. The performance was also analysed based on the gas product lower heating value (LHV) calculated using equation 6.11 (Fernandez-Lopez *et al.* 2017). The temperature was varied from 400 to 700 $^{\circ}$C while the pressure was varied from 24 to 36 MPa in the GASIFIER block. The biomass feedstock concentration was varied from 10 to 40 wt% solid content by varying the mass flow rate of WATER stream from 90 kg/hr to 15 kg/hr since a constant feed flow rate of 10 kg/hr was used in all the simulation runs.

$$LHV_{gas} = 10.8 * y_{H_2} + 12.6 * y_{CO} + 35.8 * y_{CH_4} \quad (6.11)$$

Where y_i is the mole fraction of each gas component (H_2, CO and CH_4)

6.2.5 Model Validation

The experimental data on the hydrothermal gasification of three different algae samples (*Chlorella vulgaris, Spirulina platensis*, and *Saccharina latissima*) reported by Onwudili *et al.* (2013) was used to validate and check the accuracy of the proposed Aspen Plus model. Onwudili *et al.* (2013) carried out the experimental work at a temperature of 500 ^{o}C, the pressure of 36 MPa and 5wt% biomass concentration. For the purpose of validation, Aspen Plus model was developed to simulate the hydrothermal gasification of the same three algae

samples using the same reaction conditions and feed composition, as reported in the experimental work by Onwudili *et al.* (2013). The composition (mole%) of the gaseous products obtained from the Aspen Plus simulation model was then compared with that obtained from the work of Onwudili *et al.* (2013) (Fig. 6.2). It can be seen from Fig. 6.2 that the predicted composition (mole%) of gaseous products from Aspen Plus model are in good agreement with the experimental values reported by Onwudili *et al.* (2013)), especially for the H_2, CH_4 and CO_2. The simulation results showed that Aspen Plus model underestimates the mole fraction of CO (< 6%) where the standard error of prediction value for CO appears to be greater than those of other gases (Table 6.3). This is an indication that any CO produced from steam reforming reactions was subsequently consumed, possibly in the methanation and/or water-gas shift reactions. Duan *et al.* (2018) experimentally studied hydrothermal gasification of *Chlorella pyrenoidosa* microalgae and also found the mole fraction of CO < 6% for all the temperature considered. In this study, H_2 and CH_4 were considered the gas products of focus from hydrothermal gasification process and Aspen model results for both hydrogen and methane production exhibited good agreement with the experimental values (Fig. 6.2). The slight deviation in the simulation results when compared to the experimental results was attributed to the steady-state assumption in the Aspen model where time-dependent parameters such as heating rate were kept constant in the simulation which is not the case with experimental condition. Therefore the Aspen Plus simulation model can be considered valid and reliable to describe the hydrothermal gasification process.

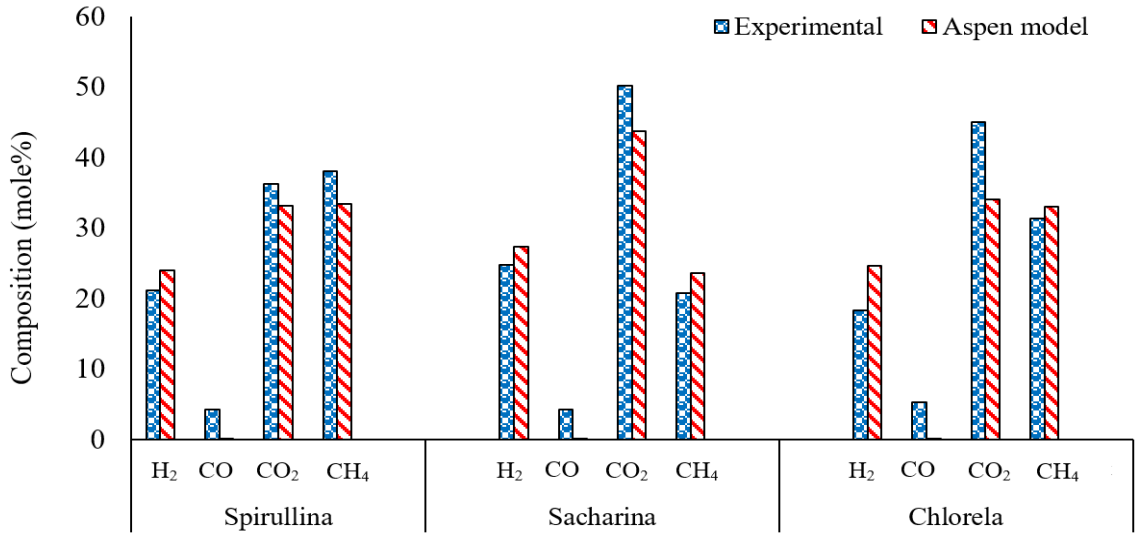

Figure 6.2. Composition of product gases from the HTG of different algae samples at 500 ˚C, 36 MPa, and 5wt% biomass feed concentration (Source of experimental data (Onwudili *et al.* 2013)).

Table 6.3. Difference in experimental and Aspen simulation model results (Experimental data – Aspen model data) (Source of experimental data (Onwudili *et al.* 2013)).

	HTG at 500 ˚C, 36 MPa, and 5wt% biomass concentration			Standard error of prediction
	Spirullina	*Sacharina*	*Chlorella*	
H_2 (mole %)	-2.88	-2.53	-6.40	0.20
CH_4 (mole %)	4.72	-2.84	-1.64	0.11
CO_2 (mole %)	3.09	6.43	10.99	0.17
CO (mole %)	4.10	4.06	5.12	0.97

6.3 Results and Discussion

6.3.1 Effect of Pressure, Temperature and Biomass Concentration

The influence of operating conditions such as pressure, temperature and biomass concentration on the yield and composition of gaseous products and lower heating value (LHV) from the hydrothermal gasification of whole *Scenedesmus obliquus* microalgae is discussed in this section. The temperature was varied from 400 °C to 700 °C while the pressure was varied from 24 MPa to 36 MPa. For the biomass concentration, the values were varied from 10 wt% to 40 wt%. The identified main components of the gaseous product from the HTG are CH_4, H_2, CO_2 with small amounts of CO, H_2S and NH_3. The present study will only focus on the H_2 and CH_4 production in the HTG process. The major reaction pathways responsible for the production of the gaseous product in HTG include steam reforming (equation 6.2), water-gas shift (equation 6.3), and methanation (equations 6.4 and 6.5). The water-gas shift and steam reforming reactions are responsible for the production of H_2 while the methanation reactions are responsible for the production of CH_4 (Onwudili *et al.* 2013; Jiao *et al.* 2017). The steam reforming reaction is endothermic and will be thermodynamically favoured at a higher temperature. On the other hand, water-gas shift and methanation are exothermic reactions favoured at relatively low temperatures. Other side reactions such as boudouard (equation 6.6), methane reforming reactions (equation 6.7 and 6.8), hydrogen sulfide formation (equation 6.9) and ammonia formation (equation 6.10) can occur in HTG(Fernandez-Lopez *et al.* 2017; Adnan and Hossain 2018a).

Fig. 6.3 shows the H_2 and CH_4 mole fraction from the HTG of the whole algae at different temperatures and pressures. As shown in Fig. 6.3, at a pressure of 36 MPa, H_2 mole fraction increased from 3.62 to 53.71 mole% while the mole fraction of CH_4 decreased from

51.99 to 10.52 mole% as the temperature was increased from 400 °C to 700 °C. The low mole fraction of H_2 observed at lower temperature could be due to contribution mainly from the exothermic water-gas shift reaction (equation 6.3) to produce H_2. But at a higher temperature, a significant increase in the mole fraction of H_2 was observed due to the steam reforming reactions (equations 6.2 and 6.7), favouring the production of more H_2 (Duan *et al.* 2018). In contrast, the CH_4 mole fraction was highest at low temperature and subsequently reduced as the temperature increased from 400 °C to 700 °C. Methanation reactions (equation 6.4 and 6.5) favour the production of methane at low temperature as they are exothermic reactions. However, as the temperature was increased, the reverse methanation occurred, which converted methane into hydrogen. Besides, methane reforming reaction favoured at higher temperature could lead to an increase of H_2 and reduction of CH_4 production observed with higher temperature. These findings are in line with the work of Atikah and Harun (2019), which also concluded that lower temperature favoured CH_4 production while H_2 production was favoured at a higher temperature. On the contrary, Duan *et al.* (2018) found that the mole composition of CH_4 significantly increased as the temperature was increased. The authors suggested that the methanation reaction may have been affected by some other parameters other than temperature. They concluded that since methanation is a volume reducing reaction which is favoured by high pressure, the retarding effect for the methanation reaction as a result of increasing temperature was offset by the significant promotion effect due to increasing reaction pressure. As shown in Fig. 6.3, CH_4 mole fraction increased from 47 mole% to 51.99 mole% when the pressure was increased from 24 MPa to 36 MPa at 400 °C. The same trend was observed when the pressure was varied at different temperatures of 400 °C, 500 °C, 600 °C and 700 °C indicating that the methanation reaction was favoured at high pressure but increase

in temperature depressed the production of CH_4. In the case of hydrogen production, the highest mole fraction of 57.97 mole% was observed at 24 MPa and 700 ˚C. The mole fraction of hydrogen decreased from 57.97 to 53.71 mole% as the pressure was increased from 24 MPa to 36 MPa. The same trend was observed for H_2 mole fraction when the pressure was varied at different temperature. The work of Adnan and Hossain (2018b)) also showed that H_2 production decreased at higher pressure. The little increase observed with the CH_4 mole fraction and slight decrease with H_2 mole fraction is an indication that pressure has minimal effect on the composition of the gaseous product when compared to the temperature effect (see Fig. 6.3).

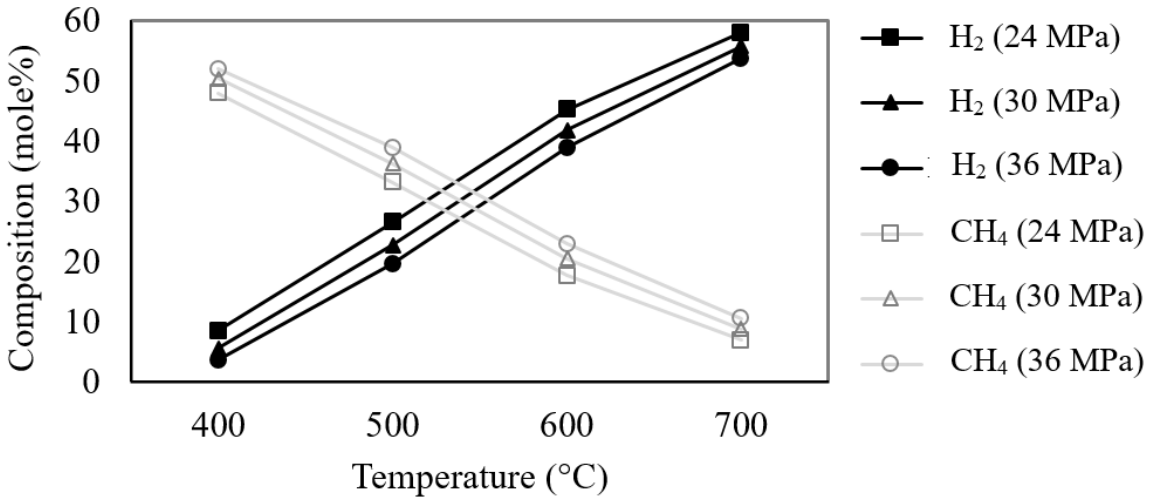

Figure 6.3. Effect of temperature at three different pressures on gas composition obtained from HTG of raw microalgae with 10 wt% biomass concentration

The influence of biomass concentration at varying temperature on the hydrothermal gasification process was explored. The biomass concentration was varied from 10 wt% to 40 wt% at temperatures of 400 ˚C, 500 ˚C, 600 ˚C and 700 ˚C. The yield and mole fraction of H_2 and CH_4 gas at varying biomass concentration and temperature are shown in Fig. 6.4. The

highest H_2 mole fraction of 55.77 mole% with a corresponding yield of 75.44 mmol/g was obtained at a biomass concentration of 10 wt% and temperature of 700 $^{\circ}$C. As the biomass concentration increased from 10 wt% to 40 wt%, the H_2 mole fraction decreased from 55.77 to 26.35 mole% and the yield also significantly reduced from 75.44 to 20.71 mmol/g. The hydrothermal gasification can be influenced by biomass concentration since water is also a reactant in the steam reforming and water-gas shift reactions. Lower biomass concentration means that more water is available for the HTG process, and the water content reduces as the biomass concentration is increased. Thus, the availability of more water at lower biomass concentration accelerated the water-gas shift and steam reforming reactions, thus favouring H_2 production. Under this condition, the methanation reaction is depressed, thereby reducing the production of CH_4. Some previous studies also found that hydrogen gasification efficiency is higher with lower biomass concentration (Chakinala *et al.* 2010; Jiao *et al.* 2017; Duan *et al.* 2018). The transfer of hydrogen atoms from excess water to the gaseous product could contribute to the higher H_2 production observed at lower biomass concentration. The work of Yanik *et al.* (2008) suggested that almost half of the H_2 production under hydrothermal gasification came from water rather than biomass.

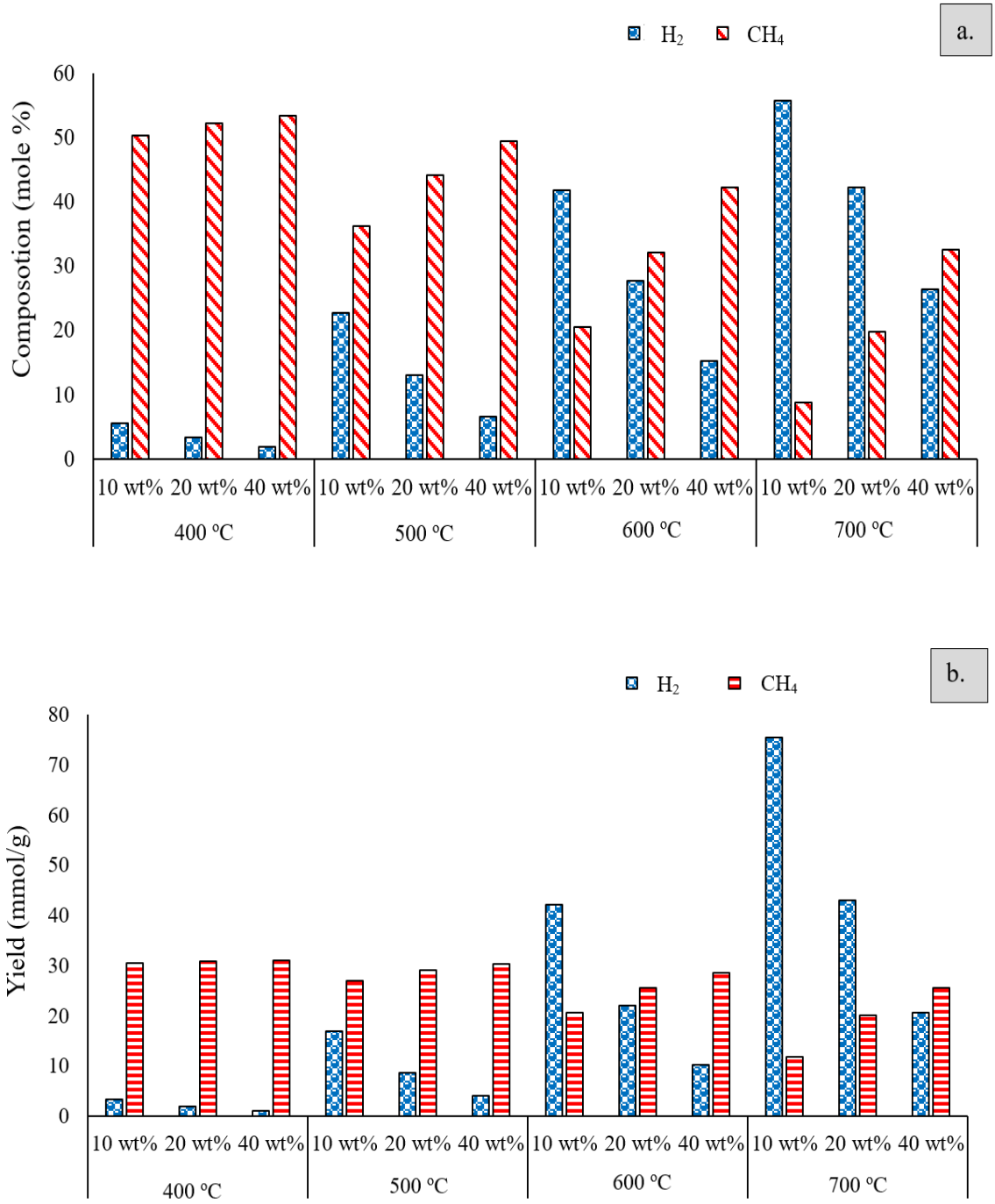

Figure 6.4. Effect of biomass concentration at different temperatures on (a) composition of H_2 and CH_4 (b) yield of H_2 and CH_4 obtained from HTG of whole algae (P = 30 MPa)

The highest CH_4 mole fraction of 53.45 mole% with a corresponding yield of 31.14 mmol/g was observed at a biomass concentration of 40 wt% and temperature of 400 °C. As the biomass concentration increased from 10 wt% to 40 wt%, the CH_4 mole fraction increased from 50.38 to 53.45 mole% and the yield also slightly increased from 30.48 to 31.14 mmol/g. Methanation reaction is primarily responsible for the production of CH_4 gas at the expense of H_2. The CH_4 yield always increased with increase in biomass concentration and reached the highest value at a biomass concentration of 40 wt% under the studied temperatures. This is an indication that the methanation reaction is accelerated at higher biomass concentration. Similar results were also observed by (Jiao *et al.* 2017). It is worth noting that the influence of varying biomass concentration on CH_4 production at a temperature of 400 °C is less compared to the obvious increment in CH_4 mole fraction observed when biomass concentration was varied at higher temperatures. This showed that methanation reaction is more dependent on the temperature than biomass concentration, especially at low temperature. This study has shown that hydrogen-rich and methane-rich gas can be produced from the hydrothermal gasification of microalgae. Hydrothermal gasification processing of high-moisture-containing biomasses such as microalgae could help to reduce or eliminate the need for drying or pretreatment costs associated with traditional gasification and pyrolysis.(Macrì *et al.* 2020) Hydrothermal gasification is a competitive technique for the production of high yield hydrogen and methane gas from microalgae mainly due to its lower cost when compared with other thermal conversion processes such as traditional gasification and pyrolysis.

The influence of biomass concentration and temperature on lower heating value (LHV) of the produced gas is explored, and the results are presented in Fig. 6.5. The composition data for H_2, CH_4 and CO in the gas products were used to determine the LHV for

the gas products using equation 6.11. As shown in Fig. 6.5, the highest LHV was observed at a temperature of 400 ºC, and little difference was observed in the LHV values as the biomass concentration was increased under this same temperature condition. The LHV values of 18.64 MJ/kg, 19.06 MJ/kg and 19.34 MJ/kg were obtained for biomass concentration of 10 wt%, 20 wt% and 40 wt% respectively. The little difference observed in the LHV values at 400 ˚C under different biomass concentration is due to the closeness of CH_4 mole fractions at 400 °C. As can be seen from equation 6.11, CH_4 is the major contributor to the LHV value, and its mole fraction has a great influence on the LHV of the product gas. In terms of high energy recovery, the temperature of 400 ˚C could be the most suitable for hydrothermal gasification of microalgae. Also, the results showed that an increase in biomass concentration increases the LHV of the product gas for all the temperature considered.

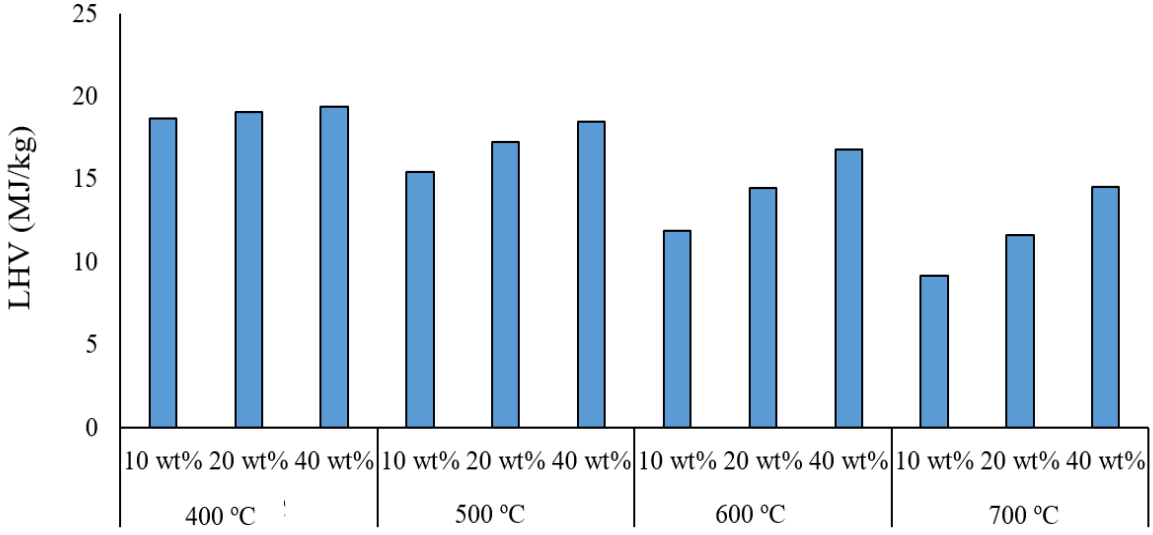

Figure 6.5. Effect of biomass concentration at different temperatures on lower heating value (LHV) obtained from HTG of *Scenedesmus obliquus* microalgae (P = 30 MPa)

6.3.2 Effect of Varying Feedstock Composition on the Hydrothermal Gasification Process

The influence of operating conditions such as temperature and biomass concentration on the yield and composition of gaseous products using different feed composition is explored. In the earlier section, the influence of the operating conditions using whole algae was discussed. In this section, the effects of operating conditions (temperature and biomass concentration) and varying feed composition resulting from derivatives of *S. obliquus* microalgae (lipid and lipid extracted algae) were compared with that of whole algae and the results presented in Table 6.4. The experiments were performed at a pressure of 30 MPa. As shown in Table 6.4, a similar trend to the results obtained with whole algae was established for the hydrothermal gasification using lipid and the lipid extracted algae (LEA) although the magnitudes are different. The variation in products distribution from the three algae samples were linked to their different biochemical compositions. This is a confirmation that the composition of feedstock (shown in Table 6.1) have a significant effect on the yield and composition of the gaseous products produced from the HTG process.

Table 6.4. Influence of operating conditions on LHV, yield, and composition of gaseous product using varying feed composition

Condition (10wt %)	H_2 mole fraction (mole %)			CH_4 mole fraction (mole %)			H_2 Yield (mmol/g)			CH_4 Yield (mmol/g)			LHV (MJ/kg)		
	Whole	Lipid	LEA	Whole	Lipid	LEA	Whole	Lipid	LEA	Whole	Lipid	LEA	Whole	Lipid	LEA
400 ˚C	5.59	4.85	5.50	50.38	58.23	49.23	3.38	4.81	3.30	30.48	57.69	29.51	18.64	21.37	18.22
500 ˚C	22.77	19.33	22.45	36.25	45.16	35.50	16.99	22.75	16.55	27.05	53.15	26.16	15.44	18.26	15.14
600 ˚C	41.86	37.38	41.45	20.46	28.80	20.06	42.18	55.45	41.10	20.62	44.25	19.89	11.85	14.35	11.66
700 ˚C	55.77	52.29	55.34	8.81	15.11	8.60	75.44	107.51	73.49	11.92	31.06	14.42	9.18	11.05	9.06
Condition (20wt %)	H_2 mole fraction (mole %)			CH_4 mole fraction (mole %)			H_2 Yield (mmol/g)			CH_4 Yield (mmol/g)			LHV (MJ/kg)		
	Whole	Lipid	LEA	Whole	Lipid	LEA	Whole	Lipid	LEA	Whole	Lipid	LEA	Whole	Lipid	LEA
400 ˚C	3.38	2.90	3.32	52.21	59.99	50.99	2.00	2.81	1.95	30.88	58.23	29.89	19.06	21.79	18.61
500 ˚C	13.08	10.80	12.87	44.19	52.83	43.24	8.64	11.46	8.40	29.18	56.01	28.24	17.23	20.08	16.87
600 ˚C	27.66	23.56	27.29	32.08	41.19	31.44	22.13	29.36	21.55	25.67	51.32	24.82	14.47	17.29	14.20
700 ˚C	42.29	37.62	41.85	19.73	28.17	19.34	42.98	58.08	41.86	20.06	43.49	19.35	11.63	14.15	11.44
Condition (40wt %)	H_2 mole fraction (mole %)			CH_4 mole fraction (mole %)			H_2 Yield (mmol/g)			CH_4 Yield (mmol/g)			LHV (MJ/kg)		
	Whole	Lipid	LEA	Whole	Lipid	LEA	Whole	Lipid	LEA	Whole	Lipid	LEA	Whole	Lipid	LEA
400 ˚C	1.88	1.61	1.84	53.45	61.70	52.20	1.09	1.49	1.06	31.14	56.90	30.15	19.34	22.26	18.89
500 ˚C	6.60	5.24	6.48	49.51	57.82	48.39	4.05	5.22	3.93	30.36	57.60	29.39	18.44	21.27	18.02
600 ˚C	15.17	12.17	14.91	42.28	51.39	41.39	10.28	13.12	9.99	28.66	55.40	27.74	16.78	19.71	16.43
700 ˚C	26.35	21.80	25.97	32.64	42.22	31.99	20.71	26.54	20.14	25.66	51.40	24.81	14.53	17.47	14.26

According to Table 6.4, the highest mole fraction and yield for CH_4 was observed at a temperature of 400 ^oC and biomass concentration of 40 wt% in all the three feedstock. CH_4 mole fraction of 53.45 mole%, 61.70 mole% and 52.20 mole% which correspond to yield of 31.14 mmol/g, 56.90 mmol/g and 30.15 mmol/g for whole algae, lipid and LEA respectively were obtained under this condition. These results showed that the CH_4 mole fraction and yield obtained from the whole algae is close to that obtained using LEA as feedstock. However, the result from lipid is almost twice the value obtained from whole algae and LEA. This was attributed to the higher carbon and low ash content present in the lipid when compared to the whole algae and lipid (Table 6.1). Besides, the high yield of CH_4 gas was linked to the degradation of the long-chain fatty acids present in lipids (Onwudili *et al.* 2013). On the other hand, the highest mole fraction and yield for H_2 was observed at a temperature of 700 $^{\circ}C$ and biomass concentration of 10 wt%. Under these conditions, the H_2 mole fraction of 55.77 mole%, 52.29 mole% and 55.34 mole% which correspond to yield of 75.44 mmol/g, 105.51 mmol/g and 73.49 mmol/g were observed for whole algae, lipid and LEA respectively. The results showed that feedstock composition has minimal effect on H_2 mole fraction and may be due to the lower hydrogen content in all the feedstock compared to the carbon content. Contrary to the trend observed with CH_4 production, H_2 mole fraction in lipid was slightly less compared to whole algae and LEA although a higher yield of H_2 was still observed with lipid. The higher H_2 mole fraction in whole algae and LEA could be due to the presence of protein and carbohydrate which have been identified to favour H_2 production (Hao *et al.* 2003; Jiao *et al.* 2017). Of the three feedstocks, the results showed that a higher yield of H_2 and CH_4 was achieved with lipid compared to the whole algae and LEA. The ranking order of the yield of H_2 and CH_4 product gas from HTG process is lipid > whole algae > LEA. With regards to the

lower heating value (LHV), the highest LHV of 19.34 MJ/kg, 22.26 MJ/kg and 18.89 MJ/kg were obtained for whole algae, lipid and LEA respectively at the same operating condition of 400 ^{o}C and 40 wt%. This is a confirmation that the LHV of the product gas is also dependent on the feedstock composition with lipid having the highest LHV and LEA with the lowest LHV for all the studied operating conditions. Previous experimental study on hydrothermal gasification of microalgae also showed that feedstock composition has a great impact on the product gas compositions.(Jiao *et al.* 2017) Microalgae biomass mainly contains high amounts of lipids, carbohydrates and protein. The degradation of the long-chain fatty acids present in lipids could be responsible for the high yield of CH_4 gas. Some previous studies have also reported that the presence of protein and carbohydrate could favor H_2 production.(Hao *et al.* 2003; Jiao *et al.* 2017) Due to the uniqueness of their composition when compared to other biomass sources (containing cellulose, hemicellulose and lignin), microalgae biomasses are suitable feedstock for the production of high yield methane and hydrogen gas via hydrothermal gasification technique.

6.4 Conclusion

The simulation model for the hydrothermal gasification process was developed using Aspen Plus V11 software. Lipids produced the highest yield of H_2 and CH_4 when compared to whole algae and lipid extracted algae. For all the three feedstocks considered, the highest mole fraction and yield of H_2 was obtained at high temperature and low biomass concentration. In contrast, the highest mole fraction and yield of CH_4 was obtained at low temperature and high biomass concentration. Higher lipid content in biomass favoured the production of CH_4 while biomass with high protein and carbohydrate content favoured hydrogen production. The lower heating value for lipid (22.2 MJ/kg) was higher when compared to whole algae (19.34 MJ/kg)

and lipid extracted algae (18.34 MJ/kg). The model will serve as a framework for optimisation studies and also for predicting the product yield and composition of gaseous products from hydrothermal gasification of microalgae at any given biomass composition and operating conditions.

CHAPTER 7

CONCLUSION AND FUTURE WORK

7.1 Conclusion

This study investigated the thermal conversion of microalgae and its derivatives into biofuels and other co-products. Based on the overall aim, the following specific objectives were achieved. (i) Characterization of lipids, lipid extracted biomass and whole cell algae grown under varying conditions. (ii) Synthesis and characterization of zeolite-supported metal catalysts for hydrothermal liquefaction process. (iii) Synthesis and characterization of metal - based catalyst loaded on different supports for the pyrolysis process. (iv) Establishing optimum process conditions for the thermal conversion processes (pyrolysis, hydrothermal liquefaction and gasification). (v) Developing predictive model for the production of biofuels from microalgae based on feedstock composition and type of thermal conversion process.

The major conclusion from this study includes:

- The results showed that nutrient stressed condition altered the microalgae compositions, especially the reduction of protein content and enhancement of the lipid and carbohydrate contents. Under the stressed condition, the protein content of the microalgae was reduced from 42.35% to 22.08% while the carbohydrate and lipid contents were increased from 25.36% to 42.55% and 17.16% to 21.62% respectively.
- The highest bio-oil yield of 52.8 wt% and 24.27 wt% were obtained from the HTL of nutrient stressed and unstressed *Scenedesmus obliquus* microalgae respectively at a temperature of 350 $^{\circ}$C in the presence of a catalyst. The use of Zr/HZSM-5 catalyst in

the HTL of nutrient stressed *S. obliquus* microalgae resulted in enhanced bio-oil yield and characteristics which compared well with petroleum crude.

- Omega-7- fatty acid (cis-vaccenic acid) was found predominant in the Bio-oil from HTL of nutrient stressed *Scenedesmus obliquus* microalgae, and this could be explored for the possibility of extracting high-value products from the bio-oil for applications other than biofuels.
- The optimum pyrolytic bio-oil yield of 46.37 wt% and 34.85 wt% were obtained at 500 °C for the nutrient stressed *S. obliquus* microalgae and its residual algae respectively, while the optimum bio-oil yield for unstressed algae (41.94 wt%) was obtained at 600 °C.
- The pyrolysis of *S. obliquus* microalgae in the presence of supported metal catalysts promotes deoxygenation, denitrogenation, aromatization and acid ketonization in the bio-oils producing high-quality bio-oils with high stability and low acidity. Also, the HHV of the pyrolytic bio-oil was increased from 38.27 MJ/kg (non-catalytic) to 39.70 – 40.78 MJ/kg in the presence of supported metal catalysts.
- Among the catalysts studied for pyrolysis, Co/Fe_3O_4-HZSM-5 catalyst showed better activity in enhancing the quality and yield of the bio-oil produced from nutrient stressed *Scenedesmus obliquus* microalgae with properties close to that of petroleum crude.
- Phenol which is of great commercial importance accounts for about 76.7% of the aromatic hydrocarbon in the bio-oil from the residual algae. The proportion of aliphatic hydrocarbons and acids in the bio-oil from nutrient stressed *S. obliquus* microalgae biomass was higher than that of residual and unstressed algae.

- The use of supported metal catalysts during pyrolysis of nutrient stressed *Scenedesmus obliquus* microalgae produces ketonic-rich bio-oils suitable for producing gasoline, diesel and jet fuels
- The nitrogen content of pyrolytic bio-oils was found to be more dependent on feedstock composition than temperature. The pyrolytic bio-oil obtained from the unstressed algae biomass has the highest proportion of nitrogen-containing compounds when compared to nutrient stressed algae and its residual algae. The proportion of nitrogen-containing compounds in bio-oil from unstressed algae was found to be 47.4% but reduced to 5.92% with the nutrient stressed microalgae biomass.
- It was also found that low temperature (400 ^{o}C) and biomass concentration of 40 wt% favored the production of methane-rich gas. In contrast, high temperature (700 ^{o}C) and low biomass concentration (10 wt%) favored hydrogen-rich gas production. This study has shown that hydrogen-rich and methane-rich gas can be produced from the hydrothermal gasification of microalgae as a function of the reaction conditions and feedstock composition.
- Artificial neural network (ANN) model was developed which can serve as a framework for the prediction of bio-oil yield from the pyrolysis of microalgae at any given biomass composition and reaction temperature.
- The model developed for the HTG of microalgae will serve as a frame work for predicting the product yield and composition of gaseous products at any given biomass composition and operating conditions.

- The suitability of nutrient stressed approach and use of catalysts to enhance the quality of bio-oil produced from the pyrolysis and HTL of *Scenedesmus obliquus* microalgae biomass was established.

7.2 Future Work

The combination of use of catalysts and nutrient stressed approach adopted in this study significantly enhanced the quality of the bio-oil produced from both the hydrothermal liquefaction and pyrolysis of *Scenedesmus obliquus* microalgae. High quality bio-oils with properties close to those of commercial petroleum crude was produced. This is a major advance in the field of microalgal biofuel technology as a sustainable alternative to fossil fuel. The bio-oils obtained from the thermal conversion process can be blended or co-processed with petroleum crude and could fit into the existing refinery eliminating the need and additional costs of building new refineries. The possible use of produced biochar or biochar/spent catalyst mix as absorbent for water treatment application need to be further investigated. The present study also showed that Omega-7- fatty acid (cis-vaccenic acid) was found predominant in the bio-oil from HTL of nutrient stressed *Scenedesmus obliquus* microalgae which is of high value as dietary supplement and have great health benefit in reducing the incidence of cardiovascular disease, cancer and obesity. This high value product could be further explored for applications other than biofuels. Co-thermal conversion of microalgae with other waste material has been proposed for improving the bio-oil quality and concurrently providing waste treatment option. Although the co-thermal conversion processes seem promising, studies in this area are still at an early stage, and further research on understanding the possible mechanism and feedstock interactions on the product quality are still needed.

REFERENCES

Abu El-Rub, Z., Bramer, E. A. and Brem, G. 2004. Review of catalysts for tar elimination in biomass gasification processes. *Industrial & Engineering Chemistry Research*, 43 (22): 6911-6919.

Adeniyi, A. G., Ighalo, J. O., Onifade, D. V. and Adeoye, S. A. 2020. Modeling the valorization of poultry litter via thermochemical processing. *Biofuels, Bioproducts and Biorefining*, 14 (2): 242-248.

Adetiba, E. and Olugbara, O. O. 2015. Lung cancer prediction using neural network ensemble with histogram of oriented gradient genomic features. *The Scientific World Journal*, 2015: 1 - 17.

Adnan, M. A. and Hossain, M. M. 2018a. Co-gasification of Indonesian coal and microalgae–A thermodynamic study and performance evaluation. *Chemical Engineering and Processing-Process Intensification*,

Adnan, M. A. and Hossain, M. M. 2018b. Gasification performance of various microalgae biomass–A thermodynamic study by considering tar formation using Aspen plus. *Energy Conversion and Management*, 165: 783-793.

Adnan, M. A., Susanto, H., Binous, H., Muraza, O. and Hossain, M. M. 2017. Feed compositions and gasification potential of several biomasses including a microalgae: A thermodynamic modeling approach. *International Journal of Hydrogen Energy*, 42 (27): 17009-17019.

Ahmad, M. S., Mehmood, M. A., Luo, H., Shen, B., Latif, M., Ghani, W. A. W. A. K., Alkhattabi, N. A., Aloqbi, A. A., Jambi, E. J. and Gull, M. 2019. Pyrolysis and thermogravimetric study to elucidate the bioenergy potential of novel feedstock produced on poor soils while keeping the environmental sustainability intact. *Sustainability*, 11 (13): 3592.

Al-Ameri, M. and Al-Zuhair, S. 2019. Using switchable solvents for enhanced, simultaneous microalgae oil extraction-reaction for biodiesel production. *Biochemical engineering journal*, 141: 217-224.

Al-Senani, G. M., Deraz, N. M. and Abd-Elkader, O. H. 2020. Magnetic and Characterization Studies of CoO/Co3O4 Nanocomposite. *Processes*, 8 (7): 844.

Andrade, L. A., Batista, F. R. X., Lira, T. S., Barrozo, M. A. S. and Vieira, L. G. M. 2018. Characterization and product formation during the catalytic and non-catalytic pyrolysis of the green microalgae Chlamydomonas reinhardtii. *Renewable energy*, 119: 731-740.

Ansari, F. A., Nasr, M., Guldhe, A., Gupta, S. K., Rawat, I. and Bux, F. 2020. Techno-economic feasibility of algal aquaculture via fish and biodiesel production pathways: A commercial-scale application. *Science of The Total Environment*, 704: 135259.

Ansari, F. A., Shriwastav, A., Gupta, S. K., Rawat, I., Guldhe, A. and Bux, F. 2015. Lipid extracted algae as a source for protein and reduced sugar: a step closer to the biorefinery. *Bioresource technology*, 179: 559-564.

Ansari, F. A., Singh, P., Guldhe, A. and Bux, F. 2017. Microalgal cultivation using aquaculture wastewater: integrated biomass generation and nutrient remediation. *Algal Research*, 21: 169-177.

Arun, J., Gopinath, K. P., SundarRajan, P., Malolan, R., Adithya, S., Jayaraman, R. S. and Ajay, P. S. 2020. Hydrothermal liquefaction of Scenedesmus obliquus using a novel catalyst derived from clam shells: Solid residue as catalyst for hydrogen production. *Bioresource technology*: 123443.

Atikah, M. and Harun, R. 2019. Simulation and optimization of Chlorella vulgaris gasification using Aspen plus. *Process Integration and Optimization for Sustainability*, 3 (3): 349-357.

Aysu, T., Fermoso, J. and Sanna, A. 2018. Ceria on alumina support for catalytic pyrolysis of Pavlova sp. microalgae to high-quality bio-oils. *Journal of energy chemistry*, 27 (3): 874-882.

Aysu, T., Ola, O., Maroto-Valer, M. M. and Sanna, A. 2017. Effects of titania based catalysts on in-situ pyrolysis of Pavlova microalgae. *Fuel Processing Technology*, 166: 291-298.

Aysu, T. and Sanna, A. 2015. Nannochloropsis algae pyrolysis with ceria-based catalysts for production of high-quality bio-oils. *Bioresource technology*, 194: 108-116.

Babich, I., Van der Hulst, M., Lefferts, L., Moulijn, J., O'Connor, P. and Seshan, K. 2011. Catalytic pyrolysis of microalgae to high-quality liquid bio-fuels. *Biomass and Bioenergy*, 35 (7): 3199-3207.

Barbarino, E. and Lourenço, S. O. 2005. An evaluation of methods for extraction and quantification of protein from marine macro-and microalgae. *Journal of Applied Phycology*, 17 (5): 447-460.

Barreiro, D. L., Prins, W., Ronsse, F. and Brilman, W. 2013a. Hydrothermal liquefaction (HTL) of microalgae for biofuel production: state of the art review and future prospects. *Biomass and Bioenergy*, 53: 113-127.

Barreiro, D. L., Zamalloa, C., Boon, N., Vyverman, W., Ronsse, F., Brilman, W. and Prins, W. 2013b. Influence of strain-specific parameters on hydrothermal liquefaction of microalgae. *Bioresource technology*, 146: 463-471.

Bennett, J. A., Parlett, C. M., Isaacs, M. A., Durndell, L. J., Olivi, L., Lee, A. F. and Wilson, K. 2017. Acetic Acid Ketonization over Fe3O4/SiO2 for Pyrolysis Bio-Oil Upgrading. *ChemCatChem*, 9 (9): 1648-1654.

Bharath, M., Raghavan, V., Prasad, B. and Chakravarthy, S. 2018. Co-gasification of Indian Rice Husk and Indian Coal with High-Ash in Bubbling Fluidized Bed Gasification Reactor. *Applied Thermal Engineering*,

Bharathiraja, B., Chakravarthy, M., Kumar, R. R., Yogendran, D., Yuvaraj, D., Jayamuthunagai, J., Kumar, R. P. and Palani, S. 2015. Aquatic biomass (algae) as a future feed stock for bio-refineries: a review on cultivation, processing and products. *Renewable and sustainable energy reviews*, 47: 634-653.

Bi, Z. and He, B. B. 2013. Characterization of microalgae for the purpose of biofuel production. *Transactions of the ASABE*, 56 (4): 1529-1539.

Biller, P., Riley, R. and Ross, A. B. 2011. Catalytic hydrothermal processing of microalgae: Decomposition and upgrading of lipids. *Bioresource technology*, 102 (7): 4841-4848.

Biller, P., Ross, A. B., Skill, S. C., Lea-Langton, A., Balasundaram, B., Hall, C., Riley, R. and Llewellyn, C. A. 2012. Nutrient recycling of aqueous phase for microalgae cultivation from the hydrothermal liquefaction process. *Algal Research*, 1 (1): 70-76.

Bligh, E. G. and Dyer, W. J. 1959. A rapid method of total lipid extraction and purification. *Canadian journal of biochemistry and physiology*, 37 (8): 911-917.

Borges, F. C., Xie, Q., Min, M., Muniz, L. A. R., Farenzena, M., Trierweiler, J. O., Chen, P. and Ruan, R. 2014. Fast microwave-assisted pyrolysis of microalgae using microwave absorbent and HZSM-5 catalyst. *Bioresource technology*, 166: 518-526.

Brennan, L. and Owende, P. 2010. Biofuels from microalgae—a review of technologies for production, processing, and extractions of biofuels and co-products. *Renewable and sustainable energy reviews*, 14 (2): 557-577.

Brindhadevi, K., Anto, S., Rene, E. R., Sekar, M., Mathimani, T., Thuy Lan Chi, N. and Pugazhendhi, A. 2021. Effect of reaction temperature on the conversion of algal biomass to bio-oil and biochar through pyrolysis and hydrothermal liquefaction. *Fuel*, 285: 119106.

Brown, T. M., Duan, P. and Savage, P. E. 2010. Hydrothermal Liquefaction and Gasification of Nannochloropsis sp. *Energy & Fuels*, 24 (6): 3639-3646.

Chagas, B. M., Dorado, C., Serapiglia, M. J., Mullen, C. A., Boateng, A. A., Melo, M. A. and Ataíde, C. H. 2016. Catalytic pyrolysis-GC/MS of Spirulina: evaluation of a highly proteinaceous biomass source for production of fuels and chemicals. *Fuel*, 179: 124-134.

Chaiwong, K., Kiatsiriroat, T., Vorayos, N. and Thararax, C. 2013. Study of bio-oil and bio-char production from algae by slow pyrolysis. *Biomass and Bioenergy*, 56: 600-606.

Chakinala, A. G., Brilman, D. W. F., van Swaaij, W. P. M. and Kersten, S. R. A. 2010. Catalytic and Non-catalytic Supercritical Water Gasification of Microalgae and Glycerol. *Industrial & Engineering Chemistry Research*, 49 (3): 1113-1122.

Channiwala, S. and Parikh, P. 2002. A unified correlation for estimating HHV of solid, liquid and gaseous fuels. *Fuel*, 81 (8): 1051-1063.

Chen, C.-Y., Zhao, X.-Q., Yen, H.-W., Ho, S.-H., Cheng, C.-L., Lee, D.-J., Bai, F.-W. and Chang, J.-S. 2013. Microalgae-based carbohydrates for biofuel production. *Biochemical engineering journal*, 78: 1-10.

Chen, W.-H., Lin, B.-J., Huang, M.-Y. and Chang, J.-S. 2015. Thermochemical conversion of microalgal biomass into biofuels: a review. *Bioresource technology*, 184: 314-327.

Chen, W.-T., Zhang, Y., Zhang, J., Yu, G., Schideman, L. C., Zhang, P. and Minarick, M. 2014. Hydrothermal liquefaction of mixed-culture algal biomass from wastewater treatment system into bio-crude oil. *Bioresource technology*, 152: 130-139.

Cheng, J., Huang, R., Yu, T., Li, T., Zhou, J. and Cen, K. 2014. Biodiesel production from lipids in wet microalgae with microwave irradiation and bio-crude production from algal residue through hydrothermal liquefaction. *Bioresource technology*, 151: 415-418.

Chew, K. W., Yap, J. Y., Show, P. L., Suan, N. H., Juan, J. C., Ling, T. C., Lee, D.-J. and Chang, J.-S. 2017. Microalgae biorefinery: High value products perspectives. *Bioresource technology*, 229: 53-62.

Chia, M. A., Lombardi, A. T., Melão, M. d. G. G. and Parrish, C. C. 2015. Combined nitrogen limitation and cadmium stress stimulate total carbohydrates, lipids, protein and amino acid accumulation in Chlorella vulgaris (Trebouxiophyceae). *Aquatic Toxicology*, 160: 87-95.

Chiaramonti, D., Prussi, M., Buffi, M., Casini, D. and Rizzo, A. M. 2015. Thermochemical conversion of microalgae: Challenges and opportunities. *Energy Procedia*, 75: 819-826.

Chiaramonti, D., Prussi, M., Buffi, M., Rizzo, A. M. and Pari, L. 2017. Review and experimental study on pyrolysis and hydrothermal liquefaction of microalgae for biofuel production. *Applied Energy*, 185: 963-972.

Cooney, M., Young, G. and Nagle, N. 2009. Extraction of bio-oils from microalgae. *Separation & Purification Reviews*, 38 (4): 291-325.

Debiagi, P. E. A., Trinchera, M., Frassoldati, A., Faravelli, T., Vinu, R. and Ranzi, E. 2017. Algae characterization and multistep pyrolysis mechanism. *Journal of Analytical and Applied Pyrolysis*, 128: 423-436.

Demirbas, A. 2002. Relationships between heating value and lignin, moisture, ash and extractive contents of biomass fuels. *Energy exploration & exploitation*, 20 (1): 105-111.

Demirbas, A. 2004. Combustion characteristics of different biomass fuels. *Progress in Energy and Combustion Science*, 30 (2): 219-230.

Depraetere, O., Deschoenmaeker, F., Badri, H., Monsieurs, P., Foubert, I., Leys, N., Wattiez, R. and Muylaert, K. 2015. Trade-off between growth and carbohydrate accumulation in

nutrient-limited Arthrospira sp. PCC 8005 studied by integrating transcriptomic and proteomic approaches. *PLoS One*, 10 (7): e0132461.

Díaz-Rey, M., Cortés-Reyes, M., Herrera, C., Larrubia, M., Amadeo, N., Laborde, M. and Alemany, L. 2015. Hydrogen-rich gas production from algae-biomass by low temperature catalytic gasification. *Catalysis Today*, 257: 177-184.

Dimitriadis, A. and Bezergianni, S. 2017. Hydrothermal liquefaction of various biomass and waste feedstocks for biocrude production: A state of the art review. *Renewable and sustainable energy reviews*, 68: 113-125.

Du, Z., Li, Y., Wang, X., Wan, Y., Chen, Q., Wang, C., Lin, X., Liu, Y., Chen, P. and Ruan, R. 2011. Microwave-assisted pyrolysis of microalgae for biofuel production. *Bioresource technology*, 102 (7): 4890-4896.

Duan, P.-G., Li, S.-C., Jiao, J.-L., Wang, F. and Xu, Y.-P. 2018. Supercritical water gasification of microalgae over a two-component catalyst mixture. *Science of The Total Environment*, 630: 243-253.

Dubois, M., Gilles, K. A., Hamilton, J. K., Rebers, P. t. and Smith, F. 1956. Colorimetric method for determination of sugars and related substances. *Analytical chemistry*, 28 (3): 350-356.

Dumas, P. and Miller, L. 2003. The use of synchrotron infrared microspectroscopy in biological and biomedical investigations. *Vibrational spectroscopy*, 32 (1): 3-21.

Ehimen, E. A., Connaughton, S., Sun, Z. and Carrington, G. C. 2009. Energy recovery from lipid extracted, transesterified and glycerol codigested microalgae biomass. *Gcb Bioenergy*, 1 (6): 371-381.

Fang, S., Gu, W., Dai, M., Xu, J., Yu, Z., Lin, Y., Chen, J. and Ma, X. 2018. A study on microwave-assisted fast co-pyrolysis of chlorella and tire in the N2 and CO2 atmospheres. *Bioresource technology*, 250: 821-827.

Fernandez-Lopez, M., Pedroche, J., Valverde, J. and Sanchez-Silva, L. 2017. Simulation of the gasification of animal wastes in a dual gasifier using Aspen Plus®. *Energy Conversion and Management*, 140: 211-217.

Folch, J., Lees, M. and Stanley, G. S. 1957. A simple method for the isolation and purification of total lipides from animal tissues. *Journal of biological chemistry*, 226 (1): 497-509.

Friedl, A., Padouvas, E., Rotter, H. and Varmuza, K. 2005. Prediction of heating values of biomass fuel from elemental composition. *Analytica Chimica Acta*, 544 (1-2): 191-198.

Gai, C., Zhang, Y., Chen, W.-T., Zhang, P. and Dong, Y. 2014. Energy and nutrient recovery efficiencies in biocrude oil produced via hydrothermal liquefaction of Chlorella pyrenoidosa. *RSC Advances*, 4 (33): 16958-16967.

Galadima, A. and Muraza, O. 2018. Hydrothermal liquefaction of algae and bio-oil upgrading into liquid fuels: Role of heterogeneous catalysts. *Renewable and sustainable energy reviews*, 81: 1037-1048.

Geun Goo, B., Baek, G., Jin Choi, D., Il Park, Y., Synytsya, A., Bleha, R., Ho Seong, D., Lee, C.-G. and Kweon Park, J. 2013. Characterization of a renewable extracellular polysaccharide from defatted microalgae Dunaliella tertiolecta. *Bioresource technology*, 129: 343-350.

Ghasemi Naghdi, F., González González, L. M., Chan, W. and Schenk, P. M. 2016. Progress on lipid extraction from wet algal biomass for biodiesel production. *Microbial biotechnology*, 9 (6): 718-726.

Gollakota, A., Kishore, N. and Gu, S. 2017. A review on hydrothermal liquefaction of biomass. *Renewable and sustainable energy reviews*,

Gong, X., Zhang, B., Zhang, Y., Huang, Y. and Xu, M. 2014. Investigation on Pyrolysis of Low Lipid Microalgae Chlorella vulgaris and Dunaliella salina. *Energy & Fuels*, 28 (1): 95-103.

González López, C. V., García, M. d. C. C., Fernández, F. G. A., Bustos, C. S., Chisti, Y. and Sevilla, J. M. F. 2010. Protein measurements of microalgal and cyanobacterial biomass. *Bioresource technology*, 101 (19): 7587-7591.

Grierson, S., Strezov, V., Ellem, G., Mcgregor, R. and Herbertson, J. 2009. Thermal characterisation of microalgae under slow pyrolysis conditions. *Journal of Analytical and Applied Pyrolysis*, 85 (1-2): 118-123.

Griffiths, M. J., van Hille, R. P. and Harrison, S. T. 2012. Lipid productivity, settling potential and fatty acid profile of 11 microalgal species grown under nitrogen replete and limited conditions. *Journal of Applied Phycology*, 24 (5): 989-1001.

Grossmann, L., Ebert, S., Hinrichs, J. and Weiss, J. 2018. Production of protein-rich extracts from disrupted microalgae cells: Impact of solvent treatment and lyophilization. *Algal Research*, 36: 67-76.

Guldhe, A., Misra, R., Singh, P., Rawat, I. and Bux, F. 2016. An innovative electrochemical process to alleviate the challenges for harvesting of small size microalgae by using non-sacrificial carbon electrodes. *Algal Research*, 19: 292-298.

Guldhe, A., Singh, B., Rawat, I., Ramluckan, K. and Bux, F. 2014. Efficacy of drying and cell disruption techniques on lipid recovery from microalgae for biodiesel production. *Fuel*, 128: 46-52.

Guo, B., Walter, V., Hornung, U. and Dahmen, N. 2019. Hydrothermal liquefaction of Chlorella vulgaris and Nannochloropsis gaditana in a continuous stirred tank reactor and hydrotreating of biocrude by nickel catalysts. *Fuel Processing Technology*, 191: 168-180.

Guo, Y., Yeh, T., Song, W., Xu, D. and Wang, S. 2015. A review of bio-oil production from hydrothermal liquefaction of algae. *Renewable and sustainable energy reviews*, 48: 776-790.

Hach, C. 1987. More powerful peroxide Kjeldahl digestion method. *J. Assoc. Off. Anal. Chem.*, 70: 783-787.

Hadhoum, L., Burnens, G., Loubar, K., Balistrou, M. and Tazerout, M. 2019. Bio-oil recovery from olive mill wastewater in sub-/supercritical alcohol-water system. *Fuel*, 252: 360-370.

Hao, X., Guo, L., Mao, X., Zhang, X. and Chen, X. 2003. Hydrogen production from glucose used as a model compound of biomass gasified in supercritical water. *International Journal of Hydrogen Energy*, 28 (1): 55-64.

He, S., Zhao, M., Wang, J., Cheng, Z., Yan, B. and Chen, G. 2020. Hydrothermal liquefaction of low-lipid algae Nannochloropsis sp. and Sargassum sp.: Effect of feedstock composition and temperature. *Science of The Total Environment*, 712: 135677.

Hernando, H., Jiménez-Sánchez, S., Fermoso, J., Pizarro, P., Coronado, J. and Serrano, D. 2016. Assessing biomass catalytic pyrolysis in terms of deoxygenation pathways and energy yields for the efficient production of advanced biofuels. *Catalysis Science & Technology*, 6 (8): 2829-2843.

Ho, S.-H., Huang, S.-W., Chen, C.-Y., Hasunuma, T., Kondo, A. and Chang, J.-S. 2013. Characterization and optimization of carbohydrate production from an indigenous microalga Chlorella vulgaris FSP-E. *Bioresource technology*, 135: 157-165.

Horne, P. A. and Williams, P. T. 1996. Influence of temperature on the products from the flash pyrolysis of biomass. *Fuel*, 75 (9): 1051-1059.

Hu, S., Guan, Y., Wang, Y. and Han, H. 2011. Nano-magnetic catalyst KF/CaO–Fe3O4 for biodiesel production. *Applied Energy*, 88 (8): 2685-2690.

Hu, X., Zhou, J., Liu, G. and Gui, B. 2016. Selection of microalgae for high CO2 fixation efficiency and lipid accumulation from ten Chlorella strains using municipal wastewater. *Journal of Environmental Sciences*, 46: 83-91.

Hu, Y., Qi, L., Feng, S., Bassi, A. and Xu, C. C. 2019. Comparative studies on liquefaction of low-lipid microalgae into bio-crude oil using varying reaction media. *Fuel*, 238: 240-247.

Hu, Z., Zheng, Y., Yan, F., Xiao, B. and Liu, S. 2013. Bio-oil production through pyrolysis of blue-green algae blooms (BGAB): Product distribution and bio-oil characterization. *Energy*, 52: 119-125.

Huang, F., Tahmasebi, A., Maliutina, K. and Yu, J. 2017. Formation of nitrogen-containing compounds during microwave pyrolysis of microalgae: Product distribution and reaction pathways. *Bioresource technology*, 245: 1067-1074.

Huang, H.-j., Yuan, X.-z., Zhu, H.-n., Li, H., Liu, Y., Wang, X.-l. and Zeng, G.-m. 2013a. Comparative studies of thermochemical liquefaction characteristics of microalgae, lignocellulosic biomass and sewage sludge. *Energy*, 56: 52-60.

Huang, X., Huang, Z., Wen, W. and Yan, J. 2013b. Effects of nitrogen supplementation of the culture medium on the growth, total lipid content and fatty acid profiles of three microalgae (Tetraselmis subcordiformis, Nannochloropsis oculata and Pavlova viridis). *Journal of Applied Phycology*, 25 (1): 129-137.

Ikaran, Z., Suárez-Alvarez, S., Urreta, I. and Castañón, S. 2015. The effect of nitrogen limitation on the physiology and metabolism of Chlorella vulgaris var L3. *Algal Research*, 10: 134-144.

Jeevan Kumar, S. P. and Banerjee, R. 2019. Enhanced lipid extraction from oleaginous yeast biomass using ultrasound assisted extraction: A greener and scalable process. *Ultrasonics sonochemistry*, 52: 25-32.

Jena, U., Das, K. and Kastner, J. 2012. Comparison of the effects of Na2CO3, Ca3 (PO4) 2, and NiO catalysts on the thermochemical liquefaction of microalga Spirulina platensis. *Applied Energy*, 98: 368-375.

Jena, U. and Das, K. C. 2011. Comparative Evaluation of Thermochemical Liquefaction and Pyrolysis for Bio-Oil Production from Microalgae. *Energy & Fuels*, 25 (11): 5472-5482.

Jena, U., Das, K. C. and Kastner, J. R. 2011. Effect of operating conditions of thermochemical liquefaction on biocrude production from Spirulina platensis. *Bioresource technology*, 102 (10): 6221-6229.

Jena, U., McCurdy, A. T., Warren, A., Summers, H., Ledbetter, R. N., Hoekman, S. K., Seefeldt, L. C. and Quinn, J. C. 2015. Oleaginous yeast platform for producing biofuels via co-solvent hydrothermal liquefaction. *Biotechnology for biofuels*, 8 (1): 167.

Jena, U., Vaidyanathan, N., Chinnasamy, S. and Das, K. C. 2011. Evaluation of microalgae cultivation using recovered aqueous co-product from thermochemical liquefaction of algal biomass. *Bioresource technology*, 102 (3): 3380-3387.

Jiao, J.-L., Wang, F., Duan, P.-G., Xu, Y.-P. and Yan, W.-H. 2017. Catalytic hydrothermal gasification of microalgae for producing hydrogen and methane-rich gas. *Energy Sources, Part A: Recovery, Utilization, and Environmental Effects*, 39 (9): 851-860.

Karatas, H. and Akgun, F. 2018. Experimental results of gasification of walnut shell and pistachio shell in a bubbling fluidized bed gasifier under air and steam atmospheres. *Fuel*, 214: 285-292.

Kassim, M. A., Kirtania, K., De La Cruz, D., Cura, N., Srivatsa, S. C. and Bhattacharya, S. 2014. Thermogravimetric analysis and kinetic characterization of lipid-extracted Tetraselmis suecica and Chlorella sp. *Algal Research*, 6: 39-45.

Kelrich, K. 1990. ur.(1990) Official methods of analysis. *Arlington, VA: Association of Official Analytical Chemists/AOAC*,

Khalil, R., Mészáros, E., Grønli, M., Várhegyi, G., Mohai, I., Marosvölgyi, B. and Hustad, J. 2008. Thermal analysis of energy crops: Part I: The applicability of a macro-thermobalance for biomass studies. *Journal of Analytical and Applied Pyrolysis*, 81 (1): 52-59.

Khoo, H., Koh, C., Shaik, M. and Sharratt, P. 2013. Bioenergy co-products derived from microalgae biomass via thermochemical conversion–life cycle energy balances and CO2 emissions. *Bioresource technology*, 143: 298-307.

Kim, S. W., Koo, B. S. and Lee, D. H. 2014. A comparative study of bio-oils from pyrolysis of microalgae and oil seed waste in a fluidized bed. *Bioresource technology*, 162: 96-102.

Kohansal, K., Tavasoli, A. and Bozorg, A. 2019. Using a hybrid-like supported catalyst to improve green fuel production through hydrothermal liquefaction of Scenedesmus obliquus microalgae. *Bioresource technology*, 277: 136-147.

Koley, S., Khadase, M. S., Mathimani, T., Raheman, H. and Mallick, N. 2018. Catalytic and non-catalytic hydrothermal processing of Scenedesmus obliquus biomass for bio-crude production–A sustainable energy perspective. *Energy Conversion and Management*, 163: 111-121.

Kostyniuk, A., Key, D. and Mdleleni, M. 2019. Effect of Fe-Mo promoters on HZSM-5 zeolite catalyst for 1-hexene aromatization. *Journal of Saudi Chemical Society*, 23 (5): 612-626.

Kumar, G., Shobana, S., Chen, W.-H., Bach, Q.-V., Kim, S.-H., Atabani, A. and Chang, J.-S. 2017a. A review of thermochemical conversion of microalgal biomass for biofuels: chemistry and processes. *Green Chemistry*, 19 (1): 44-67.

Kumar, S. J., Kumar, G. V., Dash, A., Scholz, P. and Banerjee, R. 2017b. Sustainable green solvents and techniques for lipid extraction from microalgae: A review. *Algal Research*, 21: 138-147.

Lajili, M., Guizani, C., Sanz, F. E. and Jeguirim, M. 2018. Fast pyrolysis and steam gasification of pellets prepared from olive oil mill residues. *Energy*, 150: 61-68.

Lam, M. K. and Lee, K. T. 2012. Microalgae biofuels: a critical review of issues, problems and the way forward. *Biotechnology advances*, 30 (3): 673-690.

Lamers, P. P., Janssen, M., De Vos, R. C., Bino, R. J. and Wijffels, R. H. 2012. Carotenoid and fatty acid metabolism in nitrogen-starved Dunaliella salina, a unicellular green microalga. *Journal of biotechnology*, 162 (1): 21-27.

Lee, A. K., Lewis, D. M. and Ashman, P. J. 2012. Disruption of microalgal cells for the extraction of lipids for biofuels: processes and specific energy requirements. *Biomass and Bioenergy*, 46: 89-101.

Li, T., Xu, J., Gao, B., Xiang, W., Li, A. and Zhang, C. 2016. Morphology, growth, biochemical composition and photosynthetic performance of Chlorella vulgaris (Trebouxiophyceae) under low and high nitrogen supplies. *Algal Research*, 16: 481-491.

Liang, Y. 2013. Producing liquid transportation fuels from heterotrophic microalgae. *Applied Energy*, 104: 860-868.

Liu, B., Wang, Z. and Feng, L. 2021. Effects of reaction parameter on catalytic hydrothermal liquefaction of microalgae into hydrocarbon rich bio-oil. *Journal of the Energy Institute*, 94: 22-28.

Liu, L., Huang, Y., Cao, J., Liu, C., Dong, L., Xu, L. and Zha, J. 2018. Experimental study of biomass gasification with oxygen-enriched air in fluidized bed gasifier. *Science of The Total Environment*, 626: 423-433.

Liu, T., Li, Y., Liu, F. and Wang, C. 2016. The enhanced lipid accumulation in oleaginous microalga by the potential continuous nitrogen-limitation (CNL) strategy. *Bioresource technology*, 203: 150-159.

López-González, D., Fernandez-Lopez, M., Valverde, J. and Sanchez-Silva, L. 2014. Pyrolysis of three different types of microalgae: kinetic and evolved gas analysis. *Energy*, 73: 33-43.

Lowry, O. H., Rosebrough, N. J., Farr, A. L. and Randall, R. J. 1951. Protein measurement with the Folin phenol reagent. *Journal of biological chemistry*, 193: 265-275.

Lu, J., Zhang, Z., Fan, G., Zhang, L., Wu, Y. and Yang, M. 2020. Enhancement of microalgae bio-oil quality via hydrothermal liquefaction using functionalized carbon nanotubes. *Journal of Cleaner Production*: 124835.

Lu, J., Zhang, Z., Zhang, L., Fan, G., Wu, Y. and Yang, M. 2021. Catalytic hydrothermal liquefaction of microalgae over different biochars. *Catalysis Communications*, 149: 106236.

Ly, H. V., Kim, S.-S., Choi, J. H., Woo, H. C. and Kim, J. 2016. Fast pyrolysis of Saccharina japonica alga in a fixed-bed reactor for bio-oil production. *Energy Conversion and Management*, 122: 526-534.

Ma, C., Geng, J., Zhang, D. and Ning, X. 2019. Hydrothermal liquefaction of macroalgae: Influence of zeolites based catalyst on products. *Journal of the Energy Institute*,

Ma, C., Geng, J., Zhang, D. and Ning, X. 2020. Hydrothermal liquefaction of macroalgae: Influence of zeolites based catalyst on products. *Journal of the Energy Institute*, 93 (2): 581-590.

Macrì, D., Catizzone, E., Molino, A. and Migliori, M. 2020. Supercritical water gasification of biomass and agro-food residues: Energy assessment from modelling approach. *Renewable energy*, 150: 624-636.

Maddi, B., Viamajala, S. and Varanasi, S. 2011. Comparative study of pyrolysis of algal biomass from natural lake blooms with lignocellulosic biomass. *Bioresource technology*, 102 (23): 11018-11026.

Mangla, O. and Roy, S. 2018. Monoclinic zirconium oxide nanostructures having tunable band gap synthesized under extremely non-equilibrium plasma conditions. In: Proceedings of *Multidisciplinary Digital Publishing Institute Proceedings*. 10.

Mani, T., Murugan, P., Abedi, J. and Mahinpey, N. 2010. Pyrolysis of wheat straw in a thermogravimetric analyzer: effect of particle size and heating rate on devolatilization and estimation of global kinetics. *Chemical engineering research and design*, 88 (8): 952-958.

Markou, G., Chatzipavlidis, I. and Georgakakis, D. 2012. Carbohydrates production and bio-flocculation characteristics in cultures of Arthrospira (Spirulina) platensis: improvements through phosphorus limitation process. *BioEnergy research*, 5 (4): 915-925.

Mathimani, T., Baldinelli, A., Rajendran, K., Prabakar, D., Matheswaran, M., Pieter van Leeuwen, R. and Pugazhendhi, A. 2019. Review on cultivation and thermochemical conversion of microalgae to fuels and chemicals: Process evaluation and knowledge gaps. *Journal of Cleaner Production*, 208: 1053-1064.

Meullemiestre, A., Breil, C., Abert-Vian, M. and Chemat, F. 2016. Microwave, ultrasound, thermal treatments, and bead milling as intensification techniques for extraction of lipids from oleaginous Yarrowia lipolytica yeast for a biojetfuel application. *Bioresource technology*, 211: 190-199.

Milano, J., Ong, H. C., Masjuki, H. H., Chong, W. T., Lam, M. K., Loh, P. K. and Vellayan, V. 2016. Microalgae biofuels as an alternative to fossil fuel for power generation. *Renewable and sustainable energy reviews*, 58: 180-197.

Miller, A., Hendry, D., Wilkinson, N., Venkitasamy, C. and Jacoby, W. 2012. Exploration of the gasification of Spirulina algae in supercritical water. *Bioresource technology*, 119: 41-47.

Mitran, G., Neaţu, F., Pavel, O. D., Trandafir, M. M. and Florea, M. 2019. Behavior of Molybdenum–Vanadium Mixed Oxides in Selective Oxidation and Disproportionation of Toluene. *Materials*, 12 (5): 748.

Morris, D. L. 1948. Quantitative determination of carbohydrates with Dreywood's anthrone reagent. *Science (Washington)*, 107: 254-255.

Mott, R. and Spooner, C. 1940. The calorific value of carbon in coal: the Dulong relationship. *Fuel*, 19 (226): 242.

Mustapha, S. I. and Isa, Y. M. 2020. Utilization of quaternary solvent mixtures for extraction of lipids from Scenedesmus obliquus microalgae. *Cogent Engineering*, 7 (1): 1788877.

Nagappan, S., Devendran, S., Tsai, P.-C., Dahms, H.-U. and Ponnusamy, V. K. 2019. Potential of two-stage cultivation in microalgae biofuel production. *Fuel*, 252: 339-349.

Nahak, S., Nahak, G., Pradhan, I. and Sahu, R. 2011. Bioethanol from marine algae: a solution to global warming problem. *J. Appl. Environ. Biol. Sci*, 1 (4): 74-80.

Naik, S., Goud, V. V., Rout, P. K., Jacobson, K. and Dalai, A. K. 2010. Characterization of Canadian biomass for alternative renewable biofuel. *Renewable energy*, 35 (8): 1624-1631.

Naqvi, S. R., Naqvi, M., Noor, T., Hussain, A., Iqbal, N., Uemura, Y. and Nishiyama, N. 2017. Catalytic Pyrolysis Of Botryococcus Braunii (microalgae) Over Layered and Delaminated Zeolites For Aromatic Hydrocarbon Production. *Energy Procedia*, 142: 381-385.

Nigam, P. S. and Singh, A. 2011. Production of liquid biofuels from renewable resources. *Progress in Energy and Combustion Science*, 37 (1): 52-68.

Odetoye, T., Afolabi, T., Bakar, M. A. and Titiloye, J. 2018. Thermochemical characterization of Nigerian Jatropha curcas fruit and seed residues for biofuel production. *Energy, Ecology and Environment*, 3 (6): 330-337.

Onwudili, J. A., Lea-Langton, A. R., Ross, A. B. and Williams, P. T. 2013. Catalytic hydrothermal gasification of algae for hydrogen production: composition of reaction products and potential for nutrient recycling. *Bioresource technology*, 127: 72-80.

Pan, P., Hu, C., Yang, W., Li, Y., Dong, L., Zhu, L., Tong, D., Qing, R. and Fan, Y. 2010. The direct pyrolysis and catalytic pyrolysis of Nannochloropsis sp. residue for renewable bio-oils. *Bioresource technology*, 101 (12): 4593-4599.

Peng, W., Wu, Q. and Tu, P. 2001. Pyrolytic characteristics of heterotrophic Chlorella protothecoides for renewable bio-fuel production. *Journal of Applied Phycology*, 13 (1): 5-12.

Peng, W., Wu, Q., Tu, P. and Zhao, N. 2001. Pyrolytic characteristics of microalgae as renewable energy source determined by thermogravimetric analysis. *Bioresource technology*, 80 (1): 1-7.

Peterson, A. A., Vogel, F., Lachance, R. P., Fröling, M., Antal Jr, M. J. and Tester, J. W. 2008. Thermochemical biofuel production in hydrothermal media: a review of sub-and supercritical water technologies. *Energy & Environmental Science*, 1 (1): 32-65.

Phukan, M. M., Chutia, R. S., Konwar, B. and Kataki, R. 2011. Microalgae Chlorella as a potential bio-energy feedstock. *Applied Energy*, 88 (10): 3307-3312.

Qi, P., Chang, G., Wang, H., Zhang, X. and Guo, Q. 2018. Production of aromatic hydrocarbons by catalytic co-pyrolysis of microalgae and polypropylene using HZSM-5. *Journal of Analytical and Applied Pyrolysis*, 136: 178-185.

Raheem, A., Liu, H., Ji, G. and Zhao, M. 2019. Gasification of lipid-extracted microalgae biomass promoted by waste eggshell as CaO catalyst. *Algal Research*, 42: 101601.

Rahman, N. A. A., Fermoso, J. and Sanna, A. 2018. Effect of Li-LSX-zeolite on the in-situ catalytic deoxygenation and denitrogenation of Isochrysis sp. microalgae pyrolysis vapours. *Fuel Processing Technology*, 173: 253-261.

Ramesh, D. 2013. Lipid identification and extraction techniques. *Biotechnological applications of microalgae: biodiesel and value-added products*: 89-97.

Ramesh Kumar, B., Deviram, G., Mathimani, T., Duc, P. A. and Pugazhendhi, A. 2019. Microalgae as rich source of polyunsaturated fatty acids. *Biocatalysis and Agricultural Biotechnology*, 17: 583-588.

Ranjith-Kumar, R., Hanumantha Rao, P. and Arumugam, M. 2015. Lipid extraction methods from microalgae: a comprehensive review. *Frontiers in Energy Research*, 2: 61.

Rashid, N., Rehman, M. S. U. and Han, J.-I. 2013. Recycling and reuse of spent microalgal biomass for sustainable biofuels. *Biochemical engineering journal*, 75: 101-107.

Rawat, I., Kumar, R. R., Mutanda, T. and Bux, F. 2011. Dual role of microalgae: phycoremediation of domestic wastewater and biomass production for sustainable biofuels production. *Applied Energy*, 88 (10): 3411-3424.

Ren, R., Han, X., Zhang, H., Lin, H., Zhao, J., Zheng, Y. and Wang, H. 2018. High yield bio-oil production by hydrothermal liquefaction of a hydrocarbon-rich microalgae and biocrude upgrading. *Carbon Resources Conversion*, 1 (2): 153-159.

Řezanka, T., Lukavský, J., Nedbalová, L. and Sigler, K. 2011. Effect of nitrogen and phosphorus starvation on the polyunsaturated triacylglycerol composition, including positional isomer distribution, in the alga Trachydiscus minutus. *Phytochemistry*, 72 (18): 2342-2351.

Richmond, A. 2004. *Handbook of microalgal culture: biotechnology and applied phycology*. Wiley Online Library.

Rogalinski, T., Liu, K., Albrecht, T. and Brunner, G. 2008. Hydrolysis kinetics of biopolymers in subcritical water. *The Journal of Supercritical Fluids*, 46 (3): 335-341.

Ross, A., Biller, P., Kubacki, M., Li, H., Lea-Langton, A. and Jones, J. 2010. Hydrothermal processing of microalgae using alkali and organic acids. *Fuel*, 89 (9): 2234-2243.

Saber, M., Golzary, A., Hosseinpour, M., Takahashi, F. and Yoshikawa, K. 2016. Catalytic hydrothermal liquefaction of microalgae using nanocatalyst. *Applied Energy*, 183: 566-576.

Sajjadi, B., Chen, W.-Y., Raman, A. A. A. and Ibrahim, S. 2018. Microalgae lipid and biomass for biofuel production: A comprehensive review on lipid enhancement strategies and their effects on fatty acid composition. *Renewable and sustainable energy reviews*, 97: 200-232.

Sallet, D., Souza, P. O., Fischer, L. T., Ugalde, G., Zabot, G. L., Mazutti, M. A. and Kuhn, R. C. 2019. Ultrasound-assisted extraction of lipids from Mortierella isabellina. *Journal of Food Engineering*, 242: 1-7.

Samarasinghe, N. U. and Fernando, S. D. 2015. Extraction of lipids from microalgae using monophasic-biphasic separation via hexane–acetone–water system. *Biofuels*, 6 (1-2): 129-135.

Sambusiti, C., Bellucci, M., Zabaniotou, A., Beneduce, L. and Monlau, F. 2015. Algae as promising feedstocks for fermentative biohydrogen production according to a biorefinery approach: a comprehensive review. *Renewable and sustainable energy reviews*, 44: 20-36.

Selvig, W. 1945. Calorific value of coal. *Chemistry of coal utilization*: 132-144.

Shakya, R., Adhikari, S., Mahadevan, R. and Dempster, T. A. 2017a. Catalytic Upgrading of Bio-oil Produced from Hydrothermal Liquefaction of Nannochloropsis sp. *Bioresource technology*,

Shakya, R., Adhikari, S., Mahadevan, R., Shanmugam, S. R., Nam, H. and Dempster, T. A. 2017b. Influence of biochemical composition during hydrothermal liquefaction of algae on product yields and fuel properties. *Bioresource technology*, 243: 1112-1120.

Shakya, R., Whelen, J., Adhikari, S., Mahadevan, R. and Neupane, S. 2015. Effect of temperature and Na 2 CO 3 catalyst on hydrothermal liquefaction of algae. *Algal Research*, 12: 80-90.

Sibi, G., Shetty, V. and Mokashi, K. 2016. Enhanced lipid productivity approaches in microalgae as an alternate for fossil fuels–A review. *Journal of the Energy Institute*, 89 (3): 330-334.

Sikarwar, V. S., Zhao, M., Fennell, P. S., Shah, N. and Anthony, E. J. 2017. Progress in biofuel production from gasification. *Progress in Energy and Combustion Science*, 61: 189-248.

Singh, B., Guldhe, A., Rawat, I. and Bux, F. 2014. Towards a sustainable approach for development of biodiesel from plant and microalgae. *Renewable and sustainable energy reviews*, 29: 216-245.

Singh, B., Guldhe, A., Singh, P., Singh, A., Rawat, I. and Bux, F. 2015. Sustainable production of biofuels from microalgae using a biorefinary approach. In: *Applied environmental biotechnology: Present scenario and future trends*. Springer, 115-128.

Singh, P., Kumari, S., Guldhe, A., Misra, R., Rawat, I. and Bux, F. 2016. Trends and novel strategies for enhancing lipid accumulation and quality in microalgae. *Renewable and sustainable energy reviews*, 55: 1-16.

Singh, Y. D., Mahanta, P. and Bora, U. 2017. Comprehensive characterization of lignocellulosic biomass through proximate, ultimate and compositional analysis for bioenergy production. *Renewable energy*, 103: 490-500.

Slocombe, S. P., Ross, M., Thomas, N., McNeill, S. and Stanley, M. S. 2013. A rapid and general method for measurement of protein in micro-algal biomass. *Bioresource technology*, 129: 51-57.

Sluiter, A., Hames, B., Hyman, D., Payne, C., Ruiz, R., Scarlata, C., Sluiter, J., Templeton, D. and Wolfe, J. 2005. Determination of total solids in biomass and total dissolved solids in liquid process samples. Laboratory analytical procedure (LAP). NREL/TP-510–42621. *Cited from: www. nrel. gov/biomass/pdfs/42621. pdf*,

Soji-Adekunle, A. R., Asere, A. A., Ishola, N. B., Oloko-Oba, I. M. and Betiku, E. 2018. Modeling of synthesis of waste cooking oil methyl esters by artificial neural network and

response surface methodology. *International Journal of Ambient Energy*, (just-accepted): 1-34.

Sotoudehniakarani, F., Alayat, A. and McDonald, A. G. 2019. Characterization and comparison of pyrolysis products from fast pyrolysis of commercial Chlorella vulgaris and cultivated microalgae. *Journal of Analytical and Applied Pyrolysis*, 139: 258-273.

Srivatsa, S. C., Li, F. and Bhattacharya, S. 2019. Optimization of reaction parameters for bio-oil production by catalytic pyrolysis of microalga Tetraselmis suecica: Influence of Ni-loading on the bio-oil composition. *Renewable energy*, 142: 426-436.

Stucki, S., Vogel, F., Ludwig, C., Haiduc, A. G. and Brandenberger, M. 2009. Catalytic gasification of algae in supercritical water for biofuel production and carbon capture. *Energy & Environmental Science*, 2 (5): 535-541.

Suali, E. and Sarbatly, R. 2012. Conversion of microalgae to biofuel. *Renewable and sustainable energy reviews*, 16 (6): 4316-4342.

Suárez-Garcıa, F., Martınez-Alonso, A., Llorente, M. F. and Tascón, J. 2002. Inorganic matter characterization in vegetable biomass feedstocks. *Fuel*, 81 (9): 1161-1169.

Taleb, A., Kandilian, R., Touchard, R., Montalescot, V., Rinaldi, T., Taha, S., Takache, H., Marchal, L., Legrand, J. and Pruvost, J. 2016. Screening of freshwater and seawater microalgae strains in fully controlled photobioreactors for biodiesel production. *Bioresource technology*, 218: 480-490.

Thangalazhy-Gopakumar, S., Adhikari, S., Chattanathan, S. A. and Gupta, R. B. 2012. Catalytic pyrolysis of green algae for hydrocarbon production using H+ ZSM-5 catalyst. *Bioresource technology*, 118: 150-157.

Thilakaratne, C. R. 2016. Understanding catalytic pyrolysis of biomass for production of biofuels.

Thummavichai, K., Wang, N., Xu, F., Rance, G., Xia, Y. and Zhu, Y. 2018. In situ investigations of the phase change behaviour of tungsten oxide nanostructures. *Royal Society open science*, 5 (4): 171932.

Ullah, K., Ahmad, M., Sharma, V. K., Lu, P., Harvey, A., Zafar, M. and Sultana, S. 2015. Assessing the potential of algal biomass opportunities for bioenergy industry: a review. *Fuel*, 143: 414-423.

Valdez, P. J., Nelson, M. C., Wang, H. Y., Lin, X. N. and Savage, P. E. 2012. Hydrothermal liquefaction of Nannochloropsis sp.: Systematic study of process variables and analysis of the product fractions. *Biomass and Bioenergy*, 46: 317-331.

Vassilev, S. V., Baxter, D., Andersen, L. K. and Vassileva, C. G. 2010. An overview of the chemical composition of biomass. *Fuel*, 89 (5): 913-933.

Vassilev, S. V. and Vassileva, C. G. 2016. Composition, properties and challenges of algae biomass for biofuel application: an overview. *Fuel*, 181: 1-33.

Venteris, E. R., Skaggs, R. L., Wigmosta, M. S. and Coleman, A. M. 2014. A national-scale comparison of resource and nutrient demands for algae-based biofuel production by lipid extraction and hydrothermal liquefaction. *Biomass and Bioenergy*, 64: 276-290.

Vlaskin, M., Chernova, N., Kiseleva, S. and Zhuk, A. 2017. Hydrothermal liquefaction of microalgae to produce biofuels: state of the art and future prospects. *Thermal Engineering*, 64 (9): 627-636.

Vo, T. K., Lee, O. K., Lee, E. Y., Kim, C. H., Seo, J.-W., Kim, J. and Kim, S.-S. 2016. Kinetics study of the hydrothermal liquefaction of the microalga Aurantiochytrium sp. KRS101. *Chemical engineering journal*, 306: 763-771.

Wądrzyk, M., Janus, R., Vos, M. P. and Brilman, D. W. F. 2018. Effect of process conditions on bio-oil obtained through continuous hydrothermal liquefaction of Scenedesmus sp. microalgae. *Journal of Analytical and Applied Pyrolysis*, 134: 415-426.

Wang, K. and Brown, R. C. 2013. Catalytic pyrolysis of microalgae for production of aromatics and ammonia. *Green Chemistry*, 15 (3): 675-681.

Wang, K., Brown, R. C., Homsy, S., Martinez, L. and Sidhu, S. S. 2013. Fast pyrolysis of microalgae remnants in a fluidized bed reactor for bio-oil and biochar production. *Bioresource technology*, 127: 494-499.

Wang, S., Cai, Q., Guo, Z., Wang, Y. and Wang, X. 2012. Renewable gasoline produced by co-cracking of methanol and ketones in bio-oil. *BioResources*, 7 (4): 5019-5031.

Wang, T. and Lee, H. G. 2015. Advances in research on cis-9, trans-11 conjugated linoleic acid: a major functional conjugated linoleic acid isomer. *Critical reviews in food science and nutrition*, 55 (5): 720-731.

Wang, X., Sheng, L. and Yang, X. 2017. Pyrolysis characteristics and pathways of protein, lipid and carbohydrate isolated from microalgae Nannochloropsis sp. *Bioresource technology*, 229: 119-125.

Wardani, R. K., Dahlan, K., Wahyudi, S. T. and Sukaryo, S. G. 2019. Synthesis and characterization of nanoparticle magnetite for biomedical application. In: Proceedings of *AIP Conference Proceedings*. AIP Publishing LLC, 020137.

Widjaya, E. R., Chen, G., Bowtell, L. and Hills, C. 2018. Gasification of non-woody biomass: A literature review. *Renewable and sustainable energy reviews*, 89: 184-193.

Wu, K.-T., Tsai, C.-J., Chen, C.-S. and Chen, H.-W. 2012. The characteristics of torrefied microalgae. *Applied Energy*, 100: 52-57.

Xiao, Y., Xu, S., Song, Y., Wang, C. and Ouyang, S. 2018. Gasification of low-rank coal for hydrogen-rich gas production in a dual loop gasification system. *Fuel Processing Technology*, 171: 110-116.

Xu, L., Brilman, D. W. F., Withag, J. A. M., Brem, G. and Kersten, S. 2011. Assessment of a dry and a wet route for the production of biofuels from microalgae: Energy balance analysis. *Bioresource technology*, 102 (8): 5113-5122.

Xu, Y., Hu, Y., Peng, Y., Yao, L., Dong, Y., Yang, B. and Song, R. 2020. Catalytic pyrolysis and liquefaction behavior of microalgae for bio-oil production. *Bioresource technology*, 300: 122665.

Xu, Y., Zheng, X., Yu, H. and Hu, X. 2014. Hydrothermal liquefaction of Chlorella pyrenoidosa for bio-oil production over Ce/HZSM-5. *Bioresource technology*, 156: 1-5.

Yan, W.-H., Wang, K., Duan, P.-G., Wang, B., Wang, F., Shi, X.-L. and Xu, Y.-P. 2017. Catalytic hydropyrolysis and co-hydropyrolysis of algae and used engine oil for the production of hydrocarbon-rich fuel. *Energy*, 133: 1153-1162.

Yang, C., Li, R., Zhang, B., Qiu, Q., Wang, B., Yang, H., Ding, Y. and Wang, C. 2019. Pyrolysis of microalgae: A critical review. *Fuel Processing Technology*, 186: 53-72.

Yanik, J., Ebale, S., Kruse, A., Saglam, M. and Yüksel, M. 2008. Biomass gasification in supercritical water: II. Effect of catalyst. *International Journal of Hydrogen Energy*, 33 (17): 4520-4526.

Yee, W. 2015. Feasibility of various carbon sources and plant materials in enhancing the growth and biomass productivity of the freshwater microalgae Monoraphidium griffithii NS16. *Bioresource technology*, 196: 1-8.

Yeh, T. M., Dickinson, J. G., Franck, A., Linic, S., Thompson, L. T. and Savage, P. E. 2013. Hydrothermal catalytic production of fuels and chemicals from aquatic biomass. *Journal of Chemical Technology and Biotechnology*, 88 (1): 13-24.

Yoo, G., Park, M. S., Yang, J.-W. and Choi, M. 2015. Lipid content in microalgae determines the quality of biocrude and Energy Return On Investment of hydrothermal liquefaction. *Applied Energy*, 156: 354-361.

Yu, G., Zhang, Y., Schideman, L., Funk, T. and Wang, Z. 2011. Distributions of carbon and nitrogen in the products from hydrothermal liquefaction of low-lipid microalgae. *Energy & Environmental Science*, 4 (11): 4587-4595.

Zainan, N. H., Srivatsa, S. C. and Bhattacharya, S. 2015. Catalytic pyrolysis of microalgae Tetraselmis suecica and characterization study using in situ Synchrotron-based Infrared Microscopy. *Fuel*, 161: 345-354.

Zainan, N. H., Srivatsa, S. C., Li, F. and Bhattacharya, S. 2018. Quality of bio-oil from catalytic pyrolysis of microalgae Chlorella vulgaris. *Fuel*, 223: 12-19.

Zhang, X., Zhong, J., Wang, J., Zhang, L., Gao, J. and Liu, A. 2009. Catalytic performance and characterization of Ni-doped HZSM-5 catalysts for selective trimerization of n-butene. *Fuel Processing Technology*, 90 (7-8): 863-870.

Zhou, X., Jin, W., Tu, R., Guo, Q., Han, S.-f., Chen, C., Wang, Q., Liu, W., Jensen, P. D. and Wang, Q. 2019. Optimization of microwave assisted lipid extraction from microalga Scenedesmus obliquus grown on municipal wastewater. *Journal of Cleaner Production*, 221: 502-508.

Ziolkowska, J. R. and Simon, L. 2014. Recent developments and prospects for algae-based fuels in the US. *Renewable and sustainable energy reviews*, 29: 847-853.

Zou, S., Wu, Y., Yang, M., Li, C. and Tong, J. 2010. Bio-oil production from sub-and supercritical water liquefaction of microalgae Dunaliella tertiolecta and related properties. *Energy & Environmental Science*, 3 (8): 1073-1078.

APPENDIX A (CHAPTER 3)

Table A3.1. Relative abundance (area %) of the main compounds of the pyrolytic bio-oil from N1 at 500 °C

Categories	Compounds	Area (%)
Aliphatic hydrocarbons		37.54
	Decane	1.41
	Dodecane	1.65
	9-Octadecene	3.29
	4-butylcyclopentene	0.64
	2-Hexadecene	7.84
	Hexadecane	3.72
	Heneicosane	15.56
	Heptadecane	3.43
Aromatic hydrocarbons		5.62
	Phenol	4.64
	Benzenemethanol	0.63
	Thiophene	0.35
Nitrogen-containing aliphatics		2.20
	Butanamide	0.78
	2-Propen-1-amine	0.88
	Pentanamide	0.54
Nitrogen-containing aromatics		3.72
	2-Pyrrolidinone	1.69
	4-Piperidinone	0.72
	Pyrimidinone	0.37
	Enanthamide	0.30
	Indole	0.64
Acids		26.68
	Phosphonic acid	0.98
	Hexanoic acid	0.35
	Fumaric acid	0.28
	Acetic acid	25.07
Others (Ketones, Aldehyde, Alcohol, Ethers)		24.22
	3-Penten-2-one	0.27
	2-Pentanone	9.71
	2-Furanmethanol	0.31
	Ethanol	0.56
	1,2,3-Propanetriol	1.25
	Cyclododecanol	0.19
	Methyl Ester	1.10
	5-Hydroxymethyloxolan-2-one	0.45
	Neophytadiene	9.16
	2,3-Anhydro-d-mannosan	0.38
	1,4:3,6-Dianhydro-alpha-d-glucopyranose	0.84

Table A3.2. Relative abundance (area %) of the main compounds of the pyrolytic bio-oil from R-N1 at 500 °C

Categories	Compounds	Area (%)
Aliphatic hydrocarbons		5.55
	Cycloheptene	0.24
	Hexadecane	0.36
	dodecane	2.21
	1-Hexadecene	2.74
Aromatics hydrocarbons		37.4
	Benzene	0.07
	2-Furanmethanol	4.8
	Phenol	28.67
	4H-Cyclopentafuran	3.86
Nitrogen-containing aliphatics		8.4
	Acetamide	2.7
	Propanamide	0.46
	Azetidine	0.33
	Hexanamide	2.75
	Pentanamide	2.08
	5-Aminovaleramide	0.08
Nitrogen-containing aromatics		18.66
	Piperidine-4-carbonitrile	0.48
	Pyridine	0.81
	4-Piperidinone	2.76
	1H-Pyrrole-2,5-dione	3.99
	1H-Pyrrole-2-carboxaldehyde	1.00
	1H-Indole	9.62
Acids		4.3
	Propanoic acid	0.07
	Octanoic acid	4.03
	2-Ethylbutyric acid	0.2
Others (Ketones, Aldehyde, Alcohol, Ethers)		25.68
	3-Penten-2-one	0.76
	2-Pentanone	4.76
	Ethanol	5.2
	2-cyclopentenone	3.94
	2-Methylenecyclohexanol	1.34
	1,4:3,6-Dianhydro-alpha-d-glucopyranose	9.68

Table A3.3. Relative abundance (area %) of the main compounds of the pyrolytic bio-oil from N3 at 500 °C

Categories	Compounds	Area (%)
Aliphatic hydrocarbons		13.51
	Propane	0.74
	Decane	0.62
	Dodecane	2.07
	Cyclododecane	1.08
	Tetradecane	5.87
	Hexadecane	2.24
	8-Heptadecene	0.89
Aromatic hydrocarbons		12.51
	Benzaldehyde	0.15
	Phenol	11.52
	Benzene	0.84
Nitrogen-containing aliphatics		14.67
	Acetamide	2.01
	Propanamide	0.38
	Butanamide	6.12
	2-Propen-1-amine	1.83
	Nonanenitrile	0.35
	Pentanamide	2.94
	Octanehydrazide	1.04
Nitrogen-containing aromatics		32.73
	2-Pyridinamine	1.83
	2,5-Pyrrolidinedione	2.24
	2-Pyrrolidinone	2.52
	2-Piperidinone	4.23
	Benzenepropanenitrile	3.66
	3-Methyl-2-pyrrolidinone	0.6
	1,4-Benzenediamine	0.46
	2-(1H-Imidazol-1-YL)Acetamide	1.59
	Indole	10.26
	Picolinamide	2.07
	1-Imidazolidinemethanol	3.27
Acids		2.36
	Sulfurous acid	0.33
	Cyclopropanetetradecanoic acid	0.58
	n-Pentanoic acid	1.45
Others (Ketones, Aldehyde, Alcohol, Ethers)		24.22
	2-Pentanone	10.97
	Ethanol	1.93
	Methyl ester	2.29
	Hexadecenal	4.02
	Methyl Ester	1.10

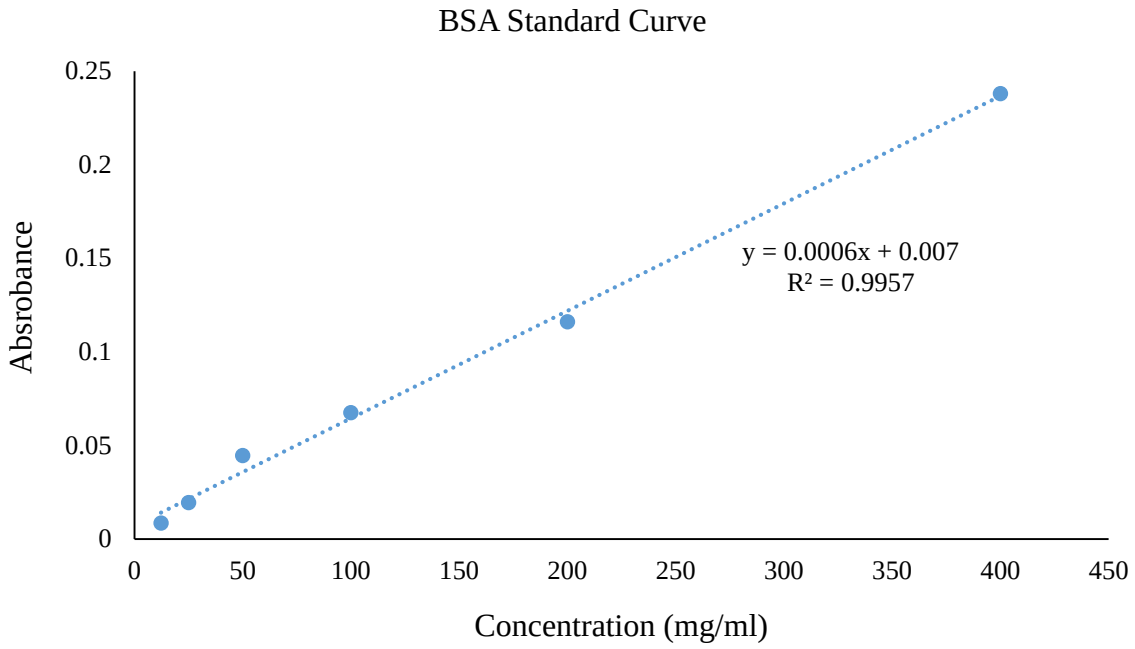

Fig. A3.1. Bovine Serum Albumin (BSA) calibration curve.

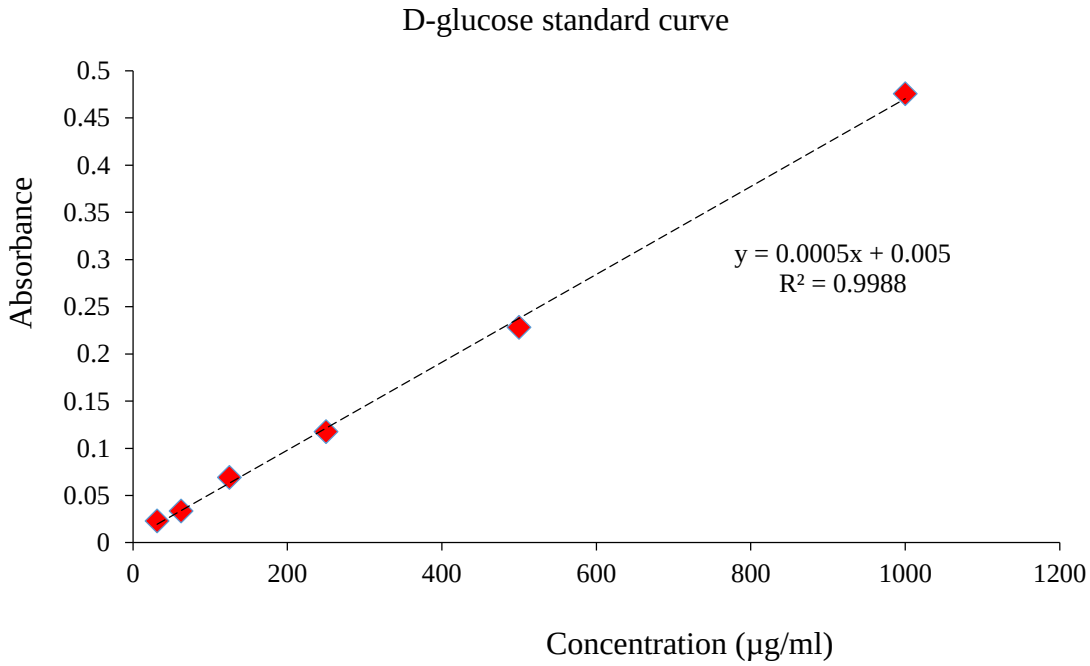

Fig. A3.2. D-glucose calibration curve.

APPENDIX B (CHAPTER 4)

Table B4.1. Relative abundance (area %) of the main compounds of the non-catalytic pyrolytic bio-oil at 500 °C

Categories	Compounds	Area (%)
Aliphatic hydrocarbons		37.54
	Decane	1.41
	Dodecane	1.65
	9-Octadecene	3.29
	4-butylcyclopentene	0.64
	2-Hexadecene	7.84
	Hexadecane	3.72
	Heneicosane	15.56
	Heptadecane	3.43
Aromatic hydrocarbons		5.62
	Phenol	4.64
	Benzenemethanol	0.63
	Thiophene	0.35
Nitrogen-containing compounds		5.92
	Butanamide	0.78
	2-Propen-1-amine	0.88
	Pentanamide	0.54
	2-Pyrrolidinone	1.69
	4-Piperidinone	0.72
	Pyrimidinone	0.37
	Enanthamide	0.30
	Indole	0.64
Acids		26.68
	Phosphonic acid	0.98
	Hexanoic acid	0.35
	Fumaric acid	0.28
	Acetic acid	25.07
Others (Ketones, Aldehyde, Alcohol, Ethers)		24.22
	3-Penten-2-one	0.27
	2-Pentanone	9.71
	2-Furanmethanol	0.31
	Ethanol	0.56
	1,2,3-Propanetriol	1.25
	Cyclododecanol	0.19
	Methyl Ester	1.10
	5-Hydroxymethyloxolan-2-one	0.45
	Neophytadiene	9.16
	2,3-Anhydro-d-mannosan	0.38
	1,4:3,6-Dianhydro-alpha-d-glucopyranose	0.84

Table B4.2. Relative abundance (area %) of the main compounds of the catalytic pyrolytic bio-oil using W/Fe_3O_4-HZSM-5 at 500 °C

Categories	Compounds	Area (%)
Aliphatic hydrocarbons		30.52
	Octane	0.92
	Undecane	0.66
	9-Eicosene	1.92
	Dodecane	2.48
	Pentadecane	2.15
	Hexadecane	3.49
	Tridecane	0.97
	Octadecane	0.35
	Cyclohexadecane	1.84
	1-Tetradecene	2.62
	1-Hexadecene	2.94
	1-Octadecene	10.18
Aromatic hydrocarbons		8.42
	Benzene	2.74
	Phenol	5.68
Nitrogen-containing compounds		2.94
	Benzenepropanenitrile	0.57
	[1,2,5]thiadiazolo[3,4]pyridine	0.3
	1H-indole	2.07
Acids		9.68
	Carbonic acid	1.15
	Oxalic acid	2.76
	Sulfurous acid	5.09
	Dichloroacetic acid	0.68
Others (Ketones, Aldehyde, Alcohol, Ethers)		48.44
	2-Pentanone	27.36
	2-Isopropyl-5-methyl-1-heptanol	2.04
	Tridecanol	0.87
	1-Hexadecanol	1.67
	n-Nonadecanol-1	8.19
	1-Hexadecanol	5.52
	Silane	0.65
	1,25-Dihydroxy vitamin	0.84
	(1-hydroxymethyl-2-phenyl-cyclopropyl)	0.73
	Ascaridole epoxide	0.57

Table B4.3. Relative abundance (area %) of the main compounds of the catalytic pyrolytic bio-oil using Zr/Fe_3O_4-HZSM-5 at 500 °C

Categories	Compounds	Area (%)
Aliphatic hydrocarbons		24.58
	Octane	2.93
	Octadecane	1.04
	Hexane	0.98
	Cyclobutane	1.15
	3-Heptene	1.17
	Heptadecane	0.71
	Nonane	1.3
	Tetradecane	15.3
Aromatic hydrocarbons		10.48
	Benzene	3.67
	Phenol	6.81
Nitrogen-containing compounds		6.25
	4-Piperidinone	0.74
	Glutarimide	1.51
	2-Propen-1-amine	0.97
	1-Ethyl-2,3-Dimethyl-4-Piperidine	0.81
	Uridine	0.69
	1,2-O-Isopropylidene	0.78
	2-Oxo-1-methyl-3-isopropylpyrazine	0.75
Acids		0.58
	Oxalic acid	0.58
Others (Ketones, Aldehyde, Alcohol, Ethers)		58.11
	2-Pentanone	52.57
	1,3-Dioxan-5-ol	0.77
	1-Heptanol	0.9
	2-Isopropyl-5-methyl-1-heptanol	0.87
	6,7-Dideuteriododec-6-enal	0.61
	1,4:3,6-Dianhydro-alpha-d-glucopyrano	1.05
	N-Butyryl-DL-homoserine lactone	0.66
	alpha-Methyl-D-mannopyranoside	0.68

Table B4.4. Relative abundance (area %) of the main compounds of the catalytic pyrolytic bio-oil using Co/Fe_3O_4-HZSM-5 at 500 °C

Categories	Compounds	Area (%)
Aliphatic hydrocarbons		27.05
	Undecane	2.9
	Cyclodecane	1.29
	Hexane	0.6
	Heptadecane	0.77
	Tetracosane	0.47
	Nonane	1.63
	1-Tetradecene	1.67
	Tetradecane	17.23
	Octadecane	0.49
Aromatic hydrocarbons		9.51
	Benzene	2.97
	Phenol	4.88
	Naphthalene	1.66
Nitrogen-containing compounds		3.11
	2-Propen-1-amine	0.69
	4-Piperidinone	0.92
	1-Ethyl-2,3-dimethyl-4-Piperidine	1.1
	Quinoline	0.4
Acids		2.73
	Carbonochloridic acid	1.21
	Benzeneacetic acid	0.73
	Phosphorus acid	0.79
Others (Ketones, Aldehyde, Alcohol, Ethers)		57.60
	2-Pentanone	53.90
	Nonanal	0.43
	2-Pentyne-1,5-diol	0.61
	1-Tridecanol	0.75
	1,3-Cyclohexadien-5-ol	0.75
	1,4:3,6-Dianhydro-alpha-d-glucopyrano	1.16

Table B4.5. Relative abundance (area %) of the main compounds of the catalytic pyrolytic bio-oil using Mo/Fe_3O_4-HZSM-5 at 500 °C

Categories	Compounds	Area (%)
Aliphatic hydrocarbons		28.56
	Octane	1.73
	Undecane	1.55
	Decane	1.33
	Tetradecane	15.59
	Pentadecane	0.86
	Hexadecane	0.68
	Heptadecane	2.64
	Hexadecane	1.32
	Nonane	1.2
	Tetracosane	0.67
	10-Methylnonadecane	0.99
Aromatic hydrocarbons		8.93
	Benzene	2.38
	2-Hydroxy-iso-butyrophenone	2.63
	2,5-Dimethyl-4-methoxyphenol	3.92
Nitrogen-containing compounds		6.55
	2-Propen-1-amine	1.21
	4-Piperidinone	0.85
	Piperidin-4-one	0.75
	2,4-Imidazolidinedione	3.11
	1,2-O-Isopropylidene	0.63
Acids		2.02
	Hexanoic acid	1.15
	Formic acid	0.87
Others (Ketones, Aldehyde, Alcohol, Ethers)		53.94
	2-Pentanone	51.35
	2-Isopropyl-5-methyl-1-heptanol	1.18
	2-Isopropyl-5-methyl-1-heptanol	0.81
	Cyclohexanol	0.60

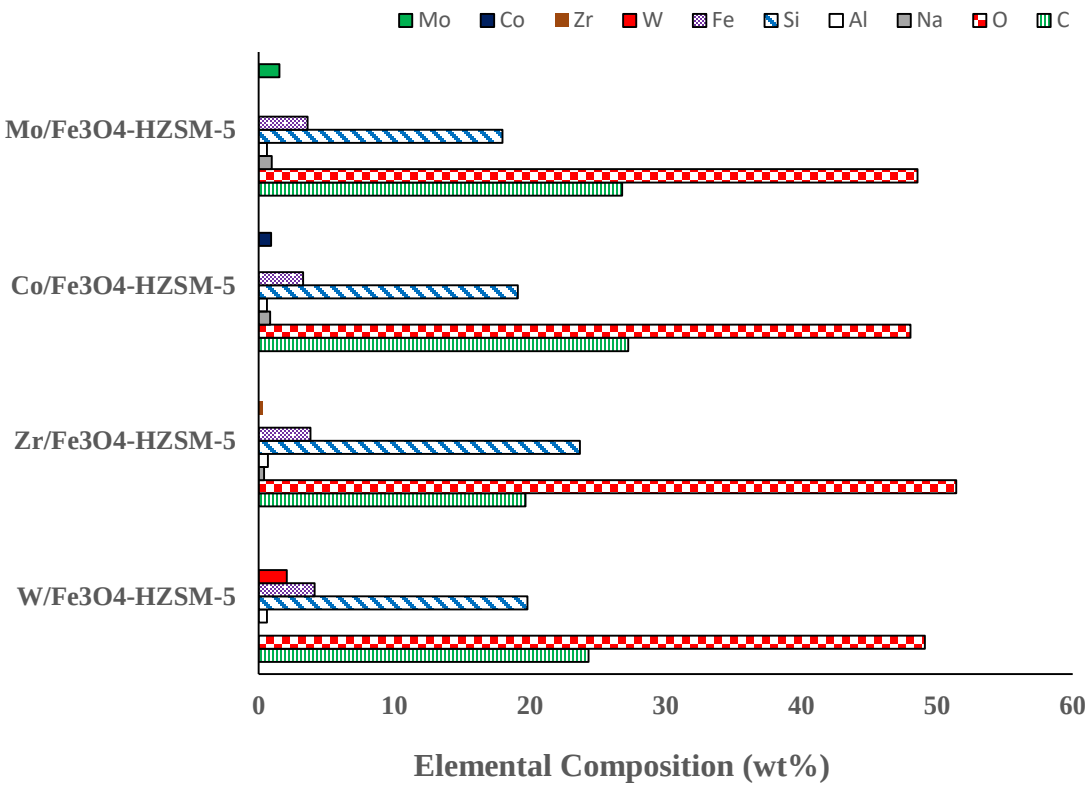

Fig. B4.1. EDS Analysis of the synthesized catalysts.

APPENDIX C (CHAPTER 5)

Table C5.1: GC-MS results of the HTL bio-oil from NSM at 300 ˚C

Retention time (min)	Compound	Area (%)	Retention time (min)	Compound	Area (%)
12.393	Heptadecane	0.22	22.735	Bis(tridecyl) phthalate, Phthalic acid	0.4
17.543	1-Hexadecen-3-ol, Isophytol	0.42	24.01	9-Octadecenoic acid (Oleic acid)	2.98
17.585	1-decene	0.34	24.375	Octadecanoic acid (Stearic Acid)	39.53
17.963	Pentadecanoic acid	1.96	24.678	13-Docosenamide	4.13
19.119	Phytol	0.22	28.36	Ergosta-7,22-dien-3-ol	0.7
19.71	9-Octadecenal (Oleic aldehyde)	24.27	28.942	Silane, dimethyl(docosyloxy)butoxy-	6.99
19.838	Octadecanoic acid (Stearic Acid)	3.36	30.863	Pentacyclo	10.3
22.643	Hexadecanoic acid (Palmitic Acid)	4.18			

Table C5.2: GC-MS results of the HTL bio-oil from NSM with a catalyst at 300 ˚C

Retention time (min)	Compound	Area (%)	Retention time (min)	Compound	Area (%)
12.699	Phenol	0.19	21.391	Decanoic acid (Capric acid)	0.63
15.651	Tetradecanoic acid (Myristic acid)	0.21	22.6	Hexadecanoic acid (Palmitic Acid)	1.24
17.475	Z,Z,Z-4,6,9-Nonadecatriene	1.56	22.73	Diisooctyl phthalate (1,2-benzenedicarboxylic acid)	0.37
17.555	1-Hexadecen-3-ol, Isophytol	2.92	23.818	1.3.5-Trisilacyclohexane, Formamide	0.65
17.59	cis-9-hexadecenoic acid (Pamitoleic acid)	1.58	23.998	9-Octadecenoic acid (Oleic acid)	2.78
17.675	Pyrrolo[1,2-a]pyrazine-1,4-dione, hexahydro-	1.16	24.235	Octadecanoic acid (Stearic Acid)	11.48
17.953	Pentadecanoic acid	19.16	26.947	2-Hexadecenoic acid	0.74
19.133	Phytol	0.72	28.36	Chondrillasterol	0.83
19.66	7-tetradecenal, aldehyde	42.37	28.911	2-tert-Butyl-4,6-bis(3,5-di-tert-butyl-4-hydroxybenzyl) phenol	2.18
19.785	Octadecanoic acid (Stearic Acid)	4.49	30.8	2-tert-Butyl-4,6-bis(3,5-di-tert-butyl-4-hydroxybenzyl) phenol	4.74

Table C5.3: GC-MS results of the HTL bio-oil from CM at 300 ˚C

Retention time (min)	Compound	Area (%)	Retention time (min)	Compound	Area (%)
12.676	Phenol	0.25	19.971	2,5-Piperazinedione	0.86
16.466	2-Pentadecanone	0.44	21.175	Cyclo-(1-leucyl-1-phenylalanyl)[piperazines]	1.25
16.687	Actinomycin	1.16	21.276	Ergotaman	2.01
17.538	1-Hexadecen-3-ol, Isophytol	2.11	21.368	Benzeneacetic acid, pentadecyl ester	1.04
17.574	5,10-Diethoxy-2,3,7,8-tetrahydro-[pyrazine]	1.81	23.955	Pentadecyl ester	2.11
17.882	Pentadecanoic acid	23.29	24.205	Octadecanoic acid (Stearic Acid)	18.96
19.111	Phytol	2.42	24.592	13-Docosenamide	1.54
19.527	7-tetradecenal, aldehyde	24.48	28.341	Chondrillasterol	2.09
19.755	2,5-Piperazinedione	4.35	28.879	Silane, dimethyl(docosyloxy)butoxy-	3.2
19.835	Hexadecanamide	0.59	30.732	Pentacyclo	6.04

Table C5.4: GC-MS results of the HTL bio-oil from CM with a catalyst at 300 ˚C

Retention time (min)	Compound	Area (%)	Retention time (min)	Compound	Area (%)
15.242	2-Hexadecene	0.31	20.788	Isovaleric acid, pentadecyl ester	0.74
16.354	Pentadecanoic acid	0.54	21.312	2-ethyl-1-butanol	1.23
16.425	Phytol	0.58	21.391	Benzeneacetic acid, pentadecyl ester	0.43
16.49	2-Pentadecanone	0.88	22.422	Nonadecanol-1	0.67
17.558	1-Hexadecen-3-ol, Isophytol	2.18	22.594	Hexadecanoic acid (Palmitic Acid)	0.8
17.62	5,10-Diethoxy-2,3,7,8-tetrahydro-[pyrazine]	0.75	22.727	Diisooctyl phthalate (1,2-benzenedicarboxylic acid)	0.87
17.71	Pyrrolo	0.92	23.813	1.3.5-Trisilacyclohexane, Formamide	0.5
17.85	Hexadecanoic acid (Palmitic Acid)	7.35	23.978	1-Heneicosanol	1.07
17.983	Eicosanoic acid (Arachidic acid)	20.44	24.234	Octadecanoic acid (Stearic Acid)	12.81
18.736	Eicosanoic acid	0.24	24.616	13-Docosenamide	0.98
19.148	Phytol	3.48	25.428	n-Tetracosanol-1	0.64
19.59	7-tetradecenal, aldehyde	22.82	28.155	Ergost-7-en-3-ol	0.62
19.667	Z,Z-3,15-Octadecadien-1-ol acetate	4.01	28.383	Stigmastorol	2.38
19.755	Octadecanoic acid (Stearic Acid)	3.54	28.904	2-tert-Butyl-4,6-bis(3,5-di-tert-butyl-4-hydroxybenzyl)phenol	1.2
19.897	Octadecanamide	0.51	30.804	2-tert-Butyl-4,6-bis(3,5-di-tert-butyl-4-hydroxybenzyl)phenol	6.51

Table C5.5: GC-MS results of the HTL bio-oil from NSM at 350 ˚C

Retention time (min)	Compound	Area (%)	Retention time (min)	Compound	Area (%)
17.53	10-Methyl-3,4,5,8,9,10-hexahydrooxecin-2-one	1.29	21.412	8-methyl-6-nonenamide	1.68
17.596	cis-9-hexadecenoic acid (Pamitoleic acid)	2.82	23.819	1,3,5-Trisilacyclohexane, Formamide	1.42
17.925	Pentadecanoic acid	14.5	23.977	2-ethylbutyric acid, eicosyl ester	1.54
19.689	cis-vaccenic acid, omega-7 fatty acid	55.94	24.229	Octadecanoic acid (Stearic Acid)	11.06
19.802	Octadecanoic acid (Stearic Acid)	3.54	30.8	2-tert-Butyl-4,6-bis(3,5-di-tert-butyl-4-hydroxybenzyl)phenol	6.21

Table C5.6: GC-MS results of the HTL bio-oil from NSM with a catalyst at 350 ˚C

Retention time (min)	Compound	Area (%)	Retention time (min)	Compound	Area (%)
11.305	Dodecane	0.2	17.901	Pentadecanoic acid	20.73
12.701	Phenol	0.2	19.611	cis-vaccenic acid, omega-7 fatty acid	47.96
13.798	Tetradecane	0.25	19.745	Octadecanoic acid (Stearic Acid)	3.74
15.643	Tetradecanoic acid (Myristic acid)	0.25	21.386	8-methyl-6-nonenamide	1.07
16.484	Acetic acid	0.32	23.814	1,3,5-Trisilacyclohexane, Formamide	1.25
16.86	3,7,11-Trimethyl-2,4-dodecadiene	0.21	23.965	2-ethylbutyric acid, eicosyl ester	1.76
17.099	3,7,11-Trimethyl-2,4-dodecadiene	0.25	24.202	Octadecanoic acid (Stearic Acid)	8.97
17.462	cis-5,8,11,14,17-Eicosapentaenoic acid	2.18	24.604	13-Docosenamide	0.81
17.552	3-Tetradecyn-1-ol	2.58	28.903	Silane, dimethyl(docosyloxy)butoxy-	0.71
17.59	Phenethylamine	1.17	30.782	Benzeneethanol	5.39

Table C5.7: GC-MS results of the HTL bio-oil from CM at 350 ˚C

Retention time (min)	Compound	Area (%)	Retention time (min)	Compound	Area (%)
12.411	Dodecane	0.71	19.424	9-Octadecenal	0.69
12.704	Phenol	0.72	19.637	Alpha- ketostearic acid	1.08
13.798	Tetradecane	0.71	20.314	2,5-piperazinedione	0.93
14.917	Dodecane	0.65	20.604	2,5-piperazinedione	0.65
15.406	Eicosane	1.25	21.148	2,5-piperazinedione	1.64
15.503	3,6-Nonadecadione	1.64	21.241	Pyrrolo	1.07
16.319	Pyrrolo	0.85	21.333	Cyclo-(1-leucyl-1-phenylalanyl)	0.79
16.48	7-Ethyl-4,6-pentadecandione	1.98	21.42	Benzeneacetic acid, pentadecyl ester	0.92
16.643	Pyrrolo	3.06	22.398	Decane	1.06
17.185	7 9-di-tert-butyl-1-oxaspiro(4 5)deca-6 9-diene-2 8-dione	1.25	23.811	1,3,5-Trisilacyclohexane, Formamide	4.74
17.5	Pyrrolo	3.11	23.968	2-ethylbutyric acid, eicosyl ester	2.38
17.59	Decane	5.85	24.215	Octadecanoic acid (Stearic Acid)	27.55
17.657	Pyrrolo	4.82	24.605	13-Docosenamide	3.37
17.784	Pentadecanoic acid	2.58	28.918	Silane, dimethyl(docosyloxy)butoxy-	11.71
18.889	2-methylhexacosane	0.64	30.784	2-tert-Butyl-4,6-bis(3,5-di-tert-butyl-4-hydroxybenzyl)phenol	11.6

Table C5.8: GC-MS results of the HTL bio-oil from CM with a catalyst at 350 ˚C

Retention time (min)	Compound	Area (%)	Retention time (min)	Compound	Area (%)
12.701	Phenol	0.32	19.73	2,5- Piperazinedione	0.8
13.795	Heptadecane	0.29	20.372	2,5- Piperazinedione	0.99
15.246	3-Methyl-1,4-diazabicyclo[4.3.0]nonane	0.64	20.657	2,5- Piperazinedione	0.73
16.041	Heptadecane	0.32	21.207	Cyclo-(1-leucyl-1-phenylalanyl)	1.4
16.125	Cyclo-(glycyl-1-leucyl) piperazinedione	0.67	21.279	Pyrrolo	1.08
16.2	Glycyl-D-threonine	0.47	21.388	Benzeneacetic acid, pentadecyl ester	1.2
16.369	Pyrrolo	0.65	21.634	Pyrrolo	0.67
16.709	Pyrrolo	2.22	22.254	1,3,5-Trisilacyclohexane, Formamide	0.26
16.855	5,8-Tridecadione	0.37	22.411	2-ethylbutyric acid, eicosyl ester	0.7
17.193	7 9-di-tert-butyl-1-oxaspiro(4 5)deca-6 9-diene-2 8-dione	0.47	22.589	Hexadecanoic acid	0.87
17.554	Pyrrolo	1.61	22.723	Diisooctyl phthalate (1,2-benzenedicarboxylic acid)	0.48
17.612	5,10-Diethoxy-2,3,7,8-etrahydro-[pyrazine]	1.66	23.814	1,3,5-Trisilacyclohexane, Formamide	2.22
17.71	2,5 Piperazinedione	4.73	23.979	Hexadecanoic acid	0.67
17.747	Pyrrolo	2.18	24.253	Octadecanoic acid (Stearic Acid)	30.84
17.787	Pyrrolo	1.3	24.625	13-Docosenamide	3.45
17.863	Pentadecanoic acid	5.6	24.81	Squalene	0.3
19.128	Phytol	0.27	26.781	Octadecyl ester	0.26
19.491	Hexadecadien-1-ol	6.49	28.366	Stigmastorol	1.07
19.571	Oxirane, hexadecyl	1.3	28.934	Silane, dimethyl(docosyloxy) butoxy-	10.4
19.689	Octadecanoic acid (Stearic Acid)	1.86	30.795	2-tert-Butyl-4,6-bis(3,5-di-tert-butyl-4-hydroxybenzyl) phenol	8.19

APPENDIX D

EXPERIMENTAL SET-UP, MATERIALS AND EQUIPMENTS

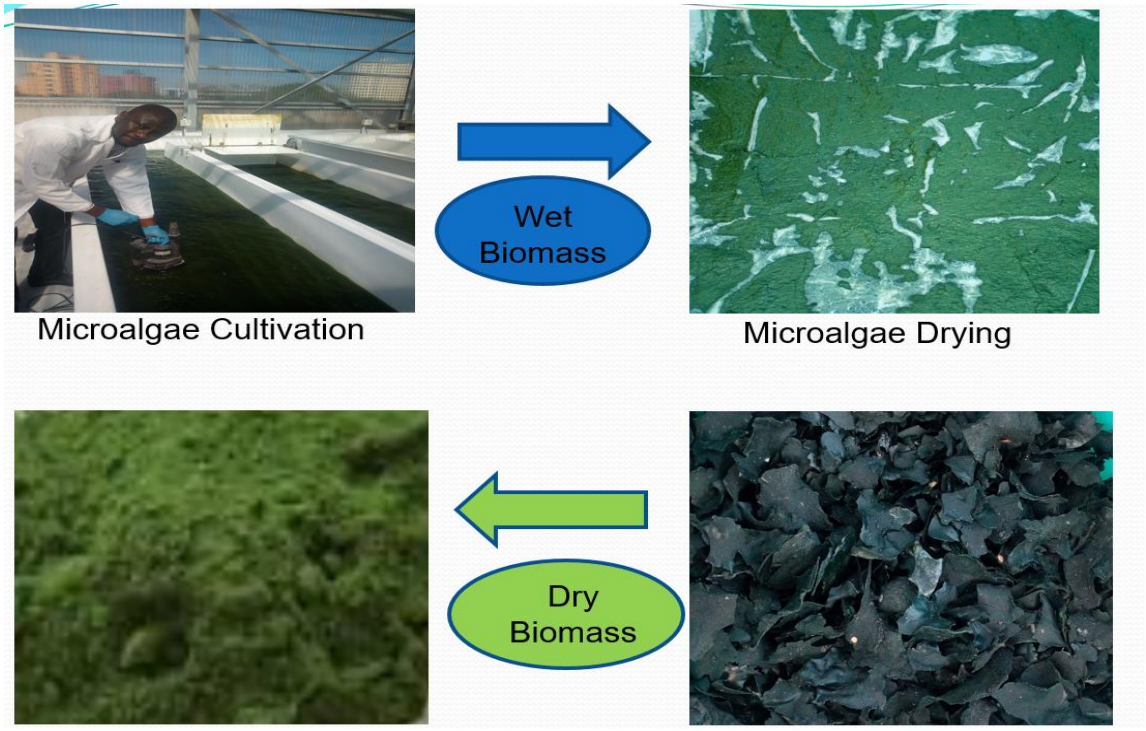

Microalgae Cultivation

Microalgae Drying

Dried and grounded microalgae biomass

Dried Microalgae Biomass

Pyrolysis Experimental Setup